

See discussions, stats, and author profiles for this publication at: <https://www.researchgate.net/publication/223963838>

# Chemistry and Biology of Acylfulvenes: Sesquiterpene-Derived Antitumor Agents

ARTICLE *in* CHEMICAL REVIEWS · APRIL 2012

Impact Factor: 46.57 · DOI: 10.1021/cr2001367 · Source: PubMed

---

CITATIONS

21

---

READS

66

## 2 AUTHORS:



[Marina Tanasova](#)

Michigan Technological University

10 PUBLICATIONS 189 CITATIONS

[SEE PROFILE](#)



[Shana J Sturla](#)

ETH Zurich

68 PUBLICATIONS 1,033 CITATIONS

[SEE PROFILE](#)

## 1 Chemistry and Biology of Acylfulvenes: Sesquiterpene-Derived 2 Antitumor Agents

3 Marina Tanasova and Shana J. Sturla\*

4 ETH Zurich, Institute of Food, Nutrition and Health, Schmelzbergstrasse 9, Zurich 8092, Switzerland

### 5 CONTENTS

7	1. Introduction	A	56
8	2. Illudins: Natural Product Precursors of Acylful-		
9	venes	B	
10	2.1. Discovery and Bioactivity	B	
11	2.2. Illudin Biosynthesis	D	
12	3. Acylfulvenes: Illudin Derivatives with Improved		
13	Therapeutic Indices for Anticancer Therapy	D	
14	3.1. Acylfulvene Discovery and Preliminary Cy-		
15	tototoxicity Data	D	
16	3.2. Acylfulvene Tumor Xenograft Activity	D	
17	3.3. Acylfulvene Tumor Selectivity	E	
18	4. Synthetic Chemistry of Illudins and Acylfulvenes	F	
19	4.1. Cycloaddition Reaction in Illudin Synthesis	F	
20	4.2. Allenic Pauson–Khand Chemistry in Acylful-		
21	vene Synthesis	G	
22	4.3. Asymmetric Metathesis for Synthesizing		
23	Acylfulvenes	H	
24	5. Metabolism and Chemical Reactivity of Acylful-		
25	venes and Illudins	I	
26	5.1. Cellular Distribution and Cytosolic Metabo-		
27	lism	I	
28	5.2. Chemical Metabolism and Reactivity toward		
29	Thiols	J	
30	5.3. Role of Glutathione in Illudin vs Acylfulvene		
31	Differential Cytotoxicity	K	
32	6. Acylfulvene-Induced Inhibition—Alkylation of		
33	Redox-Regulating Enzymes	K	
34	6.1. Acylfulvenes as Glutathione Reductase In-		
35	hibitors	K	
36	6.2. Acylfulvenes as Thioredoxin and Thioredox-		
37	in Reductase Inhibitors	K	
38	7. Structure–Activity Relationships of Acylfulvenes		
39	and Illudins	L	
40	7.1. Role of the Enone and Cyclopropyl Ring in		
41	Acylfulvene Cytotoxicity	L	
42	7.2. Role of the C10-Hydroxyl in HMAF Cytotox-		
43	icity	M	
44	7.3. Tuning Illudin Cytotoxicity and Tumor		
45	Specificity	O	
46	8. Role of Reductive Bioactivation in Acylfulvene		
47	Cytotoxicity	O	
48	8.1. Reductive Metabolism of Acylfulvenes and		
49	Illudins	P	
50	Prostaglandin Reductase 1-Mediated Acylful-		
51	vene Metabolism	P	
52	8.2. Prostaglandin Reductase 1-Mediated Illudin		
53	and Acylfulvene–GSH Interaction	Q	
54	8.3. Role of Stereochemistry in Acylfulvene		
55	Cytotoxicity	Q	
	9. Role of Uptake in Differential Cytotoxicity of		
	Illudins and Acylfulvenes	R	57
	9.1. Illudin S Uptake and Cellular Accumulation	R	58
	9.2. Acylfulvene Uptake and Cellular Accumu-		
	lation	S	60
	10. Acylfulvenes as DNA Alkylating Agents	S	61
	10.1. DNA Alkylation as a Source of Acylfulvene		
	Cytotoxicity	S	62
	10.2. DNA Alkylation through Alternative Reac-		
	tive Intermediate(s) of Acylfulvenes	T	63
	10.3. Acylfulvenes Induce DNA Double-Strand		
	Breaks and Cell Apoptosis	U	64
	11. Biochemical Pathways of Acylfulvene-Induced		
	Apoptosis	U	65
	11.1. Role of Caspases in Acylfulvene-Induced		
	Apoptosis	U	66
	11.2. Role of p53, p21, and CHK2 in Acylfulvene-		
	Induced Apoptosis	U	67
	12. Repair of Acylfulvene-Induced DNA Damage	V	68
	12.1. Brief Overview of Nucleotide Excision		
	Repair Pertinent to Illudin and Acylfulvene		
	Interactions	V	69
	12.2. Acylfulvene-Induced Cytotoxicity as a Con-		
	sequence of TC-NER Status in Cancer Cells	V	70
	12.3. Acylfulvenes Disrupt RNA Synthesis	W	71
	12.4. Homologous Recombination and Repair of		
	Acylfulvene-Induced DNA Damage	X	72
	12.5. Acylfulvene-Induced Abasic Sites and Base		
	Excision Repair	Y	73
	13. Chemically and Mechanistically Related Cyto-		
	toxins	Y	74
	13.1. Cyclopropane-Containing DNA Alkylators	Y	75
	13.2. Epoxide- and Aziridine-Containing DNA		
	Alkylators	Z	76
	13.3. Esteinascidin 743	Z	77
	14. HMAF Clinical Trials: Current Status and Results	AA	78
	14.1. Population Pharmacokinetics and Phase I		
	Clinical Trials	AA	79
	14.2. HMAF Phase II and Phase III Clinical Trials	AB	80
	15. Conclusions and Perspectives	AB	81
	Author Information	AC	82
	Corresponding Author	AC	83
	Notes	AC	84
	Biographies	AC	85
	Acknowledgments	AC	86
	References	AC	87

Received: April 23, 2011



## 1. INTRODUCTION

Illudins are naturally occurring sesquiterpene secondary metabolites of basidiomycetes found on rotten beech trees, bark, and decayed fungal fruit bodies in the United States, Canada, Japan, Norway, and Spain.<sup>1–9</sup> These natural products are proposed to be biosynthesized via farnesyl diphosphate<sup>10–13</sup> and are related to other natural sesquiterpenes, such as illudol, illudisin, fomannosin, and ptaquiloside.<sup>5,14–18</sup> Illudins S and M, the first identified examples, were isolated from *Omphalotus olearius* (Jack-o-Lantern) mushrooms in the New York Botanical Garden in the 1950s in research lead by Marjorie Anchel.<sup>1</sup> Subsequently, illudin S isolation from *Lampteromyces japonicus* (Tsukiyotake) mushrooms was reported by Nakai in 1958.<sup>3</sup> Illudins were studied extensively for their cytotoxicity in various tumor cell types and tumor xenografts. However, frequent animal deaths, associated with high **general** illudin S toxicity, restricted the potential use of illudins as anticancer agents.<sup>19</sup>

Acylfulvenes (AFs) are semisynthetic derivatives of illudin that were obtained in the course of developing cytotoxic agents with improved therapeutic characteristics. The core structure is acylfulvene, and there are various examples of further functionalized analogs, like hydroxymethylacylfulvene (HMAF). Unlike their natural product precursors, AFs are milder cytotoxins that exhibit favorable tumor specificities<sup>20,21</sup> and are more active in cells with compromised DNA repair capacities.<sup>22</sup> In cell-based cytotoxicity studies and tumor xenografts, HMAF was a more effective tumor inhibitor than cisplatin, doxorubicin, irinotecan, or mitomycin C.<sup>23</sup> In addition, AFs appear to sensitize multidrug-resistant (mdr) cells toward some conventional chemotherapeutic drugs.<sup>22,24–26</sup> Its unique tumor specificity and acceptable cytotoxicity profile advanced HMAF into human clinical trials for treatment of various solid tumors.<sup>27–29</sup>

High interest in AF bioactivity and mode of action triggered development of new synthetic strategies to AFs and their analogs. Chemical approaches involved dipolar cyclization reaction,<sup>30–34</sup> Pauson–Khand reaction,<sup>35,36</sup> and enyne ring-closing metathesis (EYRCM)<sup>37,38</sup> and provided access to racemic and enantiomerically pure AFs. Structure–activity relationship (SAR) studies resulted in identification of AF's pharmacophore<sup>39–41</sup> and provided grounds for further tuning of biological activity and tumor specificity.

A broad range of biochemical investigations has been and continues to be carried out to understand AF tumor specificity and differential activity. Cellular metabolism of AFs involves activation of the molecule via the conjugated enone; the resulting electrophilic intermediate reacts with water, glutathione (GSH), or cellular macromolecules.<sup>42–49</sup> For illudins, it appears that differences in activity across tumor cell lines depend in large part on the effectiveness of drug uptake.<sup>50</sup> For AFs, however, uptake does not sufficiently account for observed toxicity differences, and other factors such as bioactivation and repair of DNA adducts appear to play a role.<sup>47,51,52</sup>

Reductase-mediated bioactivation of AFs yields activated intermediates poised for interaction with cellular nucleophiles, such as DNA. The fulvene moiety appears to provide enough stabilization for the reactive intermediate to survive outside the enzyme active site and react with cellular macromolecules.<sup>53</sup> The positive correlation between cytotoxicity and reductase level observed for AFs suggests a direct role of reductive activation in AF tumor specificity. Prostaglandin reductase 1

(PTGR1), referred to also as alkenal(one) oxidoreductase (AOR) or leukotriene B4 12-hydroxydehydrogenase, reductively activates AFs.<sup>54</sup> AFs interact with redox-modulating enzymes, such as glutathione reductase (GR), thioredoxin (Trx), and thioredoxin reductase (TrxR), and, in some cases, covalently modify these enzymes and inhibit activity.<sup>55,56</sup> The same reactivity patterns, including dependence on bioactivation and redox-regulating enzyme inhibition, were not, however, observed for illudin S.

AFs alkylate DNA and form DNA adducts that disrupt DNA and RNA synthesis, arrest cells in G1-S phase, and induce apoptosis.<sup>57</sup> The minor groove was identified as the primary alkylation site where adducts to the 3 position of adenine are formed preferentially.<sup>58</sup> DNA lesions induced by illudins and AFs appear to be specifically recognized by transcription-coupled nucleotide excision repair (TC-NER), and TC-NER deficiency appears to contribute to the activity of AFs in lung, head, neck, prostate, and other tumors.<sup>59–61</sup> Furthermore, the specificity between AF-induced lesions and TC-NER suggests that AFs offer unique tools for studying this specific DNA repair pathway. This review offers a comprehensive description of the investigations that started with the discovery of illudins in 1950, led to HMAF clinical trials against various tumors as a single agent and in combination therapy beginning in 2002, and culminated in the past decade of advances in chemical synthesis and mechanisms of toxicity of AFs, including biotransformation processes, DNA alkylation products, unique influences of DNA repair capacities, and enzyme inhibition properties.

## 2. ILLUDINS: NATURAL PRODUCT PRECURSORS OF ACYLFULVENES

Identification of illudins as active components of *O. olearius* and *L. japonicus* prompted investigations into their biological activity and exploration of potential applications in medicine. Seminal research on illudins addressed their biogenesis, chemical and biochemical reactivity, and antitumor activity and identified their biological targets and mechanism of cytotoxicity. This section overviews the history of illudin research, which led ultimately to the discovery of the uniquely tumor-specific AFs.

### 2.1. Discovery and Bioactivity

*O. olearius* (Figure 1)<sup>63</sup> is known for causing severe abdominal cramps, vomiting, and diarrhea; they have occasionally caused fatal accidents due to their apparent similarity to edible mushrooms.<sup>64</sup> Furthermore, handling extracts leads to severe skin irritation.<sup>65,66</sup> Early bioassays involving aqueous extracts from *O. olearius* indicated high activity against *Staphylococcus aureus*, *Klebsiella pneumoniae*, and *Mycobacterium smegma* and little or no effect on *Escherichia coli*.<sup>1,3,4</sup> The active components of these extracts were determined by McMorris and Anchel<sup>10,67</sup> to be the sesquiterpenes illudin S and illudin M (Figure 2). The original 72027-S strain, isolated from *O. olearius* culture liquids, produced illudin S and illudin M in a 10:1 ratio.<sup>1</sup> After strain modification, the updated 14610-S strain produced predominantly illudin M.<sup>2</sup> Two subsequent independent reports by Matsumoto and co-workers,<sup>4</sup> and Nakanishi and co-workers<sup>5</sup> isolate a toxic substrate, Lampsterol, as an active ingredient in *L. japonicus* extract. Subsequent structural elucidation of Lampsterol revealed its identity with illudin S and established its absolute stereochemistry.<sup>5,6,46,66</sup>

Since the discovery of illudin S and M a number of other illudin-related natural products depicted in Figure 2 have been

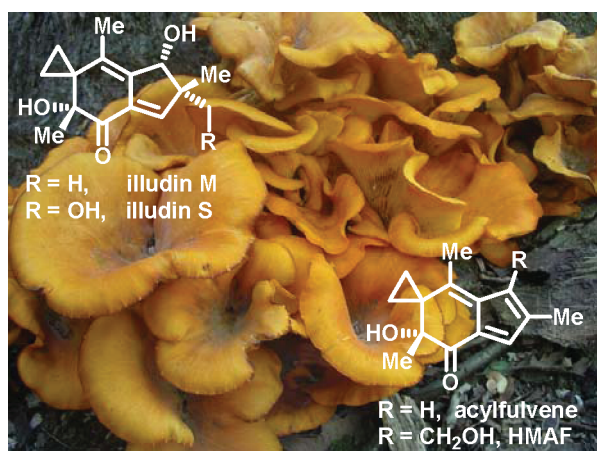


**Figure 1.** *O. leariius* (Jack-o-Lantern mushroom), fungal metabolite illudins, and semisynthetic Acylfulvene derivatives. Photograph reprinted (structures added by author) from Wikipedia Web site [http://en.wikipedia.org/wiki/File:Omphalotus\\_olearius\\_in\\_NE\\_IL.JPG](http://en.wikipedia.org/wiki/File:Omphalotus_olearius_in_NE_IL.JPG).

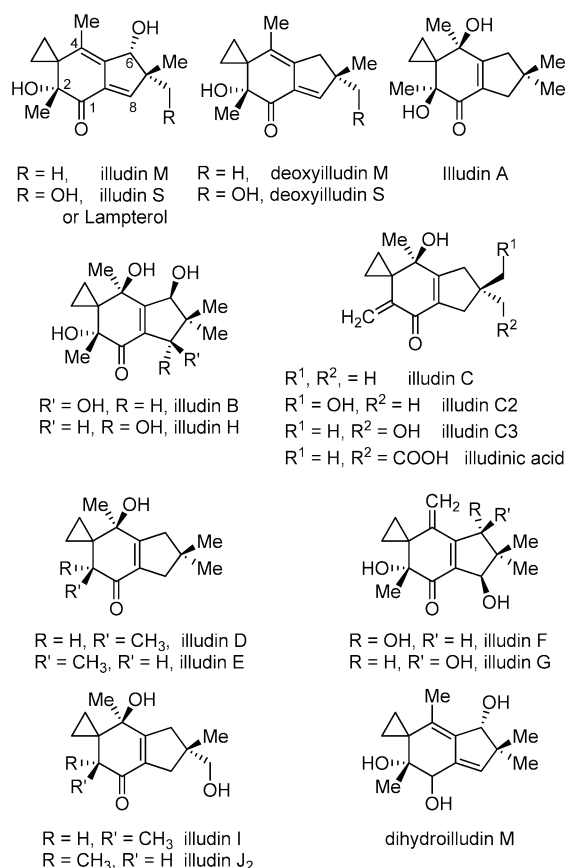


**Figure 2.** Naturally occurring illudin analogs.

222 isolated from various basidiomycetes. Illudins A–J2 are isomeric  
 223 to illudins S and M, bearing the  $\alpha,\beta$ -unsaturated ketone and  
 224 additional hydroxyl groups on C4 and the five-membered ring  
 225 of the illudane skeleton.<sup>68–71</sup> Illudins C, C2, and C3 have  
 226 unconjugated C5–C9 and C2–C10 dienes and a hydroxyl at  
 227 C4.<sup>72</sup> Illudinic acid shares the same structural features.<sup>72,73</sup>  
 228 Illudins A, B, I, and J2 have moderate antimicrobial activity  
 229 against *S. aureus* but do not exhibit significant cytotoxic  
 230 activities, except for illudin I, which is highly cytotoxic against

HepG2 hepatoma cells.<sup>68,72,74</sup> Illudinic acid shows strong  
 antibacterial activity and is also moderately cytotoxic in  
 mammalian cell cultures.<sup>74–76</sup> 6-Deoxyilludins M and S were  
 isolated from *Pleurotus japonicus* and lack the secondary  
 hydroxyl group.<sup>77</sup> They are active against illudin S-resistant  
 murine leukemia in mice xenografts.<sup>77</sup> Dihydroilludin, a  
 biological precursor to illudin M also isolated from *O. leariius*,<sup>74</sup>  
 is not significantly biologically active.

In 1987, Illudin S was tested against a variety of rodent solid  
 tumors in an NCI panel and leukemias in preclinical  
 evaluation.<sup>19</sup> It was observed that solid tumor cells are less  
 sensitive to illudin M than hematopoietic cells.  $IC_{50}$  values for  
 illudin-sensitive melanoma 242 and ovarian carcinoma 547 lines  
 are in the range of 200–300 nM. The myeloid leukemia cell  
 lines HL60 and KG-1 and the T-cell acute lymphoblastic  
 leukemia cell lines 8402 and CEM are highly susceptible to  
 illudin ( $IC_{50} = 6–11$  nM). In contrast, B-cell-derived leukemia/  
 lymphoma lines Namalva and 8392 are at least 10 times more  
 resistant to the drug. Illudins S shows relatively lower activity in  
 normal bone marrow progenitors ( $IC_{50} = 60$  nM) than illudin-  
 sensitive leukemia lines. Nonetheless, toxicity in the low  
 nanomolar range toward normal cells diminishes the overall  
 advantage of this feature.<sup>19</sup> Similarly, high activity against  
 leukemias is limited by increased mortality in illudin S-treated  
 animals.<sup>19,78–80</sup>

Illudin S has a wide range of activities in a panel of DNA  
 repair-deficient, UV-sensitive chinese hamster ovary (CHO)  
 cell lines.<sup>59</sup> It was observed that UV5, which lacks the DNA-  
 repair gene ERCC2, is 38-fold more susceptible to illudin than  
 the parent AA8 line ( $IC_{50}$  0.8 and 28 nM, respectively, after 4 h  
 exposure). The UV20, UV24, UV41, UV135, and UV61 cell  
 lines, deficient in ERCC1, ERCC3, ERCC4, ERCC5, and  
 ERCC6, respectively, are 8- to 9-fold more susceptible toward  
 illudin S. In contrast, EM9 and 5T4 cell lines, deficient in  
 XRCC1 and ERCC2, are as sensitive to illudin S as are the  
 parent AA8 line. All these observations suggest that illudin is a  
 DNA alkylating agent and that specific genes are involved with  
 the repair of illudin-induced DNA damage.

Illudin S interferes with DNA synthesis and causes a  
 complete block at the G1-S phase transition.<sup>19,81</sup> The kinetics  
 of DNA synthesis inhibition shows preferential inhibition of  
 DNA synthesis in illudin S-treated HL60 cells, followed by  
 RNA and protein synthesis. Thus, at 38 nM illudin S, less than 1  
 h is required for 50% inhibition of tritiated thymidine uptake,  
 while similar inhibition of uridine and leucine uptake requires  
 more than 2 and 24 h, respectively. These findings suggest that  
 DNA synthesis is an important target for illudin-mediated  
 growth inhibition and cytotoxicity. Cytokinetic studies using  
 HL60 cells showed that at 2 h exposure 380 nM illudin S causes  
 a block at the G1-S phase interface, indicating selective  
 apoptosis of DNA-synthesizing cells or complete inhibition of  
 new DNA synthesis.

High cytotoxicity in multidrug-resistant (mdr) cells is  
 another characteristic of illudin S.<sup>19</sup> It exhibits low micromolar  
 $IC_{50}$ s in various mdr CEM cell lines regardless of whether  
 resistance is due to gp170 expression, gp180/MRP expression,  
 GSHTR-pi expression, topoisomerase I, or topoisomerase II  
 activity or increased ability to repair DNA damage. Thus, on  
 the basis of its activity in mdr cells and nanomolar cytotoxicity  
 in leukemias and solid tumors, illudin S was explored further as  
 a potential chemotherapeutic drug. However, in subsequent  
 studies, there were high toxicities associated with illudin S and  
 high mortality rates in illudin S-treated animals.<sup>19</sup> These

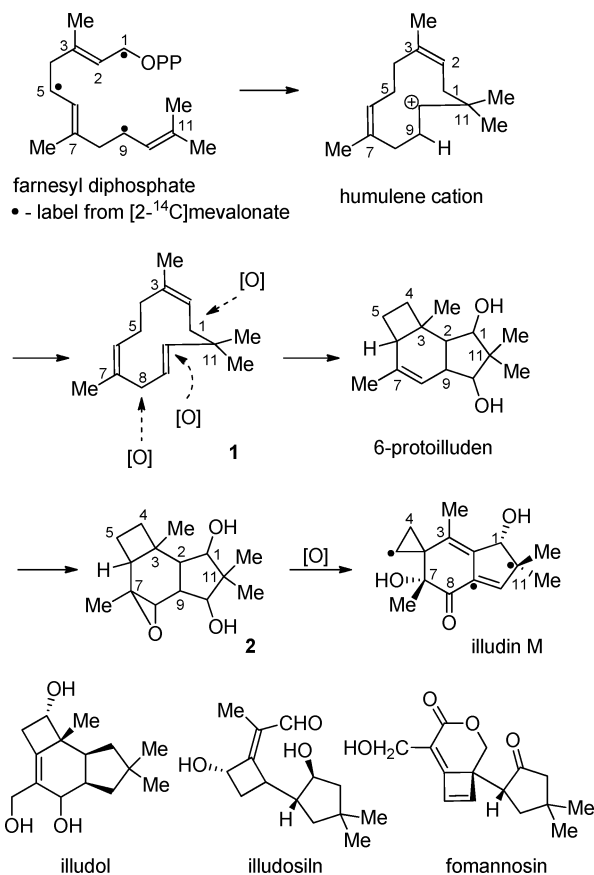


shortcomings halted the advancement of illudin S into clinical trials but sparked subsequent research to create more selective illudin analogs.

## 2.2. Illudin Biosynthesis

Biosynthesis of illudin S and M is believed to initiate from farnesyl diphosphate (Scheme 1) and involve a series of

**Scheme 1. Illudin Biosynthesis**



cyclization reactions, formulated on the basis of chemical degradation studies and *O. olerius*-mediated generation of isotopically labeled illudin M from isotopically labeled acetate and mevalonate.<sup>10</sup> Cyclization of farnesyl diphosphate to the reactive 11-membered humulene cation occurs by addition of the C10–C11 double bond to C1 in the farnesyl cation, derived from ionization of farnesyl diphosphate (Scheme 1).<sup>5,10</sup> Incorporation of three <sup>14</sup>C labels and one <sup>2</sup>H label from [4(*R*)-4-<sup>2</sup>H]-mevalonate is consistent with the mevalonoid biosynthetic pathway<sup>82</sup> and observations for related sesquiterpenes, such as illudosin and fomannosin (Scheme 1). Biosynthesis of illudin M from [5-<sup>3</sup>H]-mevalonate as a precursor yields a product containing <sup>3</sup>H at C6, suggesting that the C6 proton is derived from C1 of farnesyl diphosphate. The absolute stereochemistry of the secondary C6 alcohol is established by delivery of the 5-*pro-R*-proton of mevalonate.<sup>11</sup> Consistent with incorporation of a <sup>2</sup>H into the illudin M cyclopropyl ring, coming from [2-<sup>2</sup>H<sub>3</sub>, 2-<sup>14</sup>C]-mevalonate, humulene cyclization is thought to proceed by a nonconcerted mechanism.<sup>11,82</sup>

Completion of illudin M biosynthesis is believed to involve a series of hydride shifts and nonstereospecific deprotonations/reprotonations that occur, while the humulene cation is bound

to the cyclase active site.<sup>13</sup> The cyclization of 1 is proposed to yield 6-protoilluden, which is either released or remains enzyme-bound.<sup>13</sup> In fact, the metabolite illudol (Scheme 1) possesses the protoilluden ring system.<sup>82</sup> The cyclopropyl ring of the illudane skeleton is believed to be generated after oxidation of the C7–C8 double bond to the epoxide 2 and the following ring contraction. Subsequent dehydration and oxidation of the resulting secondary hydroxyl to the ketone could complete illudin M biosynthesis; however, to our knowledge there is no experimental information available regarding specific oxidation/reduction pathways.

## 3. ACYLFULVENES: ILLUDIN DERIVATIVES WITH IMPROVED THERAPEUTIC INDICES FOR ANTICANCER THERAPY

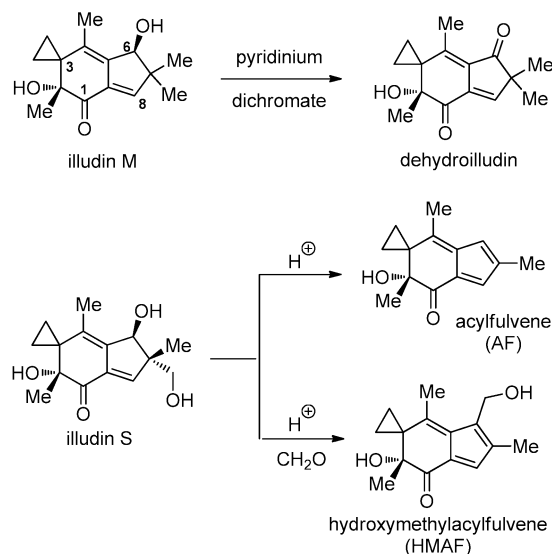
The low therapeutic indices of illudins precluded their use as anticancer drugs but stimulated a pursuit for analogs that combine high potency with better therapeutic characteristics. AFs are illudin-derived analogs with improved tumor selectivity and specificity. The SARs established on the basis of studies comparing AFs and illudins have shed light on factors that dictate tumor cell-specific toxicity. The following section summarizes the semisynthesis of AFs from illudin S and their antitumor activity and specificity in various tumor xenografts.

### 3.1. Acylfulvene Discovery and Preliminary Cytotoxicity Data

After several chemical modifications of illudin S, novel analogs were obtained, including dehydroilludin, AF, and HMAF (Scheme 2).<sup>83</sup> Dehydroilludin is derived by oxidation of illudin M with pyridinium dichromate and exhibits ~100-fold diminished cytotoxicity compared to illudin M in myeloid leukemia HL60 cells and metastatic lung carcinoma MV522 cells.<sup>83</sup> AF was first obtained by semisynthesis involving an acid-catalyzed reverse Prins reaction of illudin S in dilute sulfuric acid<sup>84</sup> and is a milder toxin than dehydroilludin in HL60 and MV522 cells.<sup>85</sup> HMAF, obtained under similar semisynthesis conditions but in the presence of excess paraformaldehyde,<sup>84</sup> has IC<sub>50</sub> values between 0.44 and 2.7 μM in ovarian carcinoma cells, 0.44 μM in colon carcinoma cells (CoLo 205), and 1.2 μM in malignant glioma cells (SNB-19 and U-251).<sup>22</sup> HMAF is active in head and neck cancer cell lines exhibiting low sensitivity toward more conventional alkylating agents like cisplatin and its analogs.<sup>22</sup> In addition, mdrr cells are highly susceptible to HMAF, suggesting that HMAF is not recognized by the P-glycoprotein and multidrug-resistance protein 1.<sup>22</sup> While potent against carcinomas, HMAF has only limited activity in sarcoma cells that are sensitive to cisplatin and other alkylating agents.<sup>22</sup>

### 3.2. Acylfulvene Tumor Xenograft Activity

HMAF demonstrated significant cytotoxic activity resulting in primary tumor growth inhibition, shrinkage of tumors, and markedly increased median life span of mice in preclinical evaluation against various tumor xenografts, including a wide range of carcinomas and some leukemias.<sup>86–88</sup> Tumor growth inhibition increased significantly with higher HMAF concentrations, and at 7 mg/kg significant tumor shrinkage in one-half the animals was observed (Table 1). In contrast, illudin S failed to demonstrate any antitumor activity in MV522 human lung adenocarcinoma xenograft models even at concentrations corresponding to 75% of LD<sub>50</sub>.<sup>85</sup> Evaluation against five lung tumor xenografts (the non-small lung cancers NCI-H460, Calu-6, and A-427 and the small-cell lung cancers NCI-H69 and LX-

**Scheme 2.** AFs: Semi-Synthetic Analogs of Illudin S

Compound	HL60 IC <sub>50</sub> , <sup>a</sup> (nM)	MV522 IC <sub>50</sub> , <sup>a</sup> (nM)
illudin S	3 ± 1	4 ± 1
dehydroilludin	296 ± 8	310 ± 3
acylfulvene	415 ± 31	350 ± 20
HMAF	73 ± 8	70 ± 8

IC<sub>50</sub> values obtained in 48-h exposure growth inhibition assays. Values are the means ± standard deviation of three to five experiments. HL60, myeloid leukemia cells; MV522, metastatic carcinoma.

**Table 1.** Cytotoxicity of HMAF in Various Lung Tumor Xenografts

drug	MV522		
	dose, (mg/kg)	tumor growth inhibition, (%)	mean tumor shrinkage, (%)
HMAF <sup>a</sup>	7	91	43
CP <sup>b,c</sup>	125	44	0
cisplatin <sup>c</sup>	3	64	0
drug	dose, (mg/kg)	tumor growth inhibition, (%)	cured mice ratio
NCI-H460			
HMAF <sup>a</sup>	7.5	100	7/7
cisplatin <sup>a</sup>	2.5	47	0/7
doxorubicin <sup>c</sup>	7.5	65	0/7
Calu-6			
HMAF <sup>a</sup>	7.5	100	4/7
cisplatin <sup>a</sup>	5	99	0/7
doxorubicin <sup>c</sup>	7.5	80	0/7
etoposide <sup>d</sup>	12.5	0	0
NCI-H69			
HMAF <sup>a</sup>	7.5	90	1/7
irinotecan <sup>d</sup>	60	86	0/6
cisplatin	12	51	0/6
A-427			
HMAF	7.5	85	2/6
LX-1			
HMAF	7.5	22	0/6
	5.0	15	0/7
	2.5	15	0/7

<sup>a</sup>Daily injections for 5 consecutive days. <sup>b</sup>Cyclophosphamide. <sup>c</sup>Drugs administered at their estimated maximum tolerance dose (MTD).

<sup>d</sup>Drugs administered daily for 4 days. <sup>e</sup>Drugs administered daily for 3 days; MV522, human lung adenocarcinoma; NCI-H460, Calu-6 and A-427, human nonsmall lung cancer; NCI-H69 and LX-1, human small cell lung cancer.

together with observed tumor shrinkage in mice, increased life span in mice, and low animal toxicity, in 1999 HMAF entered into human clinical trials in the United States.

**3.3. Acylfulvene Tumor Selectivity**

A unique and an attractive property of AFs is their cytotoxic selectivity profiles. While being significantly less cytotoxic than illudins, AFs induce apoptosis in tumor cells and are cytostatic to normal cells.<sup>21</sup> Thus, in comparison to tumor cell lines, cell lines derived from normal diploid prostate, colon, and other tissues are 3–10-fold less sensitive to HMAF than are the corresponding cancer cell lines (Table 2). Thirty-fold enhanced susceptibility to HMAF is observed for prostate cancer cells (LNCaP-LN3), as compared to normal prostate epithelial cells (PrEC).<sup>21</sup> HT-29 and CoLo 320DM colon cancer cells are also susceptible to HMAF. Even though HMAF cytotoxicity in these cells is relatively similar to that in normal colon cells (NCM 460), normal cells remain viable for a long time while tumor cell viabilities are profoundly decreased.<sup>20,21</sup> In general, these differences may arise from variations in bioactivation, intracellular distribution, or cellular uptake, and there are strong mechanistic data suggesting that preferential bioactivation contributes significantly to cytotoxicity and tumor specificity of AFs.<sup>36,54</sup>

A detailed understanding of the underlying basis of the cytotoxicity, including potencies and specificities, is important for generating improved agents and for understanding

1) revealed that antitumor activity of HMAF exceeds that of cisplatin, doxorubicin, and etoposide.<sup>23</sup> Inhibition rates greater than 58% with no animal deaths were observed for HMAF in four (NCI-H469, Calu-6, NCI-H69, LX-1) out of the five tested lung tumor xenografts, and complete tumor growth inhibition was induced in NCI-H469 and Calu-6 tumors. However, HMAF-induced cytotoxic death was noted at doses above 10 mg/kg during prolonged (10 day) treatment, and one case of death resulted for an LX-1 lung tumor xenograft at a dose of 7.5 mg/kg.<sup>23</sup> Cisplatin was effective in inducing tumor shrinkage in mice with Calu-6 tumors; however, unlike HMAF, treatment did not yield any cases of complete tumor growth inhibition.

HMAF antitumor activity was detected in MX-1 breast tumor, HT-29 colon carcinoma,<sup>86</sup> human gastric tumor (Hs746T, GT3TKB, and HGC-27) xenograft models,<sup>23</sup> and HL60/MRI myeloid leukemia.<sup>89</sup> HMAF also is active in a variety of mdr tumor xenograft models.<sup>90,91</sup> In all cases, HMAF demonstrates dose-dependent tumor shrinkage and tumor regression at the maximum tolerated dose (MTD) of 7 mg/kg. In addition, HMAF is more potent toward gastrointestinal tumors and metastatic prostate cancer than mitomycin, cisplatin, and paclitaxel.<sup>23</sup> Finally, HMAF shows synergistic activity with conventional chemotherapeutics.<sup>24–26,92–95</sup> The response to HMAF is improved when it is combined with irinotecan in pediatric solid tumor xenograft models,<sup>24</sup> with mitoxantrone or docetaxel for human prostate cancer models,<sup>25</sup> with 5-fluorouracil in colon and ovarian tumors,<sup>92</sup> and with platinum-based drugs in colon, breast, and ovarian cancer cells.<sup>26</sup> On the basis of promising tumor xenograft data,

**Table 2.** HMAF-Induced Growth Inhibition, Uptake, and Cell Viability in Tumor and Normal Cell Lines

cell line	growth inhibition GI <sub>50</sub> <sup>a</sup> (μM)	<sup>14</sup> C-HMAF uptake (pmol/1 × 10 <sup>6</sup> cells/2 h)	cell viability (%)
tumor <sup>b</sup>			
LNCaP	0.03 ± 0.01	2578 ± 255	60
LNCaP-Pro5	0.07 ± 0.008	227 ± 60	35
LNCaP-C4-2	0.11 ± 0.02	205 ± 23	20
LNCaP-LN3	0.013 ± 0.007	153 ± 30	24
PC-3	0.26 ± 0.04	97 ± 11	67
CoLo 320DM	0.21 ± 0.13	64 ± 11	ND
HT-29	0.55 ± 0.22	73 ± 15	95
CEM	1.7 ± 0.2	26 ± 5	65
normal <sup>c</sup>			
WI-38	0.37 ± 0.08	150 ± 23	ND
PrEC	0.35 ± 0.04	171 ± 12	93
NCM 460	0.43 ± 0.02	134 ± 18	96
HUVEC	0.19 ± 0.004	498 ± 78	95
RPTEC	0.11 ± 0.01	1014 ± 185	100

<sup>a</sup>GI<sub>50</sub> determined by the standard MTT assay. Values represent means from 2–4 experiments carried out in triplicate. Cell viability measured by trypan blue exclusion after 4 h treatment with HMAF followed by a 17–20 h postincubation period in drug-free medium. Sample to sample variability was 3–5%. <sup>b</sup>Tumor cell lines: LNCaP, LNCaP-Pro5, LNCaP-C4-2, LNCaP-LN3, and PC-3, human prostate carcinoma, Colo320DM; human colon carcinoma, HT-29; human colon adenocarcinoma, CEM, human leukemia. <sup>c</sup>Normal cell lines: WI-38, diploid human fibroblast; PrEC, prostate epithelia; NCM460, colon mucosa; HUVEC, umbilical vein endothelia; RPTEC, renal proximal tubule epithelia.

## 4. SYNTHETIC CHEMISTRY OF ILLUDINS AND ACYLFULVENES

445

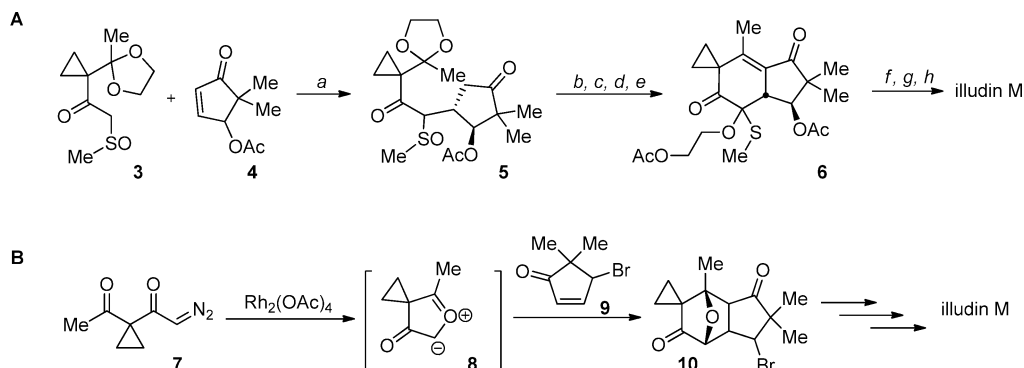
Illudins and AFs have been synthetic chemistry targets for three decades. The first general approach to illudins and AFs was based on constructing the six-membered ring of the tricyclic illudane skeleton via a dipolar cycloaddition reaction. The first racemic synthesis of illudin M was then modified to produce an enantiomerically enriched natural product and was further tuned for construction of AFs. More recent syntheses are asymmetric and amenable to structural modifications of illudins and AFs.<sup>62</sup>

### 4.1. Cycloaddition Reaction in Illudin Synthesis

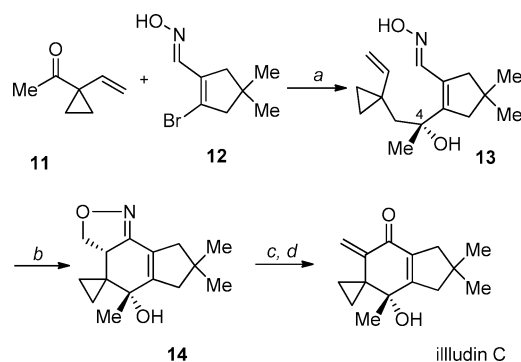
In the first racemic synthesis of illudin M, reported in 1968 by Matsumoto and co-workers,<sup>30</sup> the illudane skeleton was assembled beginning from a substituted cyclopentenone (Scheme 3A) via conjugate addition and condensation. As depicted in Scheme 3, base-catalyzed addition of β-ketosulf-oxide **3** to the ketone **4** yields conjugate addition product **5**, poised for assembly of the illudin tricyclic skeleton. The subsequent series of transformations included a Pummerer rearrangement, base-catalyzed condensation, and acylation yielding tricyclic ketone **6**. Fused functionalized indenone **6** was then transformed in three steps to illudin M. Thus, the first synthetic illudin M was obtained after eight steps, not including preparation of **3** and **4**.

An alternative six-step synthetic route to illudin M reported in 1994 by Kinder and co-workers<sup>31</sup> involved a rhodium(II)-catalyzed 1,3-dipolar cycloaddition for construction of the six-membered ring (Scheme 3B). In this synthetic sequence, cycloaddition of cyclopentenone **9** with ylide **8** derived in situ from diazo ketone **7** gives rise to tetracycle **10**, which was then converted to illudin M.<sup>31</sup> Later, in 1997, a rhodium-catalyzed cycloaddition reaction was also utilized by Padwa and co-workers<sup>96–98</sup> to access the illudane skeleton of ptaquiloside, a closely related and highly toxic natural product isolated from bracken fern.

Total synthesis of illudin C (Scheme 4), involving an alternative two-step cycloaddition, was reported by Aungst in 2001.<sup>99</sup> It is amenable for preparing other illudin analogs such as illudin C2, illudin C3, and illudinic acid.<sup>99</sup> Following this scheme, the illudane skeleton is formed via a high-yielding addition of cyclopropyl ketone **11** to alkenyl nitrile oxide **12**. The desired oxime **13** is then converted, with chloramine-T, into a single diastereomer (99%) of isoxazoline **14**. The

**Scheme 3.** Synthesis of Illudin M (A)<sup>a</sup> via Pummerer Rearrangement and (B) via 1,3-Dipolar Cycloaddition

<sup>a</sup>Reagents and conditions: (a) *t*-BuONa, (b) Pummerer rearrangement, (c) EtOH reflux, (d) *t*-BuONa, (e) AcCl, (f) MeMgBr, (g) NaBH<sub>4</sub>, (h) HgCl<sub>2</sub>.

Scheme 4. Synthesis of Illudin C<sup>a</sup>

<sup>a</sup>Reagents and conditions: (a) *t*-BuLi, THF,  $-78^{\circ}\text{C}$ , 68%; (b) chloramine-T; (c) Ra-Ni,  $\text{H}_2$ ,  $\text{B}(\text{OH})_3$ ,  $\text{MeOH}/\text{H}_2\text{O}$ ; (d)  $\text{MeSCl}$ ,  $\text{CH}_2\text{Cl}_2$ ,  $-78^{\circ}\text{C}$ ; DBU, room temperature **73%**

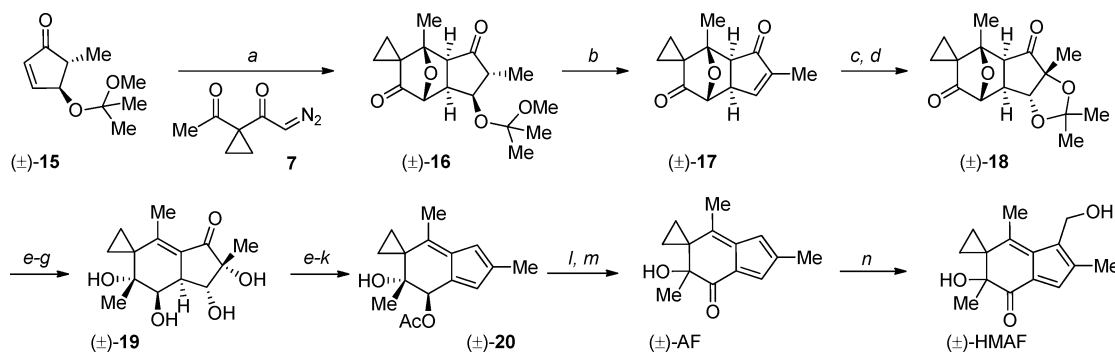
after 14 steps from 4-hydroxy-5-methyl-2-cyclopenten-1-one and 1-acetyl-1-(diazoacetyl)cyclopropane as starting materials.<sup>33</sup>

Although these racemic syntheses opened the way to synthetic AFs, they were not suitable for advancing an understanding of the influence that stereochemistry may have on AF activity. Thus, McMorris et al.,<sup>34</sup> following their own prior route, synthesized optically active AF. The synthetic approach involves enantiomerically pure 5-chloro-5-methyl-5-cyclopentenones, which controls the stereoselectivity of the cycloaddition with ylide 7.<sup>34</sup> The desired major diastereomer of the tetracycle 16 was obtained in 84% yield and further elaborated to enantiomerically pure (–)-AF. Overall, (–)-AF was prepared in 3.1% for 10 linear steps.

The cycloaddition-based approaches for synthesis of illudins and AFs follow relatively facile sequences but require complex and/or enantiomerically pure starting materials. Therefore, synthetic strategies amenable to preparing various illudin and AF structural analogs for drug development and mechanistic studies are necessary, and recent relevant solutions are described in the next section.

## 4.2. Allenic Pauson–Khand Chemistry in Acylfulvene Synthesis

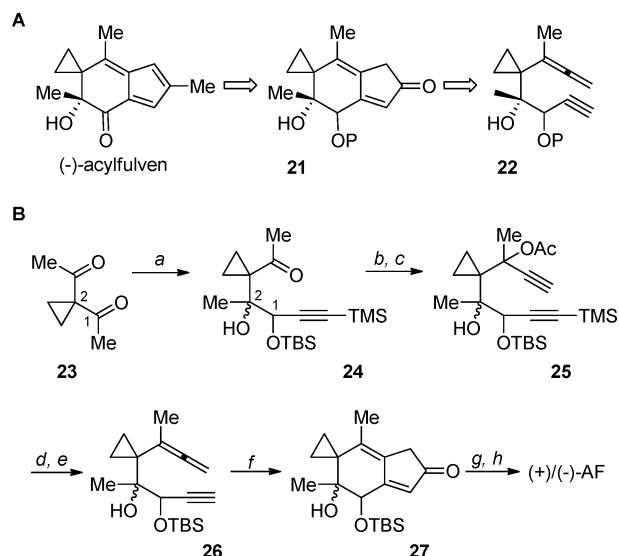
A conceptually new strategy for preparing AFs was introduced by Brummond and co-workers<sup>35,100,101</sup> in 2000 and was an excellent application of the allenic Pauson–Khand cycloaddition pioneered by the same lab. Addressing this synthesis from a retrosynthetic perspective (Scheme 6A), the fused bicyclic core of AF precursor 21 would arise from cycloaddition to the least substituted double bond of allene 22, which would be derived ultimately from 1,1-diacetylcyclopropane 23. Subsequently, base-catalyzed addition of 3-trimethylsilyl-3-propyl-1-ol to 23 yields the C2 diastereomers of 24, which after separation are carried further to enantiomeric AFs (Scheme 6B). Addition of ethynylmagnesium bromide to 24 in the presence of  $\text{CeCl}_3$  was followed by acylation of the propargyl alcohol to yield 25 as a precursor to allene 26.<sup>102</sup> Formation of allene moiety was achieved in the presence of copper hydride, and after removing the silyl protecting group, allene 26 was cyclized under conditions corresponding with the  $\text{Mo}(\text{Co})_6$ -catalyzed allenic Pauson–Khand reaction.<sup>103</sup> The exclusive product was 4-alkylidene cyclopentenone 27. Further treatment of the ketone 27 with  $\text{MeLi}$  in the presence of  $\text{CeCl}_3$

Scheme 5. Racemic Synthesis of AF and HMAF via 1,3-Dipolar Cycloaddition Reaction<sup>a</sup>

<sup>a</sup>Reagents and conditions: (a)  $\text{Rh}_2(\text{OAc})_4$ ; (b)  $\text{KOH}-\text{MeOH}$ , 95%; (c)  $\text{OsO}_4$ , NMO, THF,  $\text{H}_2\text{O}$ ; (d) dimethoxypropane, *p*-TsOH, room temperature, 2 h, 87% from (±)-15; (e)  $\text{MeMgCl}$ , THF,  $-78^{\circ}\text{C}$ ; (f)  $\text{KOH}-\text{MeOH}$ ,  $80^{\circ}\text{C}$ , 75% from (±)-18; (g) Dowex resin, 95%; (h)  $\text{CH}(\text{OMe})_3$ , *p*-TsOH, 99%; (i)  $\text{Ac}_2\text{O}$ , reflux, 1.5 h, 64%; (k)  $\text{CeCl}_3 \cdot 7\text{H}_2\text{O}$ ,  $\text{NaBH}_4$ ,  $\text{MeOH}-\text{THF}$ ,  $0^{\circ}\text{C} \rightarrow \text{room temperature}$ , 84%; (l) LAH,  $\text{Et}_2\text{O}$ ; (m) DMP,  $\text{CH}_2\text{Cl}_2$ , 71% for two steps; (n)  $(\text{CH}_2\text{O})_n \cdot \text{H}_2\text{SO}_4$ ,  $\text{H}_2\text{O}$ , acetone.



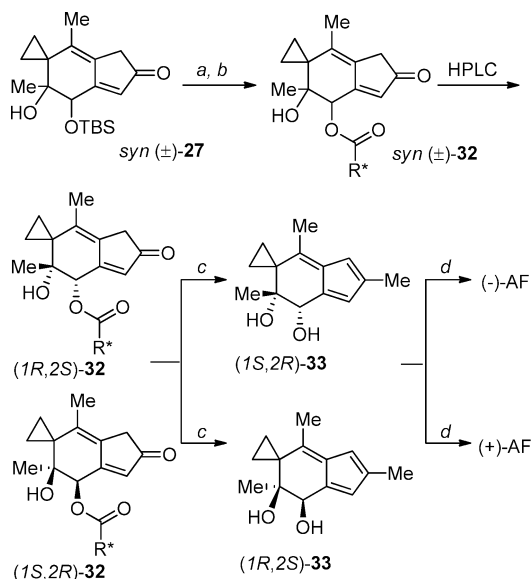
### Scheme 6. Retrosynthetic Perspective (A) and Synthesis (B) of AF via Allenic Pauson–Khand Cycloaddition<sup>a</sup>



<sup>a</sup>Reagents and conditions: (a)  $\text{TMS}\equiv\text{CH}_2\text{OTBS}$ ,  $t\text{-BuLi}$ ,  $-78\text{ }^\circ\text{C} \rightarrow 40\text{ }^\circ\text{C}$ , 57%; (b) ethynylmagnesium bromide,  $\text{CeCl}_3$ , 97%; (c)  $\text{Ac}_2\text{O}$ , DMAP,  $\text{Et}_3\text{N}$ , 98%; (d)  $[\text{CuH}(\text{PPh}_3)]_6$ , 54%; (e)  $\text{K}_2\text{CO}_3$ , MeOH,  $\text{H}_2\text{O}$ , 95%; (f)  $\text{Mg}(\text{CO})_6$ , DMSO,  $\text{PhCH}_3$ ,  $110\text{ }^\circ\text{C}$ , 30 min; (g)  $\text{CH}_3\text{Li}$ , 96%; (h)  $n\text{BuNF}$ , 97%; (i) DMP, 78%.

27 (Scheme 8) as a complementary approach to the dihydroxylation chemistry. Thus,  $(\pm)\text{-27}$  was deprotected and

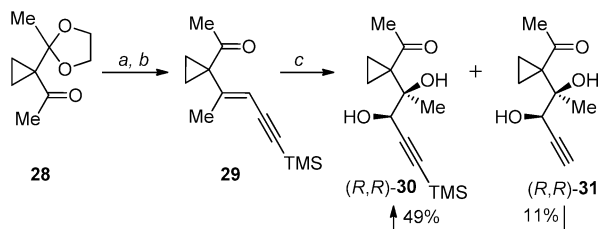
### Scheme 8. Chiral Resolution of AFs<sup>a</sup>



<sup>a</sup>Reagents and conditions: (a) TBAF, THF, 95%; (b) chiral acid, HBTU, DMAP, THF; (c)  $\text{CeCl}_3$ , MeLi, THF, 90%; (d) IBX, 88%.

yielded tertiary alcohol that underwent spontaneous dehydration to fulvene upon acidic workup. Finally, TBS-group cleavage and oxidation of the unmasked alcohol to the ketone completed the eight-step synthesis of AF in 10% overall yield.<sup>35</sup> Shortly following publication of the allenic Pauson–Khand approach to racemic AFs, Brummond and co-workers<sup>35</sup> communicated an asymmetric strategy for obtaining either enantiomer of AF via  $(R,R)\text{-30}$  (Scheme 7), an enantiomeri-

### Scheme 7. Asymmetric Strategy Toward AFs<sup>a</sup>



<sup>a</sup>Reagents and conditions: (a)  $\text{TMS}\equiv\text{CH}_2\text{P}(\text{O})(\text{OEt})_2$ ,  $n\text{-BuLi}$ , 64%,  $E/Z$ : 40:1; (b) PTSA, acetone,  $\text{H}_2\text{O}$ , 95%; (c) SAD.

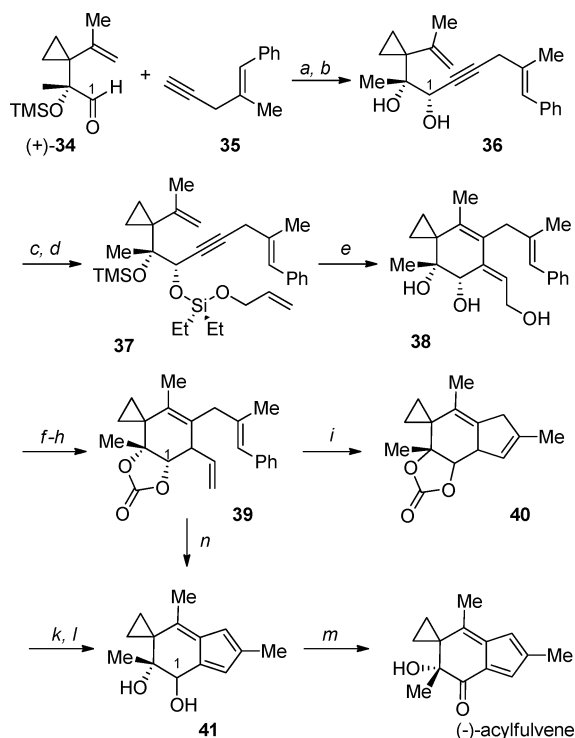
cally pure version of the cyclization precursor 24 (Scheme 6). The  $E$ -eneyne 29 was prepared from 28 and diethyl 3-(trimethylsilyl)prop-2-ynylphosphonate in high yield and degree of stereoselectivity. Subsequent dihydroxylation under standard Sharpless asymmetric dihydroxylation conditions with  $(\text{DHQD})_2\text{Pyr}$  as ligand produced the  $(R,R)$ -diol 30 in 49% yield and some of the silyl-deprotected diol 31.<sup>35</sup> Diol 30 represents a key intermediate in the formal synthesis of enantiomerically pure AF. The reliability of this strategy for total synthesis of enantiomerically pure material was confirmed by us in subsequent mechanistically centered studies.<sup>36</sup> The completed synthesis intersected Brummond's formal total synthesis and also involved chiral resolution of the cyclized intermediate

the secondary alcohol was derivatized as a series of separable diastereomeric esters 32. Methylation and removal of the chiral auxiliary was accomplished by treating with MeLi/ $\text{CeCl}_3$ , resulting in enantiomeric fulvenes 33 (Scheme 8). IBX-mediated oxidation completed the synthesis of  $(-)$ - and  $(+)\text{-AF}$  after 10 consecutive steps from diketone 23.<sup>36</sup>

### 4.3. Asymmetric Metathesis for Synthesizing Acylfulvenes

Most recently, Movassaghi and co-workers<sup>37</sup> introduced a new strategy for preparing AFs that involves an enyne ring-closing metathesis (EYRCM) reaction as a key transformation for constructing the AF six-membered ring (Scheme 9). The EYRCM precursor 36 was prepared starting with addition of lithiated 35 to  $\alpha$ -alkoxy aldehyde 34,<sup>104</sup> yielding a mixture of C1-diastereomers ( $1S/1R \approx 6:1$ ), favoring the Felkin–Ahn mode of carbonyl addition. Both diastereomers were carried forward because the C1 hydroxyl is eventually oxidized. Subsequent ring-closing metathesis of silylated 37 was performed for both diastereomers and after rearrangement of the dihydrodioxasilene intermediate yielded triol 38. The allylic transposition of 38 with the acetone hydrazone of 2-nitrobenzene-sulfonylhydrazide yielded 39. The second RCM reaction yielded 40 with the desired diastereomer as a major product ( $6S/6R$ , 7.6:1) and completed the illudane skeleton. Subsequent dehydrogenation of the major diastereomer of 40 with DDQ followed by basic hydrolysis of the cyclic carbonate yielded fulvene 41 that, after oxidation of the C1 hydroxyl, completed the synthesis of  $(-)\text{-AF}$ . Further optimization of the synthesis showed that replacing DDQ with  $p$ -chloranil allows for direct conversion of 39 to fulvene 41.<sup>38</sup> As a result, a tandem transformation including the ring-closing metathesis (RCM), dehydrogenation, and hydrolysis was employed for one-pot conversion of 39 to 41 without any intermediates in 30% yield. Overall, AF was prepared stereoselectively in 5.5% yield after 10 linear steps.

**Scheme 9. Enyne Ring-Closing Metathesis in the Construction of (–)-AF<sup>a</sup>**



<sup>a</sup>Reagents and conditions: (a) LHMDs, THF, –78 °C → 40 °C; (b) TBAF, AcOH, 75%; (c) (Et)<sub>2</sub>Si(Cl)OCH<sub>2</sub>CH=CH<sub>2</sub>, 2,6-lutidine, CH<sub>2</sub>Cl<sub>2</sub>; (d) TMSOTf, –78 °C, 83%; (e) G2 (15 mol %), 90 °C, then TBAF, AcOH, THF, 23 °C; (f) TBSOTf, 2,6-lutidine, CH<sub>2</sub>Cl<sub>2</sub>, –78 °C; (g) triphosgene; TBAF; (h) 2-NO<sub>2</sub>C<sub>6</sub>H<sub>4</sub>SO<sub>2</sub>NHN=CMe<sub>2</sub>, DEAD, Ph<sub>3</sub>P, THF, 0 °C → 23 °C; TFE, H<sub>2</sub>O, 71%; (i) G2, PhH, 68 °C, NaH, 82%, (6S:6R, 7.6:1); (k) DDQ, PhH, 93%; (l) aqueous NaOH, dioxane, 99%; (m) IBX, DMSO, 83%; (n) G2 (15 mol %), PhH, 80 °C, 50 min; NaOMe, MeOH, 23 °C; DDQ, MeCN, (37 → AF, 30%) or chloranil to isolate 41 (70%).

## 5. METABOLISM AND CHEMICAL REACTIVITY OF ACYLFULVENES AND ILLUDINS

633

Especially for chemically reactive drug candidates, understanding metabolism and cellular distribution is important for improving drug safety and effectiveness. In addition, chemical reactivity can provide insight into potential cellular targets and contribute to development of potential chemotherapeutics with improved potency. The following section covers AF cellular distribution and metabolism. It also summarizes the chemical reactivity of AFs, determined in a series of structure–activity relationship (SAR) studies carried out on the illudane skeleton.

### 5.1. Cellular Distribution and Cytosolic Metabolism

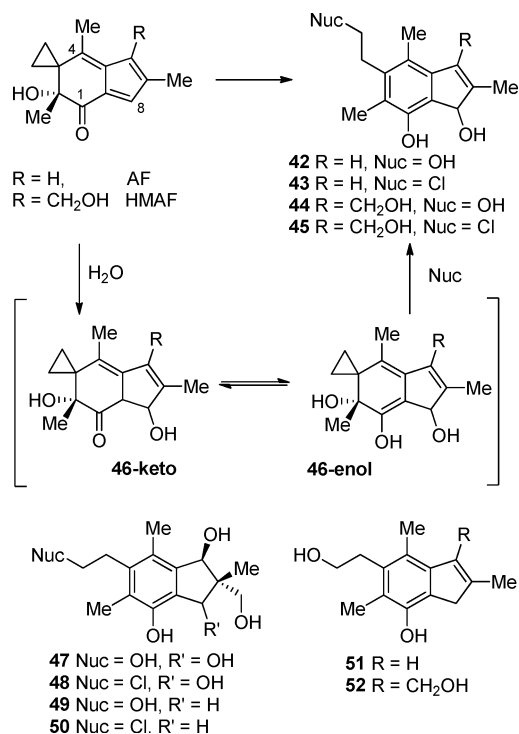
Cellular distribution of HMAF and illudin S in leukemic lymphoid CEM cells was determined by Woynarowski and co-workers in studies using the corresponding <sup>14</sup>C-labeled analogs. The nuclear fraction, containing 50% of HMAF, is identified as a major drug accumulation site.<sup>47</sup> Thirty seven percent of the drug accumulates in the cytosolic fraction and 10% in the membrane, including both outer cell and intracellular membranes.<sup>47</sup> The distribution of covalently bound HMAF after a 4 h incubation is 60% protein, 30% DNA, and 10% RNA adducts.<sup>47</sup> Illudin S has relatively higher (60%) nuclear and lower (27%) cytosolic fractions, with 11% membrane bound. In contrast, the nuclear fraction of cisplatin in rat kidney represents only 14% of total drug uptake, and the largest portion (78%) accumulates in the cytosol.<sup>105</sup> On the basis of these observations, effective nuclear incorporation of illudins and AFs may be a contributing factor to enhanced cytotoxicity as compared to cisplatin in tumor cells. Moreover, relatively low AF accumulation in the cytosol may contribute to high AF activity in cisplatin-resistant tumor cells,<sup>26</sup> where resistance correlates with more GSH-mediated inactivation and drug efflux.<sup>106,107</sup>

A major biotransformation route for AFs involves generation of aromatized metabolites typified by 42 and 45 (Scheme 10).<sup>108,109</sup> These have been isolated from the liver of rats treated with AF and HMAF, respectively. When tested themselves, these metabolites do not retain the toxic properties of their precursors. The chemical transformation that accounts for metabolite generation is proposed to proceed through hydration of the enone followed by cyclopropyl ring opening, indicating the susceptibility of these two sites toward nucleophiles (Scheme 10). Enone hydrolysis gives rise to an unstable and highly reactive intermediate 46, existing in tautomeric keto and enol forms. In this proposed intermediate, the spiro cyclopropyl ring is activated toward nucleophilic substitution, and if the nucleophile is water, the observed nontoxic metabolites 42 and 44 are generated.<sup>108,109</sup>

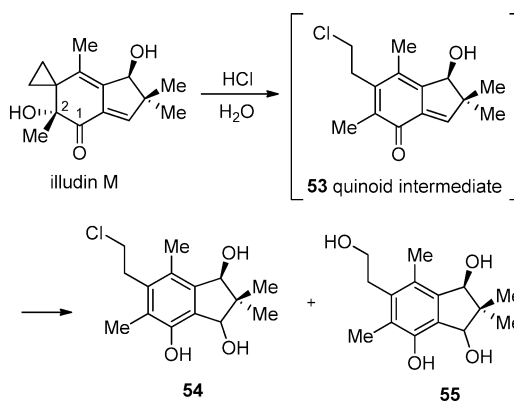
Biotransformation of illudin S by rat liver cytosol (RLC) also yields the analogous hydrated metabolite 47 (Scheme 10).<sup>42–45</sup> In addition to hydrated metabolites, the aromatized chlorinated metabolites of HMAF and illudin S (43, 45, and 48) resulting from the chlorine-mediated cyclopropyl opening were also observed in RLC.<sup>43–45</sup> Among other types of metabolites isolated from the liver cytosol of drug-treated rats are structures 49–52, formed from hydride addition to the enone. In this transformation, as opposed to the hydration pathway, the reactive intermediate is generated from reduction, and hydrolysis or chloride addition yields metabolites 49, 51, and 52 or 50, respectively.<sup>43</sup> Such reduced metabolites also were obtained through chemical reduction of illudin S, AF, or HMAF with zinc dust in the presence of dilute acid.<sup>110</sup>

Each of the synthetic approaches to AFs has relative strengths and appears to be amenable to preparation of further analogs. The allenic Pauson–Khand approach involves relatively simple starting materials, and the enantioselective dihydroxylation chemistry allows access to either AF enantiomer in only eight steps. Two carbonyl additions employed in the synthesis offer routes for further structural modifications of AFs. Use of substituted alkynes for constructing 25 and 26 offers the possibility for C8 and/or C6 functionalization, while the final Grignard addition with 27 offers the possibility of C7 modification. Similarly, the EYRCM approach allows access to C6- and C7-modified AFs after construction of suitably substituted analogs of 35, and it is an elegant illustration of RCM chemistry for synthesis of medicinally useful structures. Although the reported strategies for synthesizing illudins and AFs provide potential access to C6-, C8-, and C7-modified analogs, these methods do not provide easy access to C2- or C4-modified analogs. Although C2- and C4-modified AFs can be accessible through these routes with suitably substituted starting diketone, methodologies that would allow desired modification in the later stage of the synthesis are yet to be developed.

Scheme 10. AF in Vivo Metabolites and Proposed Route of Formation

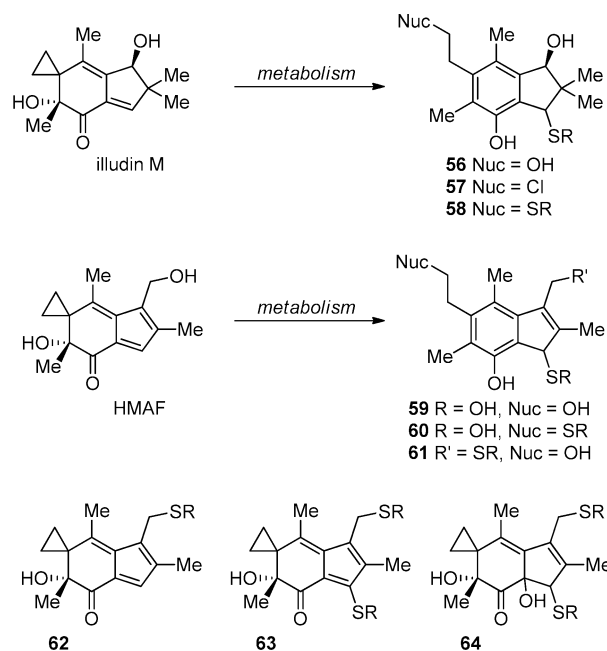


Scheme 11. Chemical Transformation of Illudin via Quinoid Intermediate



illudin to metabolites **54** and **55**. The quinoid intermediate, detected by NMR in illudin–HCl solutions, supports the fact that illudin can react with nucleophiles through additional pathways that may promote high and nonselective toxicity.<sup>46</sup>

Illudins and AFs react with free thiols, and various studies have aimed to elucidate how this chemical reactivity may affect cytotoxicity. The stereoisomeric thiolate adducts **56–60** (Figure 3) result from conjugate addition of a thiol (RSH) to



<sup>a</sup>R = alkyl, aryl, cysteine, GSH, TrxR, Trx

Figure 3. Illudin M and HMAF metabolites resulting from reactions with thiols; R = alkyl, aryl, cysteine, GSH, TrxR, **trx**.

the enone, followed by opening of the cyclopropane ring by water or chloride as a nucleophile.<sup>45,46</sup> In reactions with small thiols, illudin M yields mainly the phenolic adducts **56** and **57** (Figure 3). A small amount of **58**, a product of addition of two molecules of thiol to one of illudin M, is also generated. Under these conditions, HMAF yields analogous thiol conjugates **59** and **60** and the double-addition metabolite **61** that originates from substitution of the allylic alcohol by RSH. Similar adducts are formed in reaction of HMAF with *p*-thiocresol, benzyl

Aromatic metabolites **47–50** account for only 30% of the illudin S that is transformed by RLC,<sup>44</sup> and the remaining portion is incorporated among various cellular targets or metabolized through alternative pathways potentially contributing to the cellular activity of the drug. Urine and plasma samples obtained from illudin S-treated rats contained various GSH and glucuronide adducts that result from conjugate addition to the  $\alpha,\beta$ -unsaturated ketone and suggest a possible detoxification pathway.<sup>44,49,111</sup> Recent studies of illudins have also demonstrated that the efficiency of their interaction with GSH inversely correlates with cytotoxicity.<sup>45,46</sup>

## 5.2. Chemical Metabolism and Reactivity toward Thiols

The chemical reactivity of illudins and AFs provides additional information about potential transformations that could take place in the cellular environment. Illudin reactivity depends on the type of nucleophile encountered during the reaction and may not require enone activation. For instance, in dilute hydrochloric acid (pH 0) at room temperature, illudin M is converted to a mixture of **54** and **55** (Scheme 11) with a half-life of 147 min. At the same pH but in dilute sulfuric acid the reaction proceeds significantly slower ( $t_{1/2}$  = 1073 min) and metabolite **55** is formed.<sup>46</sup> The structural similarities between the chemically and the biologically generated metabolites suggest that illudin is transformed similarly to AF by a mechanism that involves enone-mediated activation of the cyclopropyl opening. However, a novel reactive quinoid intermediate **53**, detected in the reaction mixture (Scheme 11), suggests that cyclopropyl ring opening may occur independently of conjugate addition. This observation is in agreement with the ability of cyclopropyl rings to stabilize  $\alpha$ -cations.<sup>112</sup> Such an intermediate could be generated upon protonation of the C2 tertiary hydroxyl ( $\alpha$  to the ring) and loss of water. Subsequent conjugate addition of a nucleophile to the enone moiety of **53** could complete the transformation of



mercaptan, and ethylene glycol dimercaptoacetate, revealing the electrophilic nature of the hydroxymethylene and suggesting its possible reactivity in the cellular environment.<sup>113</sup> Unusual products **62**–**64** that have an intact cyclopropyl ring are also formed in reactions of HMAF with small thiols and are postulated to involve radical intermediates.<sup>113</sup> While illudin M and HMAF yield similar types of products, illudin M reacts much faster than HMAF, which reacts faster than AF. In radiolabeling studies, illudin S was shown to react with cysteine and cysteine-containing peptides such as GSH as well as the cysteine-rich proteins thioredoxin and Trx.<sup>47–49</sup>

### 5.3. Role of Glutathione in Illudin vs Acylfulvene Differential Cytotoxicity

Chemical reactivity profiles of illudins and AFs with thiols suggest alkylation of GSH as a possible cellular process. Indeed, illudin M effectively reacts with isolated GSH at pH 6 and yields conjugate-addition product **56** (Figure 3, SR = GSH).<sup>48</sup> Analogous adducts are formed with illudin S. This propensity for illudin–GSH reactivity supports the hypothesized GSH-mediated detoxification pathway of illudins and is completely consistent with the observed inverse relationship between cellular levels of GSH and illudin cytotoxicity. Thus, the cytotoxic activity of illudin S decreased in the leukemia HL-60 cells that overexpressed GSH and increased in the cells with GSH inhibition.<sup>48</sup>

In contrast to illudin S, reaction of HMAF with GSH yields only a trace amount of the conjugate-addition product **59** (Figure 3, SR = GSH).<sup>53</sup> This observation of low reactivity is consistent with further observation that modulating intracellular GSH levels does not significantly impact susceptibility of tumor cells to HMAF.<sup>53</sup> While GSH is not a critical cellular target, the differential reactivity of illudin M and HMAF with intracellular GSH may contribute to the differential response observed between various tumor cell lines. It is possible that the high activity of HMAF in drug-resistant tumor cells may be associated with its low reactivity toward GSH. However, to our knowledge, there is no data available for direct correlation of GSH levels in various tumor cells with AF cytotoxicity.

## 6. ACYLFULVENE-INDUCED INHIBITION–ALKYLATION OF REDOX-REGULATING ENZYMES

Cellular redox control is important in regulating cell viability, and it has been hypothesized that selective alkylation-mediated inhibition of certain thiol-containing enzymes may contribute to the cytotoxicity profiles of AFs vs illudins by disrupting redox homeostasis. Recent data suggest that AFs do inhibit some cytosolic redox-regulating thiol-containing proteins such as glutathione reductase, thioredoxin reductase, and thioredoxin. Furthermore, while illudin S is more reactive to thiol-containing small molecules, it is a worse inhibitor of these enzymes.<sup>55,56,114</sup> These observations suggest another distinguishing property that may contribute to differences in cytotoxic selectivity of these two structurally closely related types of compounds. In this section, we summarize data addressing the interactions of AFs with specific redox-regulating enzymes and how these interactions may influence cytotoxicity.

### 6.1. Acylfulvenes as Glutathione Reductase Inhibitors

Glutathione reductase (GR), a dimeric FAD-containing protein, contains a redox-active disulfide at its active site. In the presence of NADPH, GR-catalyzed reduction of oxidized glutathione (GSSG) to GSH maintains a high intracellular

GSH:GSSG ratio as a defense against oxidative stress. In the presence of NADPH, HMAF and AF inhibit GR in a time- and concentration-dependent manner such that 50% inhibition was observed at 216  $\mu\text{M}$  for HMAF and 871  $\mu\text{M}$  for AF.<sup>55</sup> Illudin S, however, does not influence enzyme activity even at elevated (2 mM) concentration. The HMAF–GR interaction exhibits irreversible inhibition characteristics, while AF is a reversible GR inhibitor. Interaction of HMAF with GR results in covalent modification of GR active site cysteine residues by two molecules of HMAF, yielding adducts typified as **59** (SR = GR, Figure 3). No adducts were observed, however, in AF-treated enzyme samples, consistent with the reversible nature of AF-mediated GR inhibition.<sup>55</sup>

In a competitive inhibition study involving GR in the presence of its natural substrate GSSG, GSSG was found to diminish the HMAF inhibitory effect.<sup>55</sup> Data from this study suggest that HMAF binds the active site of GR and other possible sites but that AF binds an allosteric GR site. The presence of alternative binding sites was further suggested by comparing reactivity profiles of reduced and nonreduced GR. Whereby the interaction of GR with other alkylating agents such as the nitrogen mustard carmustine requires prereduction of the active site, disulfide inhibition by AF or HMAF is only partially abrogated. Finally, AF induces conformational changes in GR, detectable by changes in intrinsic protein fluorescence. Micromolar AFs significantly quench GR intrinsic fluorescence regardless of the presence or absence of GSSG and NADPH. Carmustine, however, does not affect GR fluorescence at micromolar concentration and quenches 50% GR fluorescence at 1 mM drug concentration. These data suggest that the interactions between GR and AFs are more extensive (i.e., involve physical interactions that may manifest in fluorescence change) than for carmustine, which has been reported to react with one cysteine residue at the GR active site.<sup>55</sup>

### 6.2. Acylfulvenes as Thioredoxin and Thioredoxin Reductase Inhibitors

Like GR, the critical thiol- and selenol-based antioxidant enzymes thioredoxin (Trx) and thioredoxin reductase (TrxR) interact with illudins, AF, and HMAF to varying extents. HMAF covalently modifies Trx and TrxR, and the extent of binding is roughly proportional to the number of Cys residues in each enzyme.<sup>46</sup> On the basis of MS data obtained for AF- and HMAF–TrxR adducts, HMAF appears to be an irreversible inhibitor of TrxR ( $\text{IC}_{50} = 0.38 \mu\text{M}$ ), while AF is a reversible inhibitor ( $\text{IC}_{50} = 7.26 \mu\text{M}$ ).<sup>47,56</sup> In this series, illudin S is the least effective in inhibiting TrxR ( $\text{IC}_{50} = 257 \mu\text{M}$ ).<sup>55</sup> AF-induced chemical modification of TrxR is pH dependent, and due to  $\text{pK}_a$  differences of active site cysteine and selenocysteine residues (Cys 497 ( $\text{pK}_a$  8.3) and Sec 498 ( $\text{pK}_a$  5.2)) of TrxR, only the free selenol of selenocysteine is modified at pH 6.5, and both residues are modified at pH 8.5. The covalent adducts isolated after digestion of the modified enzyme were identified as conjugates typified as **59** with SR being a selenocysteine or cysteine of TrxR.<sup>56</sup> Unlike TrxR, the activity of the related selenoenzyme glutathioneperoxidase was not reduced by treatment with AF or HMAF. These data suggest that the high susceptibility of TrxR is not solely dictated by the presence of a highly reactive Sec but may also be related to the structure of the enzyme.<sup>56</sup>

For Trx, a cellular protein substrate of TrxR, AFs have been associated with a dose-dependent decrease in enzyme activity, for the isolated enzyme, and decrease in cellular protein levels, **61**



in drug-treated cancer cells (HeLa or MCF7). Analogous to reactivity patterns observed for TrxR and GR, HMAF or AF were micromolar inhibitors while illudin S did not inactivate the activity of the enzyme even at millimolar levels. Inactivation mediated by AFs was also associated with covalent modification of the enzyme, as indicated by mass spectrometry. It appears that AF monoalkylates and HMAF bisalkylates Trx and inactivates the enzyme.<sup>114</sup> The HMAF adducts appear to arise from substitution of the primary C10 hydroxyl by the thiol of the cysteine residues (conjugate **62**, SR = Trx, Figure 3) in a reaction hypothesized to be catalyzed by an aspartate residue in the enzyme active site. In cells, both illudin and AFs reduces Trx levels. Furthermore, like cisplatin, illudin S and AFs stimulate Trx nuclear accumulation,<sup>56</sup> and further studies may define the mechanisms for translocation and impact on gene transcription and toxic responses.<sup>114</sup>

These data suggest that differences in AF versus illudin S cytotoxicity may be influenced by relative propensities for interaction with redox-regulating enzymes. Consistent with the observations summarized above, HMAF appears to sensitize drug-resistant cells that show diminished response to cisplatin and mitomycin C, possibly due to elevated Trx levels.<sup>115</sup> Protein–AF interactions therefore may contribute to synergistic behavior of HMAF observed with cisplatin and mitomycin C in cancer cells and a cancer xenograft model.<sup>92,116</sup> The surprisingly low relative reactivity of illudin S vs AFs toward activated thiol or selenols of redox-regulating enzymes counters patterns of reactivity toward GSH and other small thiols. It suggests that, contrary to assumptions made prior to the availability of these data, reactions with thiol-containing enzymes does not explain the generally high toxicity of illudin. Rather, the unexpected reactivity of AFs toward certain redox-regulating enzymes, especially Trx, suggests that these interactions actually may contribute in a selective manner to AF cytotoxicity.<sup>114</sup> As the importance of redox-regulating enzymes in toxicity continues to be examined, there is an anticipated synergy between the availability of small molecules, like acylfulvenes, for probing interactions with redox-regulating enzymes, and the elucidation of the role of such enzymes in dictating cellular responses to chemical cytotoxins.<sup>117–119</sup>

## 7. STRUCTURE–ACTIVITY RELATIONSHIPS OF ACYLFULVENES AND ILLUDINS

### 7.1. Role of the Enone and Cyclopropyl Ring in Acylfulvene Cytotoxicity

Changes to the enone moiety in AF, involving masking the enone or substituting the enone, have been made with the goal of circumventing thiol-mediated drug deactivation by diminishing the reactivities of illudins and AFs toward thiols. These studies, undertaken by Arnone and co-workers,<sup>39</sup> resulted in the novel analogs **65–67** (Figure 4). Cytotoxicity tests in A2789 human ovarian cancer cells, however, revealed that removal or substitution of the enone diminishes activity compared to the original compounds.<sup>39</sup> For instance, masking the enone double bond with a cyclopropyl ring (**65**, Figure 4) results in a 10-fold loss of cytotoxicity. Methylating the enone in AF and illudin M (analog **66** and **67**) also yields a drastic drop in cytotoxicity. Additionally, the *cis*/*trans* geometry of the enone appears to play a critical role in illudin activity. Thus, *trans*-enone-containing illudin G is 2000-fold less active than *cis*-enone-containing illudin G.<sup>39</sup> These data further support the important role of the enone in AF biotransformation and

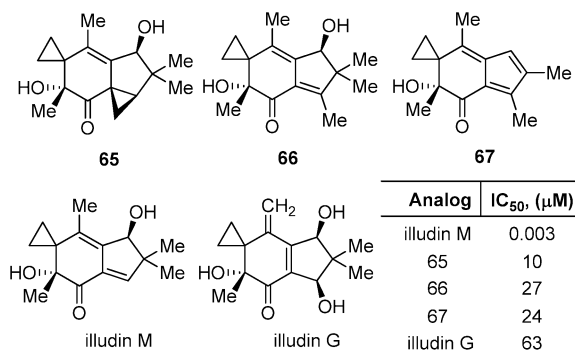


**Figure 4.** Illudin and AF analogs and cytotoxicity data in A2789 human ovarian cancer cells.

cytotoxicity. However, the fact that analogs **65–67** are still significantly cytotoxic suggests that activation of these analogs may proceed via another, as yet unidentified, pathway.

The role of the enone–cyclopropyl ring motif in AF antitumor activity was demonstrated in SAR studies of truncated bicyclic illudin analogs<sup>40</sup> that were accessed via Rh-mediated cycloaddition by Kinder and co-workers.<sup>31</sup> The truncated bicyclic core containing analogs **68** were evaluated in melanoma (A375), lung (A549), breast (MB-231), and colon (SW480) tumor cell lines, exhibits low micromolar cytotoxicity, and is highly sensitive to enone substitution (Table 3).<sup>40</sup> Thus,

**Table 3.** Truncated Illudin Analogs and SAR Data<sup>a</sup>

analog	IC <sub>50</sub> <sup>a</sup> (μM)			
	A375	A549	MB-231	SW480
<b>68a</b>	1.0	0.2	0.3	0.03
<b>68b</b>	0.004	0.15	0.11	0.12
<b>68c</b>	0.018	0.002	0.028	0.18
<b>68d</b>	0.13	0.11	0.3	0.03
<b>68e</b>	>10	1.5	4.0	2.5
<b>68f</b>	>10	>10	>10	4.0

<sup>a</sup>IC<sub>50</sub> determined by standard MTT assay. A375, human melanoma; A549, human lung carcinoma; MB-231, human breast carcinoma; SW480, human colon carcinoma.

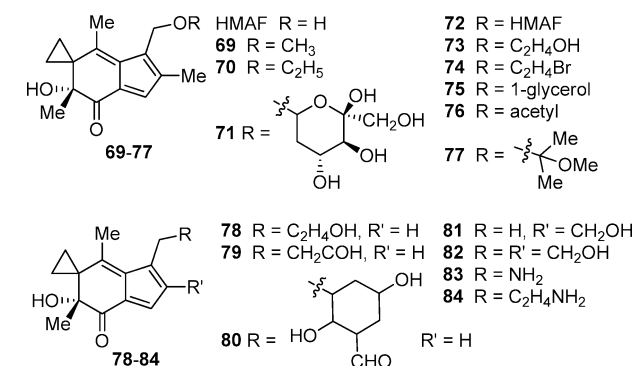
the highest IC<sub>50</sub> value is detected for **68e**, which bears a bulky phenyl ring at the enone, while the lowest IC<sub>50</sub> value is observed for the methyl analog **68b**. This observation is in agreement with previously discussed diminished cytotoxicity of illudin M and AF analogs derivatized at the enone site. Therefore, it is possible that, despite significant structural modification, the reactivity of the truncated analogs **68** relies on conjugate addition to activate the cyclopropyl ring toward cellular nucleophiles. However, there is no supporting direct experimental evidence available. Nonetheless, significant activity of **68a–d** was detected in four solid tumor cell lines, suggesting that the bicyclic enone is a main pharmacophore contributing to the cytotoxicity of illudins and AFs.<sup>40</sup> A few other illudin analogs that contain the primary enone–cyclopropyl pharmacophore have been reported by Kinder and co-workers.<sup>120</sup> Although no cytotoxicity data for them is

yet available, they are expected to be similarly cytotoxic as **68**. Finally, the importance of the cyclopropyl ring was further confirmed in SAR studies aiming to tune AF reactivity by substituting the *spiro*-cyclopropyl ring with less strained *spiro*-cyclobutyl.<sup>41</sup> Corresponding cytotoxicity data in lung (MV522), myeloid (HL60), and megacaryocyte (8392B and CHRF-2881) was 3 orders of magnitude diminished as compared to AF. Truncated analogs, as well as the cyclopentane mimics of illudins,<sup>121</sup> also show dramatic loss of activity.

## 7.2. Role of the C10-Hydroxyl in HMAF Cytotoxicity

Structural modifications of HMAF in pursuit of analogs with improved potency were carried out at C6 hydroxymethylene and at the methyl of C7. As a result, a variety of HMAF analogs depicted in Table 4 was obtained, and their cytotoxicity in

**Table 4. Cytotoxicity of C6-Substituted AF Analogs**



compound	IC <sub>50</sub> <sup>a</sup> (nM)
	MV 522
HMAF	73 ± 8
acylfulvene	350 ± 20
<b>70</b>	440 ± 60
<b>72</b>	320 ± 60
<b>73</b>	680 ± 180
<b>74</b>	930 ± 250
<b>76</b>	1400 ± 200
<b>77</b>	170 ± 180
<b>78</b>	850 ± 180
<b>79</b>	165 ± 55
<b>80</b>	270 ± 130
<b>81</b>	660 ± 200
<b>82</b>	580 ± 250
<b>83</b>	1300 ± 100
<b>84</b>	430 ± 100

<sup>a</sup>Cytotoxicity assessed by trypan blue assay after incubation for 48 h. MV522, human lung adenocarcinoma.

MV522 cells after 2 and 48 h was determined. Overall, the data obtained reflects the importance of the primary hydroxyl in HMAF activity. Thus, ethers **69** and **70** isolated from the acidified methanolic or ethanolic solutions of HMAF are about 5-fold less cytotoxic than HMAF (IC<sub>50</sub> = 73 nM, Table 4).<sup>122</sup> A relatively similar drop of activity is observed for HMAF dimer **72**, also isolated from these reactions.<sup>122</sup> Ethers **73**, **74**, and **75**, accessed by acid-catalyzed reaction of HMAF with ethylene glycol, ethylene bromohydrin, or glycerol, respectively, show more than 10-fold diminished cytotoxicity with respect to HMAF (IC<sub>50</sub>s in the range of 680–930 nM). HMAF–fructose conjugate **71**, accessed as a mixture of  $\beta$ -furanose and  $\beta$ -pyranose forms, is relatively inactive (IC<sub>50</sub> = 18000 nM) in

MV522 cells. Acylation of HMAF with acetic anhydride or benzoyl chloride yielded the corresponding methyl and phenyl esters **76** that were expected to be more cytotoxic due to the anticipated ease of displacing the acetyl versus hydroxyl group. Nonetheless, 200-fold diminished cytotoxicity activity (IC<sub>50</sub> = 1400 nM) was detected. Masking the C10-hydroxyl as a ketal also affects HMAF activity; however, the IC<sub>50</sub> of 170 nM observed for **77** makes it the most active HMAF analog in the described set.<sup>122</sup>

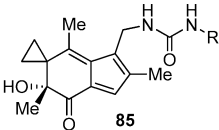
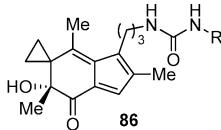
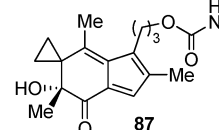
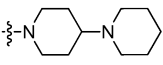
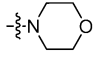
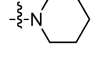
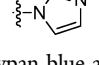
To test the influence of the length of the hydroxyl linker on HMAF activity, the methylene at C6 was replaced with a propylene linker yielding analog **78** (Table 4). As a result, more than a 10-fold decrease in cytotoxic activity (IC<sub>50</sub> = 850 nM) was observed, suggesting that the allylic nature of the hydroxyl is important for HMAF activity.<sup>122</sup> The aldehyde derivative **79** is more cytotoxic than **78** (IC<sub>50</sub> = 165 nM) and is relatively close in cytotoxicity to HMAF, suggesting possible involvement of the aldehyde moiety in the cytotoxic response. The bulky dialdehyde **80** has an IC<sub>50</sub> of 275 nM. The position of the hydroxymethylene moiety also appears to play a role in HMAF cytotoxicity. Thus, the C7-hydroxymethyl AF analog **81** exhibits 10-fold lower IC<sub>50</sub> than HMAF. Interestingly, introduction of an additional electrophilic site does not improve HMAF activity. Thus, similar to **81** the IC<sub>50</sub> is established for a diol **82**, suggesting that an additional electrophilic moiety interferes with the C10-OH reactivity or other biological processes associated with HMAF cytotoxicity.

The presented SAR study allows us to conclude that the C10-hydroxyl is involved, to some extent, in HMAF cytotoxicity and that it occupies an optimal position at the fulvene. It is noteworthy that changing the position of the hydroxymethyl or masking the free hydroxyl results in a 10-fold drop in activity, yielding IC<sub>50</sub> values similar to that of AF. Finally, the overall differences between HMAF, AF, and related analogs suggest that the main cytotoxicity is derived from the presence of the conjugated enone–cyclopropyl moiety and that the fulvene appears to tune the overall activity.

Various amine analogs of HMAF were also synthesized with the goal of enhancing AF cytotoxicity. Amine derivatives **83** and **84** mimic HMAF and **78** (Table 4).<sup>123</sup> Interestingly, propyl alcohol **78** (IC<sub>50</sub> = 850 nM) is significantly less cytotoxic than HMAF, while propyl amine **84** (IC<sub>50</sub> = 430 nM) is more cytotoxic than aminomethylene **83** (IC<sub>50</sub> = 1300 nM) in MV522 cells after 48 h exposure. Larger differences in cytotoxicity among amino-AFs were observed after shorter (2 h) exposure, where propyl amine **84** showed 8000 nM activity, while the cytotoxicity of **83** remained relatively the same (IC<sub>50</sub> = 470 nM). However, to our knowledge, there is no further insight available into the biochemical features that contribute to this difference, leaving room for further research.

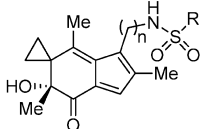
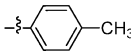
In a further series of SAR studies, electrophilic moieties at the C10 methylene were tested, resulting in analogs with cytotoxicities relatively similar to that of HMAF.<sup>124</sup> Thus, three types of analogs, ureas (**85**, **86**, Table 5), carbamides (**87**, Table 5), and sulfonamides (**88**, **89**, Table 6) bearing various N substituents at the amide, were accessed from HMAF analogs **78**, **83**, and **84**. Activities of these substrates directly correlate with the nature of the substitution and length of the fulvene–electrophile linker. On average, IC<sub>50</sub> values (MV522 cells, 48 h) are in the range of 110–190 nM for urea derivatives **85** and **86**, except **85f**, showing about 10-fold lower than average activity. Among the tested carbamates, derivatives **87a** and **87b** are the most cytotoxic (IC<sub>50</sub> of 70 and 57 nM, respectively) HMAF

**Table 5. Cytotoxicity** Data for Urea and Carbamide Analogs of AFs (IC<sub>50</sub>,<sup>a</sup> nM)

Compound	Substitution (R)	 85		 86		 87	
		MV522	8392	MV522	8392	MV522	8392
a	-NH-CH <sub>2</sub> -CH <sub>2</sub> -OH	190 ± 20	>9 000	<80	>2 800	70 ± 20	>24 000
b	-NH-CH <sub>2</sub> -CH <sub>2</sub> -Cl	110 ± 10	>8 500	170 ± 10	5 000 ± 700	57 ± 8	4 700 ± 1 200
c	-NH-CH <sub>2</sub> -CH <sub>2</sub> -F	n.s.	n.s.	n.s.	n.s.	670 ± 240	>20 000
d	-NH-CH <sub>2</sub> -CH <sub>2</sub> -Br	n.s.	n.s.	n.s.	n.s.	730 ± 140	6 600 ± 900
e	-NH-OH	190 ± 20	>9 800	150 ± 20	>9 000	460 ± 60	33 000 ± 600
f	-NH-OMe	1270 ± 10	>9 400	n.s.	n.s.	n.s.	n.s.
g		n.s.	n.s.	150 ± 20	9 000 ± 4 500	200 ± 30	610 ± 120
h		n.s.	n.s.	n.s.	n.s.	1 900 ± 450	>60 000
i		n.s.	n.s.	n.s.	n.s.	1 200 ± 250	7 100 ± 1 700
k		n.s.	n.s.	n.s.	n.s.	1 000 ± 150	>36 000

<sup>a</sup>Cytotoxicity assessed by trypan blue assay after 48 h incubation. n.s., not synthesized. MV522, human lung adenocarcinoma; 8392, B-cell-derived leukemia/lymphoma cell line.

**Table 6. Cytotoxicity** Data for Sulfonamide Analogs of AFs (IC<sub>50</sub>,<sup>a</sup> nM)

Compound	Substitution (R)	n	 	
			MV 522	8392
88a	-CH <sub>3</sub>	1	200 ± 90	>9 300
88b	-NH <sub>2</sub>	1	300 ± 20	>9 300
89a	-CH <sub>3</sub>	3	280 ± 50	>40 000
89b	-NH <sub>2</sub>	3	76 ± 17	>30 000
89c	-NH-OH	3	8 ± 1	250 ± 80
89d		3	580 ± 150	>2 900 ± 600

<sup>a</sup>Cytotoxicity assessed by trypan blue assay after 48 h incubation. MV522, human lung adenocarcinoma; 8392, B-cell derived leukemia/lymphoma cell line.

(87h), piperidine (87i), or imidazole (87k) derivatized carbamates are more than 10-fold less active than their chlorine or hydroxyl analogs (87b and 87a, respectively).

Although no data is reported regarding the mechanistic basis for the cytotoxicity of 85–87, the activity of chlorinated analogs may be attributed to in situ formation of the reactive aziridine intermediate similar to that formed with nitrogen mustards.<sup>125</sup> Furthermore, an analogous mode of reactivity is possible for hydroxylated derivatives 85a–87a, where protonation of the terminal hydroxyl may drive formation of the reactive aziridine. However, further investigations are necessary to address this hypothesis.

Among the series of HMAF sulfonamide analogs 88–89, compound 89c shows the highest cytotoxic activity (IC<sub>50</sub> = 8 nM), which exceeds that of HMAF in HMAF-sensitive MV522 cells (Table 6),<sup>124</sup> and sulfonamide 89b is as active as HMAF (78 nM). Other sulfonamide derivatives are much less cytotoxic and show activity between 200 and 300 nM. The cytotoxic activity of analogs 85–89 was also accessed in AF-resistant 8932 B cells. As a result, it was observed that the majority of new analogs exhibit 4–70-fold improved differential cytotoxicity between the target MV522 cells and nontarget 8932 B cells, and a striking >700-fold 8932 versus MV522 ratio was observed for 89c. As a result of these SAR studies, new acylfulvene-containing analogs, some exceeding the parent HMAF in cytotoxic activity, were obtained. However, considering involvement of the hydroxymethyl substituent of HMAF in interaction with cellular enzymes, further insight into the biological mechanisms associated with introduction of urea,

analogs. Among halogen-substituted ureas 87b–d, the chlorinated analog is most potent and the activities significantly diminish when chlorine is exchanged for fluorine or bromine. From the series of heteroatom-functionalized carbamates 87j–k (Table 5) the carbamate 87g is most cytotoxic, more so than fluorinated or brominated analogs 87c and 87d. Morpholine

carbamate, or sulfonamide into the molecule, and their role in the observed cytotoxicity would be of interest.

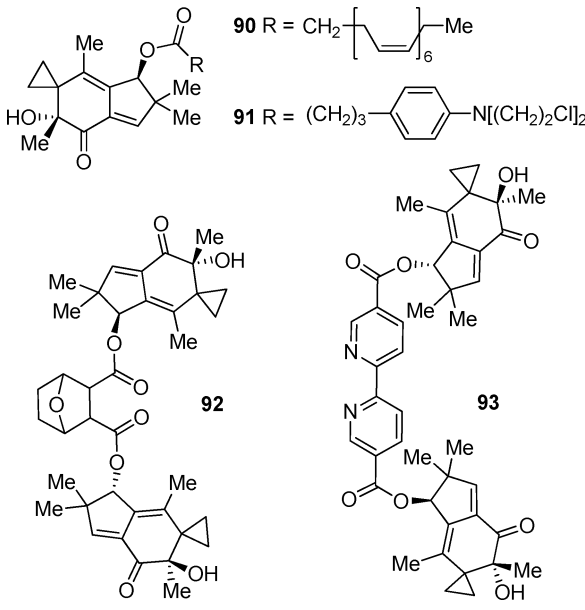
### 7.3. Tuning Illudin Cytotoxicity and Tumor Specificity

A low therapeutic index is the major drawback for illudin, and while AFs have better therapeutic characteristics, their tumor cell cytotoxicity is significantly diminished compared to illudins. In an effort to obtain illudin analogs with improved tumor specificity, Schobert and co-workers<sup>126</sup> tested various targeting elements. For example, a fatty acid-derivatized illudin M analog **90** (Table 7), chlorambucil illudin derivative **91**, endothall

concentrations ranging from 0.01 to 10  $\mu$ M. Analog **91** is weakly active in the tested tumor lines. Conjugates **92** and **93** retain the activity of illudin and show promising improvement in specificity toward tumor cells over normal fibroblasts, while **90** is drastically less cytotoxic.<sup>126</sup> The researchers indicate that further testing of these analogs in various types of liver cells and investigations on the origins of tumor selectivity are underway.<sup>126</sup>

Finally, ferrocene conjugates have been explored as a strategy for improving illudin tumor specificity.<sup>127</sup> On the basis of iron-binding metallotransferin overexpression in melanoma cells, ferrocene was expected to facilitate selective uptake of HMAF analogs by melanoma cells and open access to antimelanoma agents.<sup>127</sup> Illudin–ferrocene conjugates **94** and **95** are less toxic than illudin M in leukemia HL-60, melanoma S18A2, and human foreskin fibroblast (HF) cells (Table 8). Ferrocene

**Table 7.** Apoptosis Induction Data for Chimeric Illudin M Analogs **90**–**93**<sup>a</sup>



**90** R = CH<sub>2</sub> [CH=CH]<sub>6</sub> Me

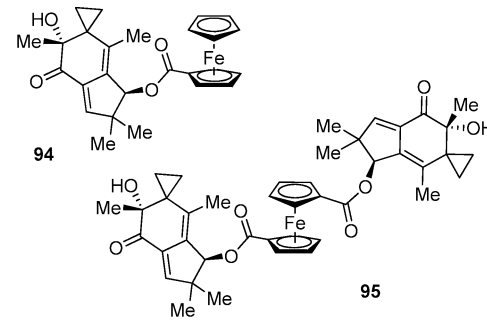
**91** R = (CH<sub>2</sub>)<sub>3</sub>–C<sub>6</sub>H<sub>4</sub>–N[(CH<sub>2</sub>)<sub>2</sub>Cl]<sub>2</sub>

compound	Panc-1 (%)	HT-29 (%)	HF (%)
vital cells			
illudin M	12.3 ± 9.6	3.8 ± 11.4	28.1 ± 14.6
<b>90</b>	103 ± 1.4	110.6 ± 4.1	80.0 ± 10.2
<b>91</b>	20.0 ± 3.4	42.7 ± 1.2	47.5 ± 3.6
<b>92</b>	7.3 ± 5.0	10.8 ± 3.9	47.8 ± 16.5
<b>93</b>	6.4 ± 7.4	3.0 ± 0.0	49. ± 10.3
apoptosis			
illudin M	86 ± 1.5	47.9 ± 0.1	88.9 ± 0.8
<b>90</b>	2.6 ± 0.9	1.9 ± 0.2	4.4 ± 1.9
<b>91</b>	36.8 ± 2.9	6.0 ± 0.9	9.5 ± 1.9
<b>92</b>	62.1 ± 15.6	21.3 ± 1.9	14.3 ± 0.5
<b>93</b>	74.0 ± 1.5	52.9 ± 1.4	33.1 ± 12.8

<sup>a</sup>Apoptosis induction data obtained after 120 h treatment. Panc-1, human pancreatic carcinoma; HT-29, human colon adenocarcinoma; HF, nonmalignant human foreskin fibroblast.

derivative **92**, and 2,2'-bipyridyl-5,5'-dicarboxylic acid (DNA intercalator)<sup>68</sup> derivative **93** were tested. The chlorambucil analog was prepared as a potential precursor of additional DNA damage, while endothall was used as a putative inhibitor of the serine–threonine protein phosphatase 2A (PP2A), which plays a role in the tumorigenic transformation, control of the cell cycle and in cell proliferation, and might be essential for the nuclear excision repair of DNA lesions. Biological evaluation of these illudin M analogs was carried out in pancreatic carcinoma (Panc-1) and colon adenocarcinoma (HT-29) cells as well as in nonmalignant human foreskin fibroblasts (HF) for 120 h at

**Table 8.** Cytotoxicity Data for Illudin M–Ferrocene Conjugates



compound	IC <sub>50</sub> <sup>a</sup> ( $\mu$ M)		
	HL-60	S18A2	HF
illudin M	0.02 ± 0.01	0.03 ± 0.02	0.13 ± 0.03
<b>94</b>	28 ± 5.3	3.6 ± 0.5	9.51 ± 2.49
<b>95</b>	3.0 ± 1.6	0.42 ± 0.08	2.99 ± 1.9

<sup>a</sup>IC<sub>50</sub> determined by standard MTT assay after 48 h treatment. HL-60, human promyelocytic leukemia cells; S18A2, human melanoma cells; HF, nonmalignant human foreskin fibroblasts. Values represent mean ± SD of three independent experiments performed in duplicate.

diminishes illudin M activity more than 100-fold (**94**), but adding a second molecule of illudin (ferrocene diester **95**) results in a compound with better, i.e., low micromolar, activity in the above three cell lines. It is noteworthy that both conjugates are about 10-fold more active in melanoma cell as compared to the leukemia cell line or nonmalignant fibroblasts (Table 8). A limiting result, however, is that there is no selectivity between tumor HL-60 and nonmalignant HF cells. Overall, studies with the ferrocene analogs, together with the previous SAR data, did not lead to significant improvements in illudin tumor selectivity but provided insight regarding the relationships between chemical structures and biological processes that influence illudin.

## 8. ROLE OF REDUCTIVE BIOACTIVATION IN ACYLFULVENE CYTOTOXICITY

Early data regarding the cellular metabolism of illudins and AFs suggests involvement of enzyme-mediated activation to electrophilic, biologically reactive intermediates.<sup>42,43,53,128</sup> Differences between illudins and AFs in their susceptibility toward metabolic activation emerge as a contributing factor for explaining AF's selectivity and specificity profiles. The following



section focuses on advances in the elucidation of illudin and AF bioactivation mechanisms.

### 8.1. Reductive Metabolism of Acylfulvenes and Illudins

The cyclopropyl ring of illudins and AFs is one of the key moieties involved in alkylation of cellular targets,<sup>10,131–134</sup> and a number of indicators suggest that it is triggered by bioreduction. Supporting evidence includes identification of metabolites such as **49** and **50** (Scheme 10), enzyme subcellular localization, cofactor preference, and metabolism inhibition profile.<sup>43,128</sup> Metabolic studies involving different subcellular liver fractions of rat liver indicate that the primary metabolic location is the cytosol, with no sign of microsomal transformation (Table 9). These data exclude involvement of

**Table 9. Cellular Localization of Illudin S-Metabolizing Enzymes**

intracellular fraction	cofactor	rate of metabolite formation ( $\mu\text{mol/g}$ liver per 10 min)	
		<b>49</b> <sup>a</sup>	<b>50</b> <sup>a</sup>
whole homogenate	NADP	1.50 $\pm$ 0.20	1.22 $\pm$ 0.22
9000 g supernatant	NADP	2.7 $\pm$ 0.55	1.51 $\pm$ 0.40
cytosol	NADP	1.83 $\pm$ 0.55	1.55 $\pm$ 0.06
microsomes	NADPH	n.d. <sup>b</sup>	n.d. <sup>b</sup>

<sup>a</sup>**49** and **50**, illudin S metabolites (Scheme 10). <sup>b</sup>n.d., not detected; each value is the mean  $\pm$  SD of the five rats.

cytochrome P-450s.<sup>43</sup> Furthermore, glutathione peroxidase also does not affect AF metabolism.<sup>42,129</sup> Drug activation and metabolite **49** and **50** formation is facile in the presence of NADPH, but no reaction is observed with NAD and NADH (Table 10). Subsequently, enone-reduced metabolites were

**Table 10. Cofactor and Oxygen Requirement for Illudin S Metabolism**

cofactor	rate of metabolite formation ( $\mu\text{mol/g}$ liver per 10 min)	
	<b>49</b> <sup>a</sup>	<b>50</b> <sup>a</sup>
NAD	n.d. <sup>b</sup>	n.d. <sup>b</sup>
NADH	n.d. <sup>b</sup>	n.d. <sup>a,b</sup>
NADP	0.84 $\pm$ 0.29	0.78 $\pm$ 0.21
NADPH	3.87 $\pm$ 0.45	3.69 $\pm$ 0.50
NADPH (anaerobic)	4.01 $\pm$ 0.98	3.92 $\pm$ 0.32

<sup>a</sup>**49** and **50**, illudin S metabolites (Scheme 10). <sup>b</sup>n.d., not detected; each value is the mean  $\pm$  SD of the five rats.

isolated from incubations of illudin S or AF with RLC in the presence of NADPH, suggesting that illudin/AF transformations are mediated by NADPH-dependent cytosolic enzymes.<sup>42,129</sup>

Toward the goal of understanding illudin/AF bioactivation pathways and identifying enzymes involved in primary activation of the drugs, some reductase-inhibition studies were performed. On the basis of suppression of illudin metabolism after enzyme activity inhibition with dicumarol,<sup>130</sup> the quinine oxidoreductase DT-diaphorase<sup>129</sup> was proposed to be involved in drug bioactivation. However, DT-diaphorase utilizes either NADPH or NADH as electron donors, while no NADH (Table 10) is involved in illudin metabolism. These data suggest the possibility of a DT-diaphorase isoenzyme being involved in catalyzing illudin metabolism.<sup>129</sup> Other inhibitors such as menadione, an inhibitor of aldehyde oxidase,

and quercetin, an inhibitor of ketone reductase and aldose reductase, partially affect illudin metabolism, suggesting either that these enzymes play a smaller role in illudin biotransformation or that they inhibit other enzymes involved in the bioactivation pathway.<sup>131,132</sup> In addition, flavoprotein enzyme inhibitors<sup>133</sup> and alcohol dehydrogenase inhibitors<sup>134</sup> do not interfere with illudin metabolism. Years later, work by Dick and Kensler<sup>53,128</sup> on characterization of the enone-reductase activity of PTGR1 highlighted its potential for AF reactivity, supporting a new avenue of investigation regarding cytotoxicity mechanisms.

### Prostaglandin Reductase 1-Mediated Acylfulvene Metabolism

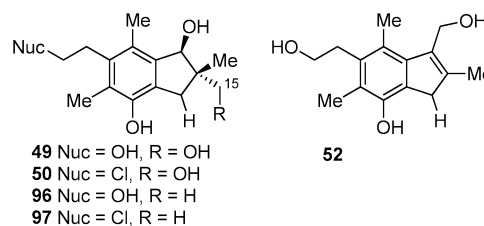
15-Oxoprostaglandin 13-reductase (PTGR1), also known as leukotriene B4 12-hydroxydehydrogenase and alkenal(one)-oxidoreductase (AOR), is an NADPH-dependent enzyme that bioactivates AFs.<sup>135–138</sup> PTGR1 reduces the carbon–carbon double bond of the enones and has been invoked in cellular detoxification of  $\alpha,\beta$ -unsaturated aldehydes and ketones. Its characterized substrates include lipid peroxidation products such as *trans*-2-alkenals, *trans*-4-hydroxy-2-alkenals, *trans*-2,4-alkadienals, and industrial chemicals such as methyl and ethyl vinyl ketones.<sup>139,140</sup> Aliphatic ketones are more efficiently reduced than aldehydes or ketones that are branched at the  $\beta$  positions or bear aromatic substituents. Cyclohexenones such as progesterone, cyclovalone, and quercetin inhibit PTGR1.<sup>140</sup> The degree of inhibition depends on the double-bond geometry; for example, *trans*-enones are noncompetitive PTGR1 inhibitors. The *cis* geometry seems to be important for proper substrate alignment in the protein active site.<sup>140</sup>

While chemical metabolism of both illudins and AFs follows the same pathway involving cyclopropyl ring opening,<sup>108,109</sup> the two processes differ in their kinetics. Illudin S is transformed by cytosolic extracts much faster than AF or HMAF, which require prolonged reaction time and increased amounts of lysate. A similar reactivity pattern is observed in PTGR1-mediated reactions. Thus, in the presence of NADPH, PTGR1-mediated metabolism of illudin S proceeds with  $V_{\text{max}}$  values more than 100 times higher than those of HMAF (Table 11).<sup>42,53</sup> This

**Table 11. Kinetic Constants for Metabolism by PTGR1<sup>a</sup>**

	metabolite	rate of metabolite formation ( $\mu\text{mol/g}$ liver per 10 min)	
		<b>49</b> <sup>a</sup>	<b>50</b> <sup>a</sup>
illudin S	<b>49</b>	65 400	486
	<b>50</b>	50 500	308
HMAF	<b>52</b>	275	145
illudin M	<b>96</b>	29 200	109
	<b>97</b>	14 900	113

<sup>a</sup> $V_{\text{max}}$ , maximum velocity, pmol/min for 10 million cells;  $K_m$ , Michaelis constant.



trend may be attributed to the diminished reactivity of the HMAF enone due to the aromaticity of the fulvene. However, illudin S exhibits weaker binding to PTGR1 as compared to HMAF, and the C15 hydroxyl appears to play a role. Thus, in

comparing the data for illudin S to illudin M, the presence of a C15 hydroxyl in illudin S appears to increase  $V_{\max}$  but diminish binding affinity for PTGR1.<sup>53</sup>

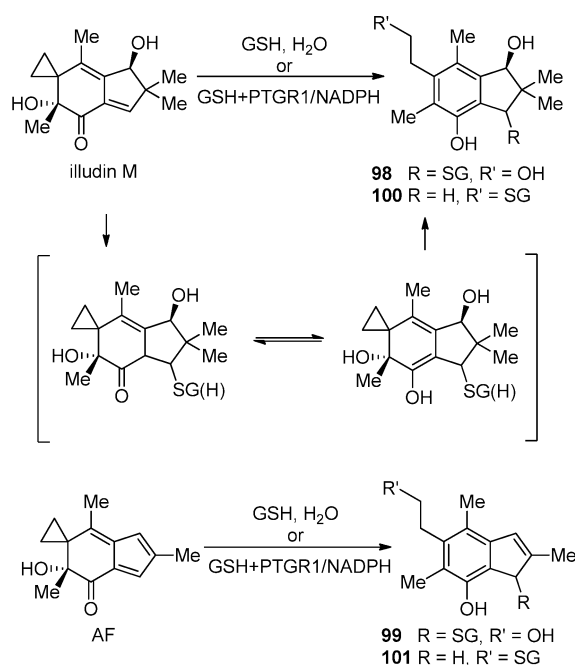
AF cytotoxicity toward cancer positively associates with reductase activity.<sup>53</sup> Among the tested cancer cell lines, leukemia cells exhibit the lowest enone reductase activity and the lowest susceptibility toward HMAF, and nonsmall lung cancer cells that exhibit the highest levels of reductase activity have the highest susceptibility toward HMAF. Furthermore, human embryonic kidney cells (HEK 293) transiently transfected with an episomal PTGR1 overexpression vector (pCEP4/PTGR1) and expressing 25-fold higher PTGR1 than control cells exhibit a >100-fold enhanced sensitivity toward HMAF. Illudin S cytotoxicity, however, does not change in PTGR1-overexpressing cells.<sup>53</sup> Therefore, regardless of the effectiveness of PTGR1-mediated metabolism of illudin S, it appears that PTGR1 does not play a role in illudin S cytotoxicity. From the perspective of chemical reactivity, illudin-mediated cytotoxicity can be considered to be significantly nonenzymatic, especially considering that many  $\alpha,\beta$ -unsaturated carbonyl compounds spontaneously react with strong nucleophiles by a conjugate addition mechanism. In contrast, distinct dependence of AF toxicity on PTGR1 levels and poor reactivity profiles in the absence of PTGR1 strongly suggest that enzyme-mediated bioactivation is an important factor dictating AF cytotoxicity. Considering the reductive environment of cancer cells, it is plausible to hypothesize that PTGR1-mediated bioactivation may also be a contributing factor to AF tumor specificity.

## 8.2. Prostaglandin Reductase 1-Mediated Illudin and Acylfulvene–GSH Interaction

PTGR1-mediated activation of AFs affects interaction with GSH by changing the regiochemistry of GSH addition.<sup>53</sup> Nonenzymatic addition of GSH to illudin M and HMAF occurs at the unsaturated carbonyl (adducts **98** and **99**, respectively, Scheme 12), whereas PTGR1/NADPH-assisted derivatization produces adducts **100** and **101**, resulting from hydride addition to the unsaturated carbonyl and GSH addition to the cyclopropyl ring. Overall, the nonenzymatic HMAF–GSH adduct **99** is 42-fold less abundant than the enzymatic adduct **101**. The activity of HMAF is not significantly altered in cells overexpressing GSH.<sup>48</sup> Despite the fact that illudin M shows no increased activation by overexpressed PTGR1 in cells,<sup>53</sup> PTGR1 does alter the illudin M–GSH adduct profile in vitro where the illudin M–GSH adduct **100** is the dominant species observed. These data suggest that PTGR1 may reduce illudins, but the resulting reactive intermediate can be rapidly trapped by GSH and thus not affect illudin S toxicity.

Considering the vastly different PTGR1/cytotoxicity relationship observed for AFs and illudins, it is plausible that upon activation these analogs form reactive intermediates of different stability. If the intermediate was rapidly trapped by nucleophiles in the enzyme active site, before it had the opportunity to react with important cellular nucleophiles (DNA or protein), metabolism by PTGR1 would result in detoxification. Alternatively, if the intermediate was stable enough to exist outside of the enzyme active site and reach important cellular nucleophiles, metabolism would serve to activate the molecule. Fast transformation of illudins into the hydroxylated and chlorinated metabolites in the presence of PTGR1 suggests formation of highly reactive and unstable intermediates. Facile reactivity of this intermediate with GSH may serve as a

**Scheme 12. Illudin M and HMAF Adducts Resulting from Spontaneous Versus PTGR1/NADPH-Mediated Glutathione (GSH) Addition**



detoxification pathway. This model is also in agreement with the findings discussed in the previous section concerning diminished cytotoxicity of illudin S in the GSH-overexpressing leukemia HL-60 cells.<sup>48</sup> AFs, however, perhaps due to additional stabilization from the aromatic fulvene, appear to form more stable intermediates that persist and react with physiologically critical cellular nucleophiles. Therefore, it can be concluded that PTGR1-mediated activation plays a small if any role in the pharmacological activity of illudins but is important for AFs.

## 8.3. Role of Stereochemistry in Acylfulvene Cytotoxicity

The cytotoxicity of AFs depends on the absolute stereochemistry of the **tertiary** hydroxyl. McMorris and co-workers<sup>34</sup> reported that a >5-fold decrease in activity was observed for (+)-AFs in MV522 adenocarcinoma cells, as compared to the corresponding (–)-AF and (–)-HMAF. In agreement with this is the higher cytotoxic activity of (–)-AFs over (+)-AFs in PTGR1-transfected HEK 293 cells.<sup>36</sup> Thus, from the four tested AFs, (–)-HMAF and (–)-AF are the two most potent compounds with IC<sub>50</sub> values of 55 and 95 nM, respectively. (+)-HMAF and (+)-AF show 25- and 50-fold diminished activity.<sup>36</sup>

Despite the evidently diminished activity of (+)-AFs in PTGR1-transfected cells, it was established that both enantiomers are effectively activated by PTGR1. The kinetic parameters for PTGR1-mediated AF metabolism are summarized in Table 12. While higher  $K_m$  values of (–)- and (+)-HMAF reflect the difference in cytotoxicity with respect to the less potent AF, the kinetic parameters are relatively similar for the two enantiomers, suggesting similarity in interaction with the enzyme. These results are consistent with earlier PTGR1 studies in which a  $K_m$  value of 145  $\mu$ M for (–)-HMAF was determined by monitoring the appearance of the hydroxyl metabolite.<sup>53</sup> Interestingly, (+)-HMAF is activated by PTGR1 twice as effectively as (–)-AF but is significantly less potent in

**Table 12. Kinetic Parameters for PTGR1-Mediated Metabolism of Enantiomeric AFs<sup>a</sup>**

substrate	$K_m$ ( $\mu\text{M}$ )	$V_{\max}$ ( $\mu\text{M}/\text{min}$ )	$V_{\max}/K_m$ ( $\text{min}^{-1}$ )
(+)-AF	465	1.7	3.7
(-)-AF	538	5.0	9.3
(+)-HMAF	243	4.5	18.5
(-)-HMAF	213	8.3	39.0

<sup>a</sup>Values represent averages determined from three runs with errors within 10%

cell-based assays. Therefore, additional biochemical factors such as cellular accumulation or deactivation or DNA interaction geometry may contribute to dictating cell sensitivity toward the (–)-enantiomer.

## 9. ROLE OF UPTAKE IN DIFFERENTIAL CYTOTOXICITY OF ILLUDINS AND ACYLFULVENES

Bioactivation, GSH reactivity, and enzyme-inhibition data described thus far clearly establish that within the cell illudins and AFs have differential activities. However, the pharmacological activity of a drug is defined by many further factors, including cellular uptake or efflux. As described in the following subsections, illudins and AFs exhibit different rates of cellular uptake. Data demonstrate that illudin activity is largely influenced by cell uptake, whereas AF activity is related to a combination of uptake and bioactivation.

### 9.1. Illudin S Uptake and Cellular Accumulation

On the basis of correlation between uptake and toxicity, cellular uptake appears to play a significant role in the differential cytotoxicity of illudins in various tumor cells. At 48 h exposure, illudin S is relatively equally reactive in the majority of the tested cancer cell lines, but a shorter incubation period is associated with distinct differential activities that, in turn, correlate with cellular uptake.<sup>50</sup> Thus, as it can be seen from Table 13, intracellular incorporation of 4  $\mu\text{M}$  illudin S after 2 h

**Table 13. Illudin S Cellular Uptake and Cytotoxicity in Various Human Tumor Cell Lines**

cell line	2 h uptake <sup>a</sup> (pM)	IC <sub>50</sub> <sup>b</sup> (nM)	
		2 h	48 h
HL60	89 ± 2	8 ± 1	3 ± 1
SW48	82 ± 6	21 ± 2	8 ± 1
HT29	59 ± 6	32 ± 2	6 ± 1
MDA231	55 ± 3	36 ± 3	1 ± 0.1
MV522	51 ± 5	79 ± 11	4 ± 1
MCF7	29 ± 4	115 ± 13	10 ± 3
8392	14 ± 2	363 ± 21	8 ± 2

<sup>a</sup>Picomoles per 10 million cells (mean ± SD of three experiments).

<sup>b</sup>Concentration producing a 50% decrease in colony formation (mean ± SD of three experiments); HL60, human promyelocytic leukemia cells; 8392, human B-cell-derived leukemia/lymphoma; MV522, human lung adenocarcinoma; HT29 and SW48, human colon adenocarcinoma; MDA231 and MCF7, human breast carcinoma.

exposure for a given cell line correlates with the IC<sub>50</sub> value. For instance, HL60 cells that are highly sensitive to illudin S at 2 h exposure exhibit effective uptake (89 pM/10<sup>6</sup> cells) and low IC<sub>50</sub> (8 nM). MCF7 and 8392 B cell lines, on the contrary, are relatively nonresponsive to illudin S and exhibit poor drug uptake. Even more prominent differences in uptake/cytotoxicity are observed at shorter exposure times. Thus, more than

99% of HL60 and MV522 cells are killed at 15 min exposure to 4  $\mu\text{M}$  illudin S, while no IC<sub>50</sub> value could be measured with 8392 B cells even at 150  $\mu\text{M}$  illudin S concentration. Subsequently, at the same concentration and time frame, HL60 and MV522 cells show high illudin S uptake, while no uptake is observed in the resistant 8392 B cells.<sup>50</sup> Extending drug treatment to 2 h enhances cytotoxicity of illudin S in MV522 cells 10-fold. Additionally, cellular accumulation does not change significantly and is 1.64 and 1.72 per 10<sup>6</sup> cells for 15 min and 2 h, respectively. Unlike MV522 cells, 2 h exposure of the 8392 B cells to illudin S displays a cytotoxic response that correlates with increased accumulation of illudin (Table 13). The relationships between uptake and drug response suggest two different uptake mechanisms for illudin S-sensitive versus illudin S-resistant cell lines.

Kinetic parameters derived for illudin S in sensitive tumor cells indicate that uptake occurs predominantly during an early rapid phase and proceeds through an energy-dependent mechanism.<sup>50</sup> Uptake in HL60 and MV522 cells saturates, is temperature sensitive, and has equivalently high  $V_{\max}$  and low  $K_m$  and  $V_d$  values (Table 14), which is characteristic of energy-

**Table 14. Kinetic Characteristics for Cell Uptake of Illudin S, HMAF, and AF**

cell line	constant	illudin S	HMAF	AF
HL60	$V_{\max}$	28.7	14	3.6
	$K_m$	7.1	11	7.8
	$V_d$	0.34	<0.005	0.018
MV522	$V_{\max}$	33.6	18	348
	$K_m$	5.6	25	18.1
	$V_d$	0.13	<0.005	0.013
8392 B	$V_{\max}$	6.0	n.d. <sup>b</sup>	n.d. <sup>b</sup>
	$K_m$	81.0	n.d. <sup>b</sup>	n.d. <sup>b</sup>
	$V_d$	0.05		0.01

<sup>a</sup> $V_{\max}$ , maximal velocity, pmol/min for 10 million cells;  $K_m$ , Michaelis constant,  $\mu\text{M}$ ;  $V_d$  in min  $\sim 1$  for 10 million cells. <sup>b</sup>n.d., not detected.

dependent uptake. This observation is in agreement with the rapid accumulation of illudin S in MV522 cells during 15 min exposure. In contrast, no evidence of rapid energy-dependent uptake was detected for the resistant 8392 B cells.  $V_{\max}$  for the 8392 cell line is markedly below that of HL60, and  $K_m$  is more than 10-fold higher, suggesting minimal involvement of energy-dependent transport in this cell line. However, with the use of <sup>3</sup>H-labeled illudin S and an incubation time four times longer than used for the sensitive cells, evidence of low-capacity transport in 8392 B cells was detected. Hence, it appears that relatively sensitive tumor cells rapidly take up illudin S by a saturable energy-dependent mechanism, whereas resistant cells use passive diffusion.<sup>50,78</sup>

A distinct illudin S uptake–cytotoxicity correlation also is observed in multidrug-resistant (mdr) cell lines (Table 15).<sup>50</sup> It has been noted previously that CEM mdr cells are relatively sensitive to illudin,<sup>19</sup> despite marked resistance to conventional anticancer agents. It is noteworthy that the 8226/LRS cell line is significantly more sensitive to illudin S and takes up illudin S more rapidly (46 pM per 10<sup>6</sup> cells) than the parent 8226 line (13 pM per 10<sup>6</sup> cells). Illudin S uptake evaluated in MCF7 and MCF-7/ADR cell lines does not show a significant difference, which correlates with the relatively similar cytotoxicity values detected for these cell lines.<sup>50</sup> Hence, it appears that the activity of an energy-dependent uptake in tumor cells affects the



**Table 15. Illudin S Cytotoxicity in Multidrug-Resistant Cell Lines**

cell line	resistance mechanism	IC <sub>50</sub> <sup>a</sup> (μM)
CEM parent		11 ± 1
VM-1	topoisomerase II	13 ± 1
MDA-231 parent		0.9 ± 0.2
3-1	Gp170/mdr1	0.9 ± 0.4
MCF7 parent		0.9 ± 0.1
ADR	GSHTR-pi	3 ± 1
HL60 parent		3 ± 1
ADR	Gp180/MRP	2 ± 1
2008 parent		55 ± 5
cisplatin	DNA repair	52 ± 3
8226 parent		316 ± 53
LR5	thiol content	6 ± 1
DC3F parent		24 ± 7
C-10	topoisomerase I	17 ± 3

<sup>a</sup>Concentrations producing a 50% decrease in the cell count after 48 h exposure (mean ± SD for 3–5 determinations by standard MTT assay). CEM, human T-cells; MDA-231 and MCF7, human breast carcinoma; HL60, human promyelocytic leukemia cells; 2008, human ovarian cancer, 8826, myeloma; DC3F, murine cancer cells.

cytotoxic response to illudin S and contributes to differential tumor cytotoxicity.

## 9.2. Acylfulvene Uptake and Cellular Accumulation

In contrast to illudins, AF uptake in sensitive cells proceeds in two distinct phases.<sup>47,51,52</sup> The time course data for treatment of CEM cells with 10 μM <sup>14</sup>C-HMAF displays an early rapid component of drug uptake and a slower but sustained uptake that continues for several hours. The rapid phase is dominant up to 10 min but diminishes with time and at 4 h accounts for only 25% of total cell-associated HMAF.<sup>47</sup> Continuous slow uptake is detected even after 14 h of incubation.<sup>52</sup> Measurable accumulation is also detected at pharmacologically relevant levels of HMAF (2 μM, IC<sub>50</sub> 1.7 μM).<sup>20</sup> Similar to illudin S,<sup>50</sup> the cell lines previously noted to display energy-dependent uptake are more sensitive to the AF analogs during 2 h exposure, while the 8392 B cell line, previously shown to lack energy-dependent accumulation, is resistant to AFs (Table 16). Overall, with the exception of

**Table 16. Acylfulvenes Cellular Uptake and Cytotoxicity in Various Human Tumor Cell Lines**

cell line	HMAF		AF	
	uptake <sup>a</sup> (pM/10 <sup>6</sup> cells)	IC <sub>50</sub> <sup>b</sup> (nM)	uptake <sup>a</sup> (pM/10 <sup>6</sup> cells)	IC <sub>50</sub> <sup>b</sup> (nM)
HL60	9 ± 2	825	24 ± 1	443
SW48	10 ± 2	1220	17 ± 1	1180
HT29	17 ± 1	1060	190 ± 10	379
MDA231	11 ± 1	350	n.r.	190
MV522	14 ± 2	1200	147 ± 8	447
MCF7	33 ± 5	160	n.r.	212
8392	3.7 ± 0.5	26 000	7.4 ± 1	17 670

<sup>a</sup>Amount of a drug (pmol) accumulated intracellularly in 10 million cells after 2 h exposure to HMAF (407 nM, 100 ng/mL) or AF (462 nM, 100 ng/mL), respectively. <sup>b</sup>Concentration producing a 50% decrease in colony formation after 2 h exposure (mean ± SD, *n* = 3).

MDA231 and HL60 cells, HMAF and AF activity diminishes with decreased drug uptake. These correlations suggest that in

sensitive cells AFs and illudin S are taken up by a similar energy-dependent transport mechanism. In agreement with this are high *V*<sub>max</sub> and *K*<sub>m</sub> values measured for HMAF in HL60 and MV522 cell lines. These values, with the exception of *V*<sub>max</sub> for HL60 (Table 16, HMAF), support involvement of energy-dependent transport of HMAF. The kinetic parameters for AFs in 8392 B cells were not measured due to low cellular uptake of the drug.

While kinetic parameters for HMAF uptake are relatively similar to that of illudin S, a 10-fold increase in *V*<sub>max</sub> is observed for AF in MV522 cells (Table 16, AF). The *V*<sub>max</sub> value (348 pM/min for 10<sup>6</sup> cells) assessed for AF in MV522 cells is about 20-fold higher than the ones derived for HMAF. The 8392 B cell line, lacking the energy-dependent process, has a markedly lower *V*<sub>d</sub> coefficient. Together these two findings may explain the increased in vivo efficacy of AF compared with illudin S. The higher *V*<sub>max</sub> allows increased uptake of AF into tumor cells. The markedly higher *K*<sub>m</sub> and relatively lower *V*<sub>d</sub> coefficients result in a reduction in the number of molecules entering nontumor cells, consistent with the decrease in nonspecific in vivo toxicity of AF as compared to illudin S.

Continuous AF influx is attributed to its effective binding to cellular macromolecules, leading to low intracellular concentrations of free drug.<sup>47</sup> After 4 h exposure of CEM cells to 5 mM HMAF approximately 70% of the drug is covalently bound to macromolecules. Total drug uptake reflects internalized drug and drug associated with the outer cell surface. The total concentration of intracellular <sup>14</sup>C-HMAF in CEM cells exceeds the extracellular concentration of the drug by 15-fold. However, concentrations of unbound intracellular HMAF are comparable with extracellular concentrations, suggesting that continuous HMAF uptake is driven by covalent binding of the drug to cellular targets.<sup>47</sup>

Drug efflux does not appear to influence illudin S or AF activity. In studies performed with HL60 cells treated with <sup>3</sup>H-labeled illudin S (28 nM), there was no release of the drug after 2 h. Moreover, no drug efflux was detected even after increasing the concentration of illudin S 200 times over the IC<sub>50</sub> value, suggesting that illudin S cellular metabolism exceeds the rate of efflux and/or is a result of binding of the drug with intracellular target(s).<sup>50</sup>

Overall, the available uptake data suggest that differential toxicity of illudin S primarily, if not solely, depends on uptake. Reactivity of AF and HMAF, however, differs with respect to the type of the tumor cell, implying that metabolism and bioactivation are major factors contributing to AF differential cytotoxicity. In agreement with this model is the observation that even though AF uptake in MV522 and HT29 cells drastically exceeds that of illudin S, the inhibitory concentration for AFs in these cell lines is 6–10-fold lower than that of illudin S.<sup>51,141</sup>

## 10. ACYLFULVENES AS DNA ALKYLATING AGENTS

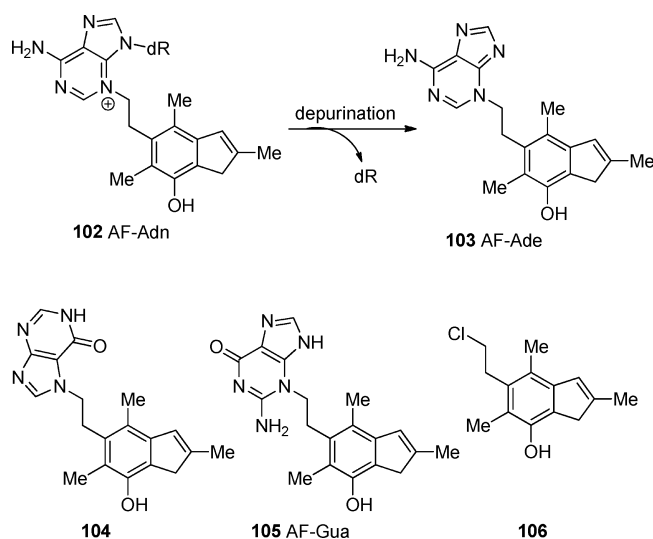
Although alkylation of redox-mediated enzymes may contribute to AF cytotoxicity, DNA alkylation is considered a major source of the observed cellular response to AFs. DNA damage resulting from AF–DNA alkylation blocks the cell cycle and induces apoptosis. This section provides an overview of AF-induced DNA damage and possible cellular pathways involved in AF-induced apoptosis.



### 10.1. DNA Alkylation as a Source of Acylfulvene Cytotoxicity

The electrophilic nature of AFs in conjunction with nuclear incorporation<sup>20,47</sup> suggests that AF and HMAF could produce DNA adducts, DNA–protein cross-links, and/or DNA–DNA cross-links. Experiments to assess DNA–protein and DNA–HMAF–DNA adducts, however, suggest that **neither is formed** nor they are formed at levels that cannot be detected.<sup>57</sup> Covalent DNA monoadducts, on the other hand, have been detected and characterized.<sup>58</sup> MS analysis of the in vitro combination of monomeric deoxynucleotides with AF in the presence of PTGR1/NADPH showed that DNA, predominantly at purine bases, reacts to form covalent adducts. Further analysis revealed the 3 position of deoxyadenine (dAdn) as a primary site of alkylation yielding adducts **102** (Scheme 13). Alkylation of deoxyguanine (dGuo)

Scheme 13. AF–DNA Adducts



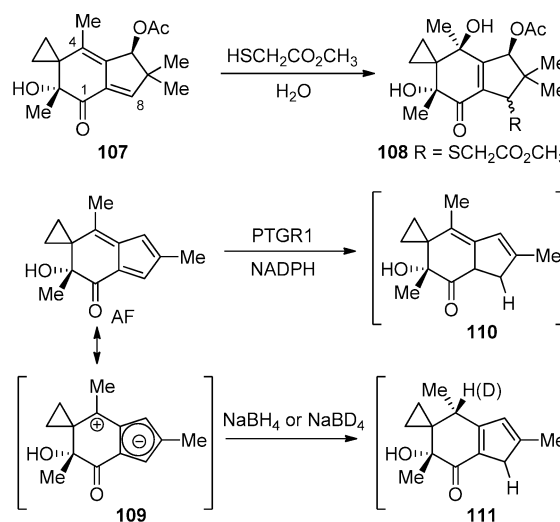
also occurs and produces 3- and 7-AF adducts. AF–dAdn and AF–dGuo adducts depurinate under physiological conditions and yield adducts **103**–**105** that are expected from a reductase-mediated reaction pathway. Independent chemical synthesis of conjugates **103**–**105** from adenine, guanine, and indene **106** confirmed the structures as AF–dAdn and AF–dGuo adducts.<sup>58</sup> Alkylation of dAdn, mediated by PTGR1, is about 100 times more efficient than reaction with dGuo.<sup>54</sup> Similar results were obtained after allowing calf thymus DNA, a convenient source of naked duplex DNA, to react with AF in the presence of PTGR1/NADPH. After isolating alkylated DNA, subsequent enzymatic neutral or thermal hydrolysis gave rise to AF adducts **103**–**105**, detected by MS/MS analysis. The relative abundance of AF–dAde (**103**) is 100 times higher than that of AF–dGua (**105**), indicating that under the same conditions reaction between dAdn and AF in the presence of PTGR1 is about 100 times more efficient than that of dGuo. AF–Ade and AF–Gua adducts have been also isolated from the cellular DNA of AF-treated cells (HEK293) that were transfected to overexpress PTGR1. The AF–DNA adducts are formed at 5–10 times higher levels in the PTGR1 transfected cells that **produced** a 7–8-fold higher expression of PTGR1 than in control cells.<sup>58</sup> On the basis of data regarding reaction of AF with a sequence-defined DNA plasmid, AF-induced damage does not

appear to depend on DNA sequence. Treating the plasmid with AF in the presence of PTGR1/NADPH yields DNA cleavage at all dGuo and dAdn sites. Analogous experiments carried out with dimethyl sulfate/piperidine or formic acid/piperidine yielded similar DNA fragments cleaved nonspecifically at dGuo and dAdn, indicating that AF preferentially alkylates purine bases but does not exhibit any sequence specificity.<sup>58</sup> These observations from cell-free systems are consistent with HMAF-induced DNA fragmentation in CEM cells,<sup>57</sup> suggesting that both AFs may exhibit a similar mode of interaction with DNA. However, further studies are needed to establish whether the patterns of DNA alkylation by HMAF and distribution of DNA versus protein alkylation are analogous to those of AF or whether HMAF's hydroxymethylene substituent has a significant influence on DNA/protein reactivity.

### 10.2. DNA Alkylation through Alternative Reactive Intermediate(s) of Acylfulvenes

An important chemical process in biochemical or chemical transformations of AFs or illudins involves conjugate addition at C8 (i.e., the enone) followed by opening of the cyclopropyl ring (Schemes 10 and 12).<sup>108,109</sup> However, an alternative mode of reactivity involves addition of nucleophile or hydride to C4 (Scheme 14). For example, **108** (Scheme 14) was isolated from

Scheme 14. C8 as Alternative Site of AF Transformation



reaction of **107** with methyl glycolate.<sup>39</sup> Identification of **108** suggests that the reactive diene intermediate, generated after nucleophilic addition to the enone, could trap nucleophiles at C4 possibly contributing to cytotoxicity. Further, while it appears that enzymatic (PTGR1-mediated) reduction of AF proceeds by 1,4-conjugate addition of hydride, giving rise to intermediate **110** (as originally proposed by McMorris and co-workers,<sup>113</sup>), chemical (NaBH<sub>4</sub>-mediated) reduction of AF gives rise to an isomeric intermediate **111**, arising from 1,8-conjugate addition (Scheme 14). Structural elucidation of **111**, facilitated in part by preparation of its deuterated analog by reduction with NaBD<sub>4</sub>, suggests that the hydride is delivered at C4 and that delivery is diastereoselective, leading to formation of (S)-**111**.<sup>142</sup> The regioselectivity of this chemical reduction may be rationalized on the basis of the dipolar resonance structure **109** (Scheme 14) containing an aromatic cyclopentadiene ring and with C4 activated toward nucleophilic attack.<sup>143,144</sup> In addition, the carbonyl may tune the reduction

potential of the fulvene, making it particularly susceptible to reduction with  $\text{NaBH}_4$ , suggesting also a possible route for modifying the reactivity of the molecule.

The chemically reduced AF analog **111** reacts with nucleophiles in the same manner as PTGR1-activated AF, giving rise to aromatic products resulting from the opening of the cyclopropane ring. Furthermore and also consistent with the enzymatic reaction of AF with purine nucleosides, the activated AF **111** reacts with dAdn and dGuo and forms adducts that, after thermal hydrolysis, depurinate and yield **103–105** (Scheme 14). Reaction of **111** with calf thymus DNA also yields AF–Ade and AF–Gua adducts as observed for AF.<sup>142</sup> While product formation in both reactions is diminished as compared to the enzyme-mediated reactions of AF, this novel reduced AF analog is a potentially useful chemical probe for investigating the role of adducts in cytotoxicity without confounding differences in enzymatic activation.

### 10.3. Acylfulvenes Induce DNA Double-Strand Breaks and Cell Apoptosis

AFs disrupt DNA synthesis, block the cell cycle, and induce DNA strand breaks and cell death. Thus, after 17 h of treatment of CEM cells with 3.4 and 8.5  $\mu\text{M}$  HMAF, the S-phase fraction increased to 77% and 80% of cells, respectively, as compared with 43% for the untreated control.<sup>57</sup> This result is hypothesized to be linked to inhibition of DNA synthesis by HMAF-induced damage. In agreement with this hypothesis is partial inhibition of  $\beta$ -globin gene amplification at 25–250  $\mu\text{M}$  HMAF, with no dependence on concentration. DNA synthesis inhibition by HMAF ( $\text{IC}_{50} = 2 \mu\text{M}$ ) was also established on the basis of [ $^3\text{H}$ ]-thymidine incorporation.<sup>57</sup> HMAF inhibits RNA synthesis, albeit at higher concentrations (20  $\mu\text{M}$  HMAF), and protein synthesis at elevated (70  $\mu\text{M}$ ) concentration.

HMAF causes widespread DNA damage even after the drug is removed from the surrounding media, and damage results in irreversible strand cleavage. Thus, during the initial 4 h period of treating CEM cells with HMAF, relatively large fragments (~80 kb) of DNA resulting from DNA double-strand breaks (DSBs) is detected and up to 35% of total cellular DNA is fragmented. Comparable DNA fragmentation is observed upon lowering HMAF concentration to 5  $\mu\text{M}$  and extending the drug-treatment time to 24 h. Moreover, DNA fragmentation levels increase upon postincubation of drug-treated cells for another 24 h, with the majority of the released DNA fragments being 8–15 kilobase (kb) pairs in size.<sup>57</sup> HMAF-mediated inhibition of DNA synthesis, formation of DNA fragments from 50 to >400 kb, and cell cycle arrest in S phase and at G2/M checkpoint was also observed in breast and ovarian cancer cell lines.<sup>145</sup> The interference of HMAF with DNA synthesis suggests that processing of HMAF adducts at the replication fork may contribute to formation of replication-dependent DSBs. This hypothesis is further supported by chromosomal breaks observed to generate upon HMAF treatment.<sup>145</sup>

In contrast to tumor cell lines, low levels of apoptosis are detected in normal cells. Even after prolonged treatment with HMAF at concentrations that exceeded tumor cell  $\text{IC}_{50}$  values 15–800-fold, DNA fragmentation levels do not exceed 10% of total cellular DNA.<sup>20</sup> This resistance of normal cells to HMAF-induced apoptosis cannot be accounted for by differences in drug accumulation or drug covalent binding to intracellular targets.<sup>20</sup> In fact, a relatively similar level of HMAF uptake occurs in tumor versus normal cells. Nonetheless, about 3-fold

more potent growth inhibition is observed for the tumor cell lines.<sup>20</sup> Therefore, additional mechanisms, possibly HMAF activation and also DNA repair, may contribute to minimizing HMAF-induced damage in nontumor cells.

## 11. BIOCHEMICAL PATHWAYS OF ACYLFULVENE-INDUCED APOPTOSIS

AFs are potent inducers of apoptosis. AF cytotoxicity induces activation of caspases, p21, and CHK2 and is independent of p53. This section summarizes the studies addressing biochemical pathways of AF-induced cell death.

### 11.1. Role of Caspases in Acylfulvene-Induced Apoptosis

AFs induce cell death by apoptosis. Caspases, which are cysteine–aspartic acid proteases, activate and execute apoptosis and necrosis and contribute to the apoptotic effects of various chemotherapeutic agents.<sup>146–148</sup> Briefly, cellular apoptotic responses are coordinated by initiator caspases (caspase-8 and caspase-9) that activate executioner caspases (for instance, caspase-3) responsible for biochemical and morphological changes yielding cell death. Thus, elevated caspase-3 levels are linked to enhanced apoptosis, while caspase-3 deficiency correlates with tumor growth.<sup>149–151</sup> The involvement of caspase-3 in HMAF-induced apoptosis was studied with caspase-3-deficient MCF-7 and caspase-3-proficient MDA-MB-231 breast cancer cell lines along with healthy breast cells (HMEC).<sup>152</sup> Despite the differential pattern in caspase-3, HMAF induces apoptosis in both cancer cell lines at the same level, suggesting a minimal role of caspase-3 in AF-induced cytotoxicity. In contrast, MCF-7 cells require caspase-3 transfection to be sensitized to tumor necrosis factor plus cycloheximide or staurosporine-, cisplatin-, doxorubicin-, or etoposide-induced apoptosis.<sup>152–154</sup> However, MCF-7 cells undergo apoptosis with glycerol nitrate (nitric oxide donor) and with tumor necrosis factor plus actinomycin D in the presence of iron sulfate, causing distortion of redox homeostasis.<sup>155–157</sup> Hence, it is possible that HMAF reactivity with redox enzymes may contribute to the apoptotic response observed in MCF-7 cells. However, additional data is required to verify this connection.

Regardless of its caspase-3 independence, HMAF-induced cell death appears to be a caspase-dependent process. Thus, treating MCF-7 cells or the caspase-3 proficient breast cancer cells (CEM, LNCaP, and LNCaP-Pro-5) with a broad-spectrum caspase inhibitor results in inhibition of HMAF-induced DNA fragmentation. These data suggest involvement of alternative executioner caspases in HMAF cytotoxicity.<sup>152,158</sup> Other studies suggest involvement of initiators caspase-6, caspase-8, and caspase-9 in the cellular response to HMAF.<sup>158,159</sup> Finally, correlating drug activity between MDA-MB-231 and HMEC shows significant susceptibility of the former to HMAF treatment. Cellular caspase profile is therefore a possible contributing factor to AF tumor selectivity.<sup>20,160</sup>

### 11.2. Role of p53, p21, and CHK2 in Acylfulvene-Induced Apoptosis

Similar response to the cytotoxic effect of HMAF in p53-proficient versus p53-deficient cells suggests that AF cytotoxicity is independent of cellular p53 status. p53 is a transcription factor. It is expressed at relatively low levels in the absence of cellular stress, and its expression is induced by various stimuli, including alkylation-induced DNA damage. Alkylation-induced cell death, in most of cases, is linked to p53 and p21 function as apoptosis triggers. For example, DNA-binding compounds

display ~4-fold diminished activity in the HCT-116 p53<sup>−/−</sup> cell line versus p53-proficient HCT-116 cells.<sup>161,162</sup> In contrast, no significant alteration in HMAF activity is observed in these cell lines.<sup>22</sup> Furthermore, treatment of HCT-116 cells with isotoxic doses of cisplatin and HMAF induces p53 accumulation at similar levels, suggesting that the drug-induced p53 is transcriptionally active. HMAF-mediated cytotoxicity is also independent of the cyclin-dependent kinase inhibitor p21. This was concluded after monitoring HMAF activity in HCT-116 p21<sup>−/−</sup> cells. Thus, the cellular activity of HMAF is independent of both p53 and p21.<sup>22</sup>

Studies also indicate involvement of the CHK2 kinase-dependent DNA damage pathway.<sup>163</sup> CHK2 regulates G1 arrest,<sup>164,165</sup> S-phase checkpoint,<sup>166,167</sup> or G2/M transition<sup>168,169</sup> following DNA damage. It is yet to be determined whether CHK2 activation might also play a role in repairing HMAF-elicited DNA lesions; however, CHK2 activation and overexpression were observed upon treating ovarian cells (A2780, A2780/CP70, CAO3, SKOV3, and OVCAR3) with HMAF. Therefore, CHK2 activation may contribute to HMAF-mediated cell cycle arrest.<sup>163</sup> To understand the possible role that HMAF-induced CHK2 activation might play in cell cycle arrest, the isogenic HCT116 cells and CHK2 knockout derivatives were examined after HMAF treatment. As a result, CHK2 was only expressed and activated in the parental HCT116 (CHK2+/+) cells. It was also observed that 3 h HMAF treatment induces a 4-fold enhancement of S-phase cell arrest in CHK2+/+ compared to CHK<sup>−/−</sup> cells. This trend is maintained throughout the 24 h period after drug removal. Thus, HMAF-mediated CHK2 activation contributes to S-phase cell cycle arrest and apoptosis.<sup>163</sup>

## 12. REPAIR OF ACYLFULVENE-INDUCED DNA DAMAGE

DNA repair may significantly impact the cellular response to AFs and illudin S, and the TC-NER subpathway of NER appears to be most involved in recognition and removal of corresponding lesions.<sup>59,60,170–173</sup> This section provides first a brief pertinent overview of TC-NER. Because the roles of various NER proteins have been assigned to particular pathways, it can be informative to test which are relevant in the biological response of a particular DNA-alkylating agent by testing the relative cytotoxicities of these chemicals in patient-derived cells with altered expression levels of individual or groups of proteins. Very interesting data has emerged when such studies have been performed with illudin S and HMAF, and the results and implications of these studies are presented here. In addition to TC-NER, homologous recombination is implicated in repair of AF-induced DSBs. This section summarizes, therefore, the role of TC-NER and RNA Pol II as well as homologous recombination in the cytotoxic activity of illudins and AFs.

### 12.1. Brief Overview of Nucleotide Excision Repair Pertinent to Illudin and Acylfulvene Interactions

The NER pathway accounts for more than 30 of the over 130 identified DNA repair-associated proteins in human tissue.<sup>174</sup> These proteins process lesions that interfere with DNA replication or transcription and distort the shape of the double helix. Upon activation, NER removes single-stranded DNA segments that include the lesion and creates a single-strand DNA gap. This gap is subsequently filled by DNA polymerases that use the undamaged strand as a template.

NER is divided into two subpathways: global genome GG-NER and TC-NER.<sup>170,172,174,175</sup> GG-NER is responsible for repairing transcriptionally inactive parts of the genome and nontranscribed gene segments, and GG-NER sites are typically evenly distributed throughout the genome.<sup>176</sup> TC-NER sites are uniquely localized at specific chromosomal domains and restricted to transcribed gene strands. GG-NER deficiency is associated with the cancer-prone syndrome xeroderma pigmentosum (XP),<sup>177</sup> while defective TC-NER results in Cockayne Syndrome (CS)<sup>178</sup> and trichothiodystrophy.<sup>179</sup>

GG-NER and TC-NER differ with respect to damage recognition and repair initiation and use different enzymes to execute DNA repair (Table 17).<sup>170,172,174,175</sup> For GG-NER,

**Table 17.** NER-Associated Genes and Proteins

implicated gene	HUGO nomenclature (CG)	GG-NER	TCR-NER	cancer prone deficiency <sup>b</sup>
XPA	XPA (XPA)	+	+	+
XPB	ERCC3 (XPB)	+	+	+
XPC	XPC (XPC)	+	−	+
XPB	ERCC2 (XPB)	+	+	+
XPD	ERCC2 (XPD)	+	+	+
XPE	DDB1/DDB2 (XPE)	+	+	+
XPF	ERCC4 (XPF)	+	+	+
XPG	ERCC5 (XPG)	+	+	+
CSA	ERCC8 (CSA)	−	+	−
CSB	ERCC6 (CSB)	−	+	−
ERCC1	ERCC1	+	+	unknown

<sup>a</sup>+ and − indicate involvement of a specified gene in GG-NER or TCR-NER. <sup>b</sup>+ and − indicate relationship of specified gene deficiencies and cancer development; DDB2, DNA damage-binding-2; ERCC, excision repair cross-complementing; GG-NER, global genomic nucleotide excision repair; HUGO, Human Genome Organisation; CG, complementation group; TCR-NER, transcription-coupled nucleotide excision repair.

damage recognition initiates with the binding of XPC-Rad23B and/or heterodimeric DDB1-DDB2 (XPE) binds to the damaged DNA segment. The XPC-Rad23B complex recognizes major distortions in DNA, and DDB1-DDB2 recognizes some UV irradiation-induced DNA dimers.<sup>180–182</sup> In TC-NER (Figure 5), blocked RNA pol II serves as a damage recognition signal.<sup>185,194</sup> In mammalian cells, TC-NER initiation is assigned to CSB and CSA.<sup>171,183–186</sup> CSA has been proposed to serve as a molecular chaperone, while CSB is an ATP-dependent chromatin remodeling factor<sup>187</sup> that is believed to interact with the stalled elongating RNA pol II and remodel the polymerase–DNA interface at the lesion.<sup>188</sup> CSB also serves to recruit factors CSA.<sup>171</sup> Damage recognition yields recruitment of transcription factor II H (TFIIH) and repair of the identified lesion via a common pathways for both GG-NER and TC-NER. The TFIIH constituent XPB and XPD helicases unwind DNA 5′ and 3′ of a damaged base, respectively, to create a 10–30 nucleotide bubble.<sup>182,189,190</sup> Finally, the ERCC1–XPF endonuclease complex incises the damaged DNA 5′ to the damage site, endonuclease XPG cuts out the bubble at the 3′ site of the damaged strand,<sup>170,172,191–194</sup> and XPA and RPA are verifying complex formation and orienting endonucleases.<sup>194–197</sup> Data from multiple independent studies suggest that illudin- and AF-induced damage is repaired by TC-NER.<sup>59,60,170–173</sup>



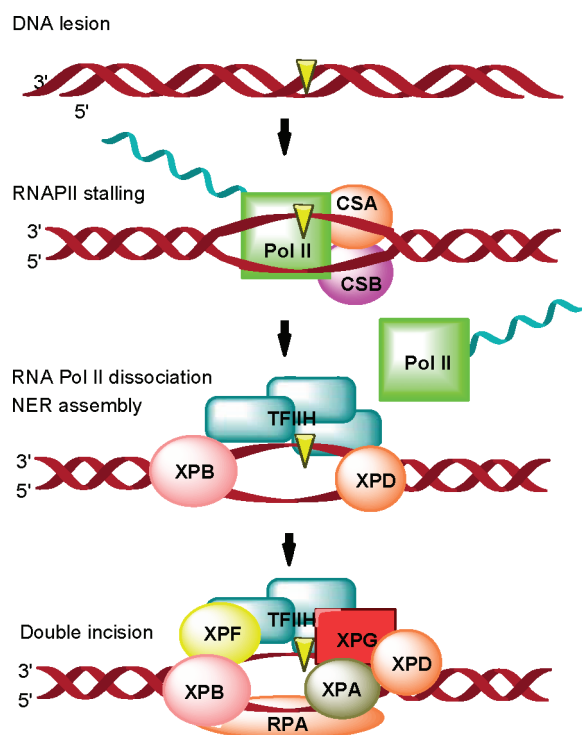


**Figure 5.** Transcription-coupled NER (TCR-NER) initiates after stalling of Pol II at the lesions (schematic representation). Colored boxes represent the enzymes involved in damage recognition, DNA unwinding, and damage removal.

## 12.2. Acylfulvene-Induced Cytotoxicity as a Consequence of TC-NER Status in Cancer Cells

Early information regarding which DNA repair pathways might be associated with AF-induced cell death resulted from cytotoxicity studies comparing the sensitivity of various UV-sensitive CHO cells to a number of drugs, including illudin S.<sup>59</sup> Thus, cells were exposed to illudin S, cisplatin, mitomycin C, or carmustine for 4 or 48 h and then evaluated for colony formation. From over a dozen tested UV-sensitive lines, growth of five lines (Table 18, entries 2–7) was inhibited ( $IC_{50} = 0.8$ –

mitomycin C, and carmustine, while UV5, UV24, and UV135, which are deficient in XPD, XPB, and XPG, were not. Drug uptake data for these cell lines indicates that illudin S accumulates equally in each type of cell and therefore cannot explain the differential cytotoxicity of illudin S.<sup>59</sup> Further, the transgenic cell line ST4-12, a UV5 derivative that expresses human ERCC2 and ERCC3, does not differ in illudin uptake (after 4 h) from the parent cell line but is resistant to the drug even after 49 h. These data suggest that ERCC2 and ERCC3 are involved in repairing illudin S-induced DNA damage and that cellular susceptibility to the drug relates to deficiencies in these components of NER.<sup>59</sup>

Cytotoxicity data for illudin S and AFs in cell lines derived from XP patients and mice suggest that TC-NER is a specific repair pathway for illudin S- and HMAF-induced DNA damage.<sup>60</sup> Thus, UV-sensitive NER-deficient XPA fibroblasts show about 10-fold enhanced susceptibility to illudin S ( $IC_{50} = 0.036$  nM) than normal control cells (SV40-transformed human fibroblasts,  $IC_{50} = 0.26$  nM).<sup>60</sup> Illudin S is highly toxic to other UV-sensitive cell lines that are deficient in XPB, XPD, XPF, and XPG enzymes, confirming the requirements of NER for drug-induced damage repair. In contrast, the XPC strains (XP21RO, XP3SRO, and XP4LE) and XPC-defective mouse fibroblasts (UV-sensitive, GG-NER-deficient) are resistant to illudin S. XPE cells, which are deficient in GG-NER-associated XPE helicase, are also resistant to illudin S. In contrast, XPF cells with residual GG-NER levels similar to XPC cells but deficient in TC-NER components are sensitive to illudin S well as to UV. Considering that XPC and XPE are proteins associated with GG-NER and that their deficiency does not affect the survival of illudin S-treated cells, it appears that the DNA lesions induced by illudin S are recognized preferentially by TC-NER. Consistent with this hypothesis is that TC-NER-deficient cells from CS<sup>178</sup> patients (CSA, CSB) are more sensitive to illudin S than to UV light. Again, because UV damage is repaired by both GG-NER and TC-NER and XPC and XPE cells are TC-NER deficient, illudin S adducts appear to be invisible to GG-NER.<sup>60</sup>

Like illudin S, HMAF-mediated cytotoxicity also appears to be TC-NER dependent.<sup>61</sup> Thus, HMAF is up to 30-fold more cytotoxic for NER-deficient XPA cells compared to repair-proficient human cells.  $IC_{50}$  values for HMAF in 20 tumor cell lines derived from eight solid tumor types correlate with NER deficiency of the tested cell lines.<sup>61</sup> On average, HMAF is significantly more active ( $IC_{50} = 0.34$   $\mu$ M) than cisplatin ( $IC_{50} = 2.1$   $\mu$ M) in all of the tested cell lines, including head and neck, lung, colon, breast, ovary, prostate, and glioma cells. XPB and XPD helicase-deficient cells are up to 20-fold more sensitive to HMAF than repair-proficient cells.<sup>61</sup> CSB-deficient CS539VI cells are more than 10-fold more sensitive to HMAF than normal 198VI cells, while XPC cells (deficient in GG-NER) are not affected by HMAF. HMAF also is highly active in NER-deficient XPF and XPG cell lines. It has been observed that HMAF cytotoxicity correlates with expression levels of the XPG endonuclease, while there is no consistent correlation with levels of other TC-NER-associated enzymes. These observations suggest that the response to HMAF-induced DNA damage directly depends on the effectiveness of TC-NER and that XPG might be a rate-limiting step in TC-NER-mediated repair of AF–DNA lesions.<sup>61</sup>

**Table 18.** Illudin S Cytotoxicity in UV-Sensitive Cell Lines

cell line	designation <sup>a</sup>	$IC_{50}^b$ (nM)
AA8	WT	$28.6 \pm 2.5$
UV20	ERCC1	$3.7 \pm 0.1$
UV5	ERCC2 (XPD)	$0.8 \pm 0.1$
UV24	ERCC3 (XPB)	$2.3 \pm 0.1$
UV41	ERCC4 (XPF)	$3.2 \pm 0.1$
UV135	ERCC5 (XPG)	$3.2 \pm 0.1$
UV61	ERCC6 (CSB)	$4.0 \pm 0.5$
UV40	XRCC9/FANCG	$16.7 \pm 1.6$
UVS1	ERCC11	$19 \pm 1.7$
EM9	(XRCC1)	$25.9 \pm 2.4$
7PVTOR	ERCC9	>30
4PVTOR	ERCC10	>30

<sup>a</sup>Designation indicates proteins compromised in the specified cell line.

<sup>b</sup>Concentrations producing a 50% decrease in the cell count after 4 h exposure (mean  $\pm$  SD for 3–5 determinations by standard MTT assay).

4.0 nM/L) by illudin S. Of these, UV20 and UV41 cell lines deficient in ERCC1 and XPF also are sensitive to cisplatin,



### 12.3. Acylfulvenes Disrupt RNA Synthesis

AF-induced cell death also may be mediated by suppressed RNA synthesis,<sup>57</sup> due to stalling of the elongating RNA pol II at the AF-induced DNA lesion.<sup>171,198</sup> RNA synthesis is reduced by 50% within HeLa cells exposed to 2  $\mu$ M HMAF.<sup>57</sup> HMAF does not, however, arrest RNA synthesis completely even at high doses, suggesting that the drug inhibits only certain types of polymerases.<sup>198</sup> Comparative inhibition studies with actinomycin D (nucleoplasmic transcription inhibitor), 5,6-dichloro-1-beta-D-ribofuranosylbenzimidazole (DRB, RNA pol II inhibitor), bromouridine (inhibitor of mitochondrial and nucleoplasmic RNA synthesis), and HMAF showed that HMAF inhibits only nucleoplasmic incorporation and does not affect mitochondrial RNA synthesis. The disruption of RNA synthesis is reversible. Cells initially incubated with HMAF recover RNA synthesis once the HMAF is removed from the cell culture and TC-NER is complete. These data suggest that suppression of RNA synthesis by AFs is due largely to disruption of DNA translation and not damage to the RNA polymerases.<sup>198</sup>

Effective TC-NER requires access to the DNA damage site for incision and removal of the lesion. However, RNA pol II, stalled at the AF–DNA lesion site, hinders approach of the repair factors. This was clearly observed in bacterial systems where stalled RNA pol II blocked the access of photolyase.<sup>199,200</sup> Similarly, RNA pol II accumulates at HMAF-induced DNA lesions, and the fraction of the engaged enzyme is increased in a dose-dependent manner, but the non-committed RNA pol II is not impacted.<sup>198</sup> Hence, the question requiring attention is the fate of the stalled RNA pol II after initiation of repair and whether stalling is toxic.

Transcript elongation by RNA pol II is accompanied by frequent pausing. Consequently, efficient transcription requires removal of the stalled protein. Two possible outcomes are TC-NER initiation or RNA pol II degradation.<sup>61</sup> RNA pol II-mediated transcription is strand specific and does not involve special lesion-bypass polymerases, such as those involved in DNA replication. Hence, irreversible stalling of RNA pol II at the AF–DNA lesion site has to be overcome either by repair or by physical removal of the polymerase, and evidence for both exists.<sup>201</sup> It was observed that pol II is ubiquitinated and degraded through proteolysis. At the same time, the necessity of transcriptional recovery and natural degradation of the stalled RNA pol II suggests that the polymerase stalling by itself does not contribute to cell death.<sup>202</sup> All these findings suggest that HMAF-mediated apoptosis of TC-NER-deficient CS cells is triggered through accumulation of the stalled RNA pol II on the DNA lesion due to insufficient ubiquitylation and proteolysis.<sup>203,204</sup> However, a direct comparison of TC-NER-deficient and proficient cells reveals that the only difference in the ubiquitylation and proteolysis of RNA pol II is in the kinetics of the processes (the CSB or CSA cells are less efficient). This finding diminishes the role of RNA pol II stalling in cell apoptosis and invokes the possibility of RNA pol II degradation in initiating apoptosis.<sup>205</sup>

On the basis of the observation that even in the presence of a stalled RNA pol II XPG, and XPF endonucleases effectively doubly incise AF-induced DNA damage, AF cytotoxicity appears to depend on the effectiveness of TC-NER and not on RNA pol II stalling.<sup>184,206</sup> There is therefore a possible conformational change of RNA pol II induced by either XPG or TFIIH that allows DNA repair. In vitro studies with a 10 nucleotide DNA bubble showed that addition of RNA pol II,

prior to XPG, blocked incision by 90% as compared to the complete incision observed in the absence of polymerase.<sup>197</sup> This result is attributed to preferential complexation of XPG with stalled polymerase as opposed to recognition of the DNA bubble. However, the effective incision of XPG is not due to the release of stalled RNA pol II but due to TFIIH-induced modification of the stalled RNA pol II that allows XPG to access the DNA bubble bound to the RNA pol II and cut it.<sup>197</sup> This model correlates with an enhanced activity of AFs in XPG-deficient cells and with the critical role of XPG in TC-NER of AF-induced lesions.

Published findings suggest that TC-NER plays a unique role in AF cytotoxicity and that TC-NER deficiency controls AF-induced damage. It is noteworthy that TC-NER deficiency is not limited to XP or CS cells but is also observed in solid tumors. For instance, upon treatment of cells from patients with lung, head, and neck cancers with HMAF, decreased DNA repair caused by host-cell deactivation of a damaged reporter plasmid was observed.<sup>207</sup> In agreement with this observation is loss of heterozygosity of genes encoding the NER proteins in ovarian tumor and carcinoma cells<sup>208</sup> and malignant gliomas, lung, and colon tumor cells.<sup>209–212</sup> Overall, these observations are fully consistent with the strong cytotoxicity of AF in certain types of cells, such as ovarian, lung, colon, and head and neck.

### 12.4. Homologous Recombination and Repair of Acylfulvene-Induced DNA Damage

Homologous recombination (HR) is another DNA repair pathway that affects AF cytotoxicity. This has been concluded from the dependence of HMAF cytotoxicity on the status of BRCA and Fanconi anemia proteins (FANCD2),<sup>145,213</sup> which are involved in homology-directed repair of double-strand breaks.<sup>214–216</sup> For these studies, BRCA1-proficient or -deficient HCC1937 cell lines were used to compare AF–DNA damage repair dynamics.<sup>145</sup> After 1 h of treatment with HMAF, the number of genomic DNA fragments (from 50 to >400 kb) gradually increased in the BRCA1-deficient (i.e., vector-transfected) HCC1937 cells over a period of postincubation in drug-free media for 6–48 h. In BRCA1-transfected HCC1937 cells, DSBs were repaired under the same treatment conditions, suggesting the involvement of BRCA1 in the repair of AF-induced DSBs.<sup>145</sup> Further, BRCA1-knockout SKOV3 cells were used to evaluate chromosome aberrations upon HMAF treatment. The level of chromosome breaks increased in untreated BRCA1 knockout SKOV3 cells, as compared to the normal control, and further exacerbated after HMAF treatment, suggesting that BRCA1 maintains chromosome integrity in response to AF-induced DNA damage.<sup>145</sup>

RAD51 is a DNA recombinase critical for initiation of HR repair of DSBs.<sup>217</sup> To establish the connection between HMAF-induced DSBs and BRCA1, HR, and RAD51 foci formation in BRCA1-transfected HCC1937 cells was evaluated relative to those in blank-transfected HCC1937 cells. As evidenced by immunofluorescent staining data while inducing analogous levels of DNA fragmentation, HMAF induces larger accumulation of RAD51 in BRCA1-transfected HCC1937 cells (from 4.7% of untreated cells to 40.3%) than in vector-transfected HCC1937 cells (from 2.8% to 13.2%), suggesting that RAD51 accumulation and, therefore, subsequent HR activation is dependent on BRCA1. With respect to the role of BRCA1 in repairing HMAF-induced DSBs, these results demonstrate that RAD51-dependent HR repair is involved and that BRCA1 is critical for this process.<sup>145</sup>

The involvement of HR in repairing AF-induced DBSs has also been addressed by testing the role of FANCD2, which is generally necessary for homology-directed repair of DSBs. DNA damage-induced monoubiquitination of FANCD2 leads to its colocalization with BRCA1.<sup>216</sup> HMAF-treating ovarian cancer cells (SKOV3) that were stably transfected with short hairpin FANCD2 lead to monoubiquitination of FANCD2,<sup>213</sup> suggesting recognition of AF-induced DSBs by HR. The fact that FANCD2 is monoubiquitinated in response to HMAF also suggests that HMAF-induced DSB is a replication-associated DNA damage.<sup>218</sup> Overall, while formation of DSBs may be contributing to AF cytotoxicity, the status of HR, in addition to TC-NER, should be considered as a factor, dictating the expected outcome of AF treatment.

### 12.5. Acylfulvene-Induced Abasic Sites and Base Excision Repair

AF-induced DNA alkylation yields abasic sites as a result of depurination of Ade and Gua adducts (section 9.1);<sup>58</sup> however, data from studies in which cells that are compromised in their capacity to repair abasic sites are treated with illudin S or AFs do not suggest a role for abasic sites in AF or illudin S cytotoxicity.<sup>59</sup> EM9 cells deficient in XRCC1 endonuclease, a critical base excision repair (BER) enzyme, are as resistant to AFs as fully repair-proficient cells.<sup>59</sup> BER typically copes effectively with abasic sites in the range of  $10^5$  per diploid per day.<sup>219</sup> It involves the three distinct phases of lesion recognition/strand scission, DNA gap tailoring, and DNA synthesis/ligation. Each are coordinated by the XRCC1/DNA Ligase III $\alpha$  and Poly[ADP-ribose] polymerase 1 (PARP1) scaffold protein complexes and associated interacting proteins.<sup>220</sup> Therefore, XRCC1 deficiency can be considered a global deficiency of BER. Accordingly, resistance of BER-deficient EM9 cells to AFs suggests that AF-induced damage may be recognized by TC-NER faster than adduct depurination, which would result in a BER-processed abasic site. These data suggest that previously characterized depurinating AF adducts<sup>54,57,142</sup> are sufficiently stable in cells to contribute directly to cellular responses and/or that biologically important and chemically stable AF–DNA adducts are as yet uncharacterized. Further research needed to reconcile these toxicological possibilities, which are important not only for these molecules but of fundamental relevance to addressing biological responses of DNA-reactive cytotoxins on a chemical level.<sup>221–224</sup>

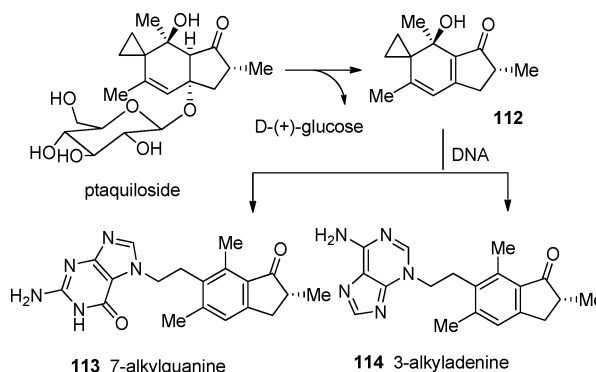
## 13. CHEMICALLY AND MECHANISTICALLY RELATED CYTOTOXINS

DNA alkylation is the oldest mode of chemotherapeutic cytotoxicity, and there are several natural products that alkylate DNA by reacting at an electrophilic cyclopropane ring. Examples include ptaquiloside, CC-1065, duocarmycin, and yatakemycin.<sup>18,225–228</sup> Some other chemotherapeutics, such as mitomycin, involve aziridines and epoxides to induce DNA damage. All of these agents, including AFs, appear to be pro-apoptotic DNA minor-groove binders. With the goal of establishing a greater understanding of the chemical and biochemical basis of drug cytotoxicity in cancer cells, it is extremely valuable to compare and contrast their biological impacts on the basis of their chemical structures.

### 13.1. Cyclopropane-Containing DNA Alkylators

Ptaquiloside (Scheme 15) is a norsesquiterpene glucoside natural product of the illudane type most closely structurally related to AFs. It was isolated from the bracken fern, *Pteridium*

**Scheme 15.** Natural Product Ptaquiloside Forms Guanine and Adenine Adducts



*aquilinum*, and is toxic for livestock, causing bracken poisoning.<sup>14–16,18,229</sup> Humans are exposed to ptaquiloside poisoning by direct consumption or via milk contaminated from cows feeding on bracken, and the poisoning is thought to be causally associated with an increased incidence of gastric cancer.<sup>230–233</sup> The carcinogenicity of ptaquiloside in rats was supported by data reported in 1984 by Hirono and co-workers.<sup>234,235</sup> Further, the role of ptaquiloside in the characteristic biological effects of bracken, such as acute bracken poisoning, bright blindness in sheep, mutagenicity, clastogenic effects, and genotoxicity, have been assessed in various studies.<sup>234,235</sup> Other studies showed that *P. aquilinum* depresses bone marrow activity in rats and results in severe leucopenia, thrombocytopenia, and the hemorrhagic syndrome.<sup>236–238</sup>

Ptaquiloside is unstable in acid or base and forms an aromatic indanone in a transformation that proceeds through the highly reactive dienone 112 and subsequent nucleophilic addition to yield ring-opened products 113 and 114 (Scheme 15). Under physiological conditions, ptaquiloside modifies DNA very much like AFs, with the corresponding aromatic moiety linked to the 7 position of guanine and 3 position of adenine.<sup>228,239</sup>

CC-1065 (Figure 6), a highly toxic cyclopropane ring-containing antibiotic isolated from *Streptomyces zelensis*,<sup>240</sup> is

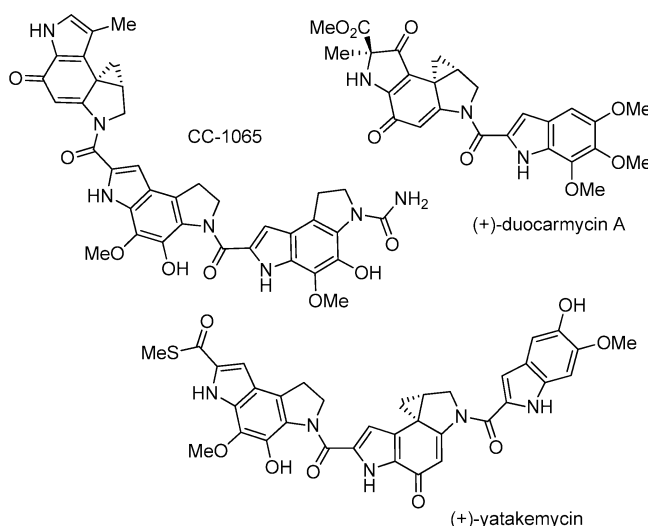


**Figure 6.** CC-1065, (+)-duocarmycin, and (+)-yatakemycin as chemical and biochemical analogs of AFs.

cytotoxic in vitro, displays antitumor activity in vivo, and is significantly more toxic than actinomycin or vinblastine.<sup>241</sup> CC-1065 interacts with double-stranded DNA, is specific for adenine (A)- and thymine (T)-rich sites, and appears to exert its cytotoxic effects by disrupting DNA synthesis. However, unlike other conventional DNA-alkylating agents causing DNA strand breaks, CC-1065 stabilizes the DNA helix. It raises the thermal melting temperature of DNA, inhibits the ethidium-induced unwinding of DNA, and inhibits susceptibility of DNA to nuclease S1 digestion.

Duocarmycins and yatakemycin (Figure 6), the natural compounds isolated from a culture broth of *Streptomyces* species, also act as DNA-alkylating agents on the basis of the electrophilicity of the fused cyclopropyl ring. These compounds are unreactive toward general nucleophiles at physiological pH but are highly efficient in reacting with DNA to form adducts at the minor groove in adenine/thymidine (A/T)-rich regions and alkylate adenine at the 3 position. These reactivity patterns are thought to arise from shape-dependent catalysis involving molecular recognition-mediated activation of the molecules as a result of noncovalent DNA binding.<sup>242</sup> Despite their structural relationship with one another, these compounds demonstrate clear differences in sequence-dependent DNA reactivity. Thus, duocarmycin A preferentially alkylates the 3'-terminal adenine of five base-pair A/T tracts, while duocarmycin SA interacts with a three to four base-pair A/T tracts.<sup>225,243–245</sup> An even more significant difference observed for yatakemycin is that the two subunits interact with DNA to form DNA duplex sandwiched complexes.<sup>243,246,247</sup> All three natural products possess remarkably high cytotoxicity with pM IC<sub>50</sub> values established in L1210 cells.<sup>248</sup>

### 13.2. Epoxide- and Aziridine-Containing DNA Alkylators

Mitomycin C (MMC, Figure 7A) shares a close mechanistic basis with AF-alkylating agents, and information regarding its

activity is highly instructive in this regard. As AFs, MMC is reductively bioactivated prior to DNA alkylation by trans-formation of quinone into an aromatic hydroquinone, causing elimination of CH<sub>3</sub>OH and formation of a bioactivated alkylation agent **115** and the resonance indolohydroquinone **116** (Figure 7A).<sup>249</sup> Modification of DNA by **116** occurs via opening of the aziridine moiety and results in a monoalkylated DNA adduct **117**. The formed adduct is identified to lose a carbamate moiety and form an intermediate poised to the second nucleophilic attack by DNA, giving bifunctionally alkylated end product and resulting in DNA–DNA cross-links.<sup>250</sup>

Azinomycin B (carzinophilin) and its structurally related analog azinomycin A are DNA-alkylating agents with high antitumor activity (Figure 7B).<sup>251–253</sup> Similarly to AFs, the cytotoxicity of azinomycins is based on formation of covalent DNA adducts through alkylation by electrophilic aziridine and epoxide moieties.<sup>254</sup> Cross-linking mediated by azinomycins proceeds in two steps, the first being alkylation of the 7 position of adenine and the second step taking place between the epoxide and the 7 position of guanine.<sup>254</sup> The corresponding lesions interfere with gene transcription and lead to cell death. However, unlike AFs, azinomycins tend to form covalent interstrand cross-links within the major groove of duplex DNA at 5'-GXC or 5'-GXT. The in vivo therapeutic potential of the azinomycins has not been well addressed despite their antimicrobial activity and high in vitro cytotoxicity. A main limiter is the low chemical stability of the compounds. However, structural analogs of azinomycin have been assessed, and studies of the role of DNA alkylation in the activity of the drug are in progress.<sup>255–258</sup>

### 13.3. Eteinscadin 743

Dependence of cellular cytotoxicity on the status of DNA repair is a feature that links AFs and Eteinscadin 743 (ET-743, Figure 8), a natural DNA-alkylating tetrahydroisoquinolone

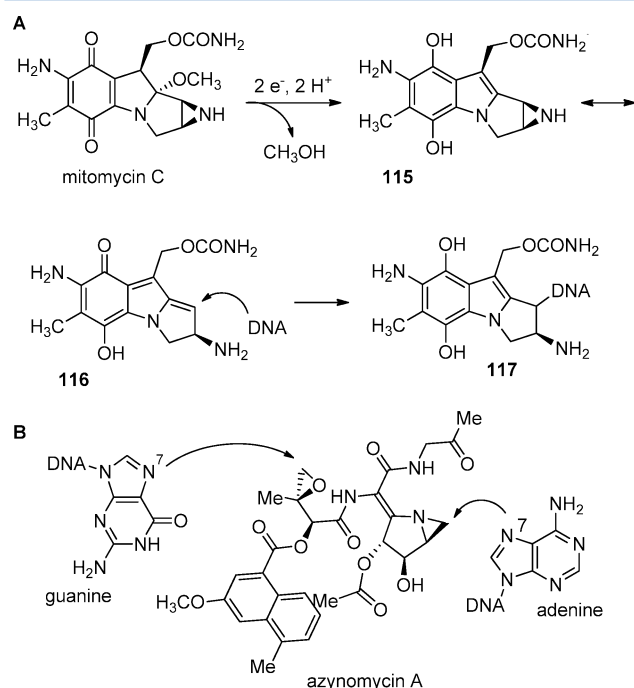


**Figure 7.** Bioactivated mitomycin C and azinomycin A as chemical and biochemical analogs of AFs.

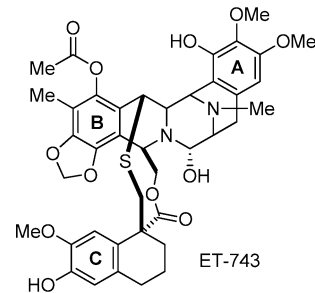


**Figure 8.** ET-743 as mechanistic analog of AFs.

alkaloid and currently used anticancer agent.<sup>259–261</sup> Similar to HMAF, ET-743 is a DNA minor-groove binder. It alkylates guanines at the N<sup>2</sup>-position and induces a bend in DNA toward the major groove. ET-743-induced damage, in analogy to AFs, stalls DNA replication and induces replication-dependent DSBs that are repaired via homologous recombination.<sup>145,262</sup> ET-743 is highly potent against breast, nonsmall-cell lung, and ovarian cancers and melanomas.<sup>263</sup> Comparative cytotoxicity studies of ET-743 with a variety of DNA damage-oriented chemotherapeutics in various cell lines revealed a high activity of the alkaloid in cells resistant to cisplatin and adriamycin and high potency in paclitaxel-resistant cells (breast, melanoma, nonsmall lung, and ovarian cell lines). ET-743 is currently approved in the European Union as a drug for soft tissue sarcomas and



also in clinical studies for breast, ovarian, and prostate cancers and pediatric sarcomas.<sup>264</sup>

Cytotoxicities of AFs and ET-743 in various cell lines are complementary to one another and correlate with TC-NER status, i.e., while AFs are more active in cells with compromised TC-NER, ET-743 is active in TC-NER-proficient cells.<sup>22</sup> Thus, XPA-, XBD-, XPF-, XPG-, CSA-, and CSB-deficient cells are 10–23-fold more resistant to ET-743 than their isogenic parental cells. The efficacy of ET-743 in repair-proficient cells was correlated with two factors: bending of DNA toward the major groove at an angle of about 17°, causing a significant distortion of the duplex, and interaction with XPG.<sup>265</sup> The structure of ET-743 consists of three subunits A, B, and C and a carbonilamine center. Subunits A and B are responsible for binding to the minor groove, while DNA alkylation with the carbinilamine moiety occurs at the N<sup>2</sup> position of guanine in GC-rich regions, with preferences for 5'-GGC, 5'-AGC, and 5'-GGG sequences.<sup>263,266</sup> In such an arrangement, the C subunit is directed out of the minor groove and proposed to interact with XPG, thus trapping the XPG–DNA complex at single-strand breaks and preventing further repair of DNA damage. The resulting inhibition of the regulation of gene transcription possibly contributes to the cytotoxic activity of the compound.<sup>265–269</sup>

## 14. HMAF CLINICAL TRIALS: CURRENT STATUS AND RESULTS

The promising therapeutic properties and satisfactory pre-clinical evaluation of HMAF led to more advanced human clinical trials where the compound was tested as a drug against various types of cancer, including renal cell carcinoma and melanoma. Several studies were carried out to evaluate HMAF toxicity and pharmacologic behavior,<sup>270</sup> population pharmacokinetics,<sup>271</sup> clinical tolerability,<sup>28</sup> MTD, and dose-limiting toxicities (DLT) in combination with other chemotherapeutics.<sup>29,272</sup> This section provides a brief overview of HMAF phase I, II, and III clinical trials and outcomes.

### 14.1. Population Pharmacokinetics and Phase I Clinical Trials

HMAF toxicity was determined when administered as a 5 min intravenous dose daily for 5 days every 4 weeks to 46 patients with advanced solid malignancies. Patients were treated with doses ranging from 1.0 to 17.69 mg/m<sup>2</sup>, and the pharmacokinetic studies were performed on days 1 and 5 to characterize the plasma disposition of HMAF. After a total of 92 courses of HMAF the dose limiting toxicity (DLT) on this schedule was myelosuppression and renal dysfunction at up to 14.15 mg/m<sup>2</sup>. A higher dosage of the drug (17.69 mg/m<sup>2</sup>) produced level four neutropenia and renal toxicity. Other common toxicities included mild to moderate nausea, vomiting, facial erythema, and fatigue. Pharmacokinetic studies of HMAF revealed dose-proportional increases in both maximum plasma concentrations and area under the concentration–time curve, while the agent exhibited a rapid elimination half-life of 2–10 min. As a result the recommended dose was 10.64 mg/m<sup>2</sup> as a 5 min IV infusion daily for 5 days every 4 weeks. Effective antitumor activity was documented in a patient with advanced pancreatic cancer.<sup>270</sup>

The MTD, DLT, and plasma pharmacokinetics of HMAF in children (<21 years of age) with refractory/recurrent malignancies were also reported after a phase I trial. Thirty-four patients received HMAF daily for 5 days every 28 days

over 10 min, following pretreatment with ondansetron<sup>7</sup> (0.45 mg/kg) and dexamethasone (12 mg/m<sup>2</sup>). Dose limitation varied with pretreatment. Thus, in heavily pretreated patients dose-limiting thrombocytopenia was observed at 6–8 mg/m<sup>2</sup>/day. In less heavily pretreated patients, doses of 13–17 and 10 mg/m<sup>2</sup>/day were proposed as the MTD.<sup>273</sup>

A population pharmacokinetic model for and evaluation of variables that might affect HMAF pharmacokinetics were derived from phase I studies with 59 cancer patients. HMAF was administered by 5- or 30-min intravenous infusion, and blood samples were collected over 4 h. Plasma samples were analyzed to quantitate HMAF, and population pharmacokinetic analysis was performed using a nonlinear mixed effects modeling program, MP2. Final parameter estimates of clearance and central volume of distribution were 616 and 37 L/h, respectively, resulting in a very short terminal half-life of less than 10 min and were not significantly influenced by individual characteristics, i.e., body weight, body surface area, age, and gender. In addition, the optimal sampling schedule for clearance estimation was 0.35–0.45, 0.80, and 1–1.2 h from the beginning of a 30 min infusion.<sup>271</sup>

HMAF clinical tolerability was derived from a different phase I trial, where HMAF was given as a 30 min intravenous infusion daily for 5 days every 28 days. Ten patients were treated with 6, 8, and 11 mg/m<sup>2</sup> per day. After infusions, HMAF reached steady-state concentrations and disappeared rapidly from plasma within 15–30 min. The mean half-life of HMAF in plasma was 4.91 min, and the mean clearance was 4.57 L/mm per m<sup>2</sup>. Thus, the recommended dose for the phase II clinical trials was 6 mg/m<sup>2</sup>.<sup>28</sup>

HMAF was taken into phase I clinical studies in patients with primary refractory or relapsed acute myeloid leukemia, acute lymphocytic leukemia, or myelodysplastic syndromes, and the toxicity profile and activity of the drug were investigated.<sup>274</sup> It was given as a 5 min intravenous infusion daily for 5 days with the starting dose of 10 mg/m<sup>2</sup>/day (50 mg/m<sup>2</sup>/course). Courses were scheduled to be given every 3–4 weeks to 20 patients according to toxicity and antileukemic efficacy. Nausea, vomiting, hepatic dysfunction, weakness, renal dysfunction, and pulmonary edema were the dose-limiting toxicities, occurring in 2 of 5 patients treated at 20 mg/m<sup>2</sup>/day and 2 of 3 patients treated at 12.5 mg/m<sup>2</sup>/day. The MTD was defined as 10 mg/m<sup>2</sup>/day for 5 days. One patient with primary resistant acute myeloid leukemia achieved complete remission in this study. As a result, HMAF was proposed for phase II studies in patients with this type of acute myeloid leukemia and in other hematological malignancies, both as a single agent and in combination regimens, particularly with topoisomerase I inhibitors.<sup>274</sup>

Phase I studies also covered the use of HMAF in combination therapy. The MTD, recommended dose, DLT, safety, and pharmacokinetics were investigated for HMAF/capecitabine<sup>29</sup> and HMAF/cisplatin<sup>272</sup> combinations in advanced solid tumor patients. HMAF/capecitabine and HMAF/cisplatin were adequately tolerated, and evidence of antitumor activity was observed. The recommended doses for HMAF/capecitabine and HMAF/cisplatin were 0.4 mg/kg HMAF and 2000 mg/m<sup>2</sup> capecitabine per day and 0.4 mg/kg HMAF and 30 mg/m<sup>2</sup> cisplatin per day, respectively.

As of 1998, clinical trial results indicated that significant doses of HMAF could be administered to humans before a dose-limiting degree of bone marrow suppression was observed.<sup>144</sup> Unique tumor specificity and promising antitumor

effects of HMAF observed on intermittent dosing schedules supported further disease-directed evaluations in phase II clinical trials.

#### 14.2. HMAF Phase II and Phase III Clinical Trials

Despite promising results in phase I clinical trials, there were disappointing patient responses to HMAF in phase II trials. Thirteen patients with advanced renal cell carcinoma,<sup>275</sup> 16 patients with stage IV melanoma,<sup>276</sup> patients with advanced nonsmall cell lung cancer previously treated with chemotherapy (carboplatin and paclitaxel  $\pm$  radiation, cisplatin and CPT-11),<sup>277</sup> and patients with nonsmall lung carcinoma<sup>278</sup> were treated with 11 mg/m<sup>2</sup> HMAF by 5 min intravenous infusion on 5 consecutive days every 28 days. No significant response to the treatment was detected.

The most common patient toxicities toward HMAF were grade 1/2 nausea, vomiting, fatigue, anemia, and thrombocytopenia. Patients with recurrent or metastatic gastric cancer tolerated HMAF at a dose of 0.45 mg/kg administered intravenously over a 30 min infusion (up to a maximum of 50 mg); however, no antitumor activity was detected.<sup>279</sup> Patients with recurrent ovarian cancer who received extensive prior chemotherapy were treated with HMAF every 14 days with a dose of 24 mg/m<sup>2</sup> and showed unanticipated retinal toxicities. The dose was changed to 0.55 mg/kg on the same schedule with a maximum individual dose of 50 mg. Nevertheless, out of 148 women, including patients with platinum-resistant disease and with platinum-sensitive disease, 30 women experienced visual symptoms. The majority of visual toxicities resolved either during treatment or post-treatment with HMAF. There was one partial response among 19 women with platinum-resistant disease and for 1 among 8 women having platinum-sensitive diseases. Yet, HMAF demonstrated only limited antitumor activity.<sup>280</sup>

In contrast, encouraging results and an acceptable safety profile were derived from trials for patients with hormone-refractory prostate cancer. The trials were performed to assess HMAF antitumor activity by measuring a sustained decrease of 50% or greater in serum prostate-specific antigen levels. Forty-two patients (median age, 73 years) who had pathologically confirmed metastatic hormone-refractory adenocarcinoma of the prostate and had not received prior cytotoxic chemotherapy received at least one dose of 10.6 mg/m<sup>2</sup> HMAF per day on days 1–5 every 28 days. Four patients (13%) achieved a partial response, with a median duration of 2.9 months (range, 2.6–5.8 months), 27 patients (84%) had disease stabilization, and 1 patient (3%) progressed on study. Median progression-free survival was 3.2 months (95% confidence interval, 2.3–4.2 months) for all patients, compared to 4.2 months (range, 3.5–6.9 months) for responders. The most common treatment-related grade 3 nonhematologic toxicities included asthenia, vomiting, nausea, and infection without grade 3/4 neutropenia.

Multicenter phase II trials were also conducted to evaluate the activity and toxicity of HMAF in patients with previously treated adenocarcinoma of the endometrium. Patients were treated at an intravenous dose of 11 mg/m<sup>2</sup>/day for 4 days every 28 days. Doses were escalated or reduced based on previous cycle toxicity. Out of 25 enrollees, there was 1 (4%) with confirmed complete response. Seven (28%) patients had stable disease, with a median duration of 10.4 (range 4.4–21.6) months. Patients received a median of one (range 1–5) cycle of protocol treatment. There were 3 early treatment-related deaths due to renal failure and severe electrolyte disturbances. HMAF

was concluded to be minimally active and significantly toxic at this schedule and dose.<sup>281</sup>

Visual symptoms induced by HMAF led to studies aiming to better characterize the visual adverse events of HMAF and provide treatment guidelines. Clinical data from 277 patients entered in single-agent phase I/II clinical trials who received HMAF were included in this multiparameter analysis. Overall, 74 patients (27%) experienced visual symptoms. The most frequently reported symptoms were flashing lights, blurred vision, and photosensitivity. The occurrence and severity of visual events were dose dependent, with no grade 3 visual events occurring at low doses (0.50 mg/kg) and grade 1–2 events occurring in small numbers of patients at doses between 0.50 mg/kg (12%) and 20 mg/m<sup>2</sup> (8%). Grade 1–2 toxicity was reversible in most patients.<sup>282</sup>

The U.S.-based biopharmaceutical company MGI PHARMA supported the advancement of HMAF into phase III clinical trials for refractory pancreatic cancer patients. These trials were prematurely terminated in April 2002 however. Despite favorable HMAF activity, preliminary analysis of the phase III data by an independent board suggested that the comparison arm involving 5-fluorouracil (5-FU) demonstrated a greater than expected survival benefit and that it would be statistically improbable that HMAF would outperform 5-FU in this study. For about the 5 subsequent years, MGI PHARMA continued to pursue trials and AF analogues with improved therapeutic properties; however, since acquisition of MGI by the Japanese pharmaceutical company Eisai was announced in late 2007, to our knowledge no further trials or reports of AF-related advances outside of basic academic research have appeared.

## 15. CONCLUSIONS AND PERSPECTIVES

Research centered on AFs have advanced cancer drug development by providing a test system for exploring factors that impact tumor specificity, such as preferential bioactivation, cellular uptake, DNA alkylation patterns, DNA repair, inhibition of redox-regulating enzymes, and understanding how all of these biological processes are influenced by changes in chemical structure. These data provide a rational basis for further tuning AF activity and designing novel analogs that will exploit the biological factors that influence AF cytotoxicity. Studies centered on AF and illudin chemical reactivity and chemical transformations identified modes of metabolism, biomolecule alkylation, enzyme inhibition properties, and possible means of resistance. AFs are reductively bioactivated, and data suggests that the tumor specificity characteristic for these compounds depends on reductase activity in tumor cells. Bioactivation results in formation of a reactive intermediate that alkylates cellular nucleophiles and genomic DNA. Resulting DNA adducts interfere with transcription, induce single-strand breaks, and initiate apoptosis.

Without the requirement for reductive bioactivation, AFs react with and inhibit cellular thiol-containing redox-regulating proteins. Aspects of illudin versus AF potency toward enzymes counter expectations established from small-molecule studies and suggest a potential role for AF-mediated interactions with proteins as a contributor to toxic selectivity. This possibility has implications for the activity of AFs in combination with conventional therapeutics and therefore requires further investigation. Finally, illudins and AFs have emerged as a unique tool to study DNA damage repair and specifically TC-NER and its role in chemotherapy independent of the actions of the GG-NER pathway.

After more than 50 years of illudin investigation and the more recent 15 year focus on the derivative AFs, our understanding of how chemical and biological factors come together to dictate the selectivity and effectiveness with which natural products kill cancer cells has vastly improved. Fundamental questions remain that may be addressed by building on the knowledge gained from illudin and AF research and by a combination of existing and new chemistries and structural analogs. Intriguing outstanding questions include, but are not limited to, modulating AF-toxicity-controlling enzymes and elucidating the molecular basis of the specificity of the interactions of AF–DNA damage with NER machinery. Understanding the chemical and biological factors that contribute to AF activity could open new research areas involving application of AF analogs, related natural or natural product-derived cytotoxins, and novel chemical structures, as well as biological strategies that selectively modulate pathways targeted by AFs.

## AUTHOR INFORMATION

### Corresponding Author

\*E-mail: sturlas@ethz.ch.

### Notes

The authors declare no competing financial interest.

### Biographies



Marina Tanasova was born in 1974 in Tbilisi, Republic of Georgia. She obtained her B.S. (1996) and M.S. (1998) degrees in Chemistry at Georgian Technical University and Ph.D. degree in Chemistry at Michigan State University in 2009. Marina is a Postdoctoral Fellow of the Susan G. Komen for the Cure Foundation and since 2010 has been a Postdoctoral Associate at the University of Minnesota and the ETH Zurich. Her research aims involve understanding acylfulvene mechanisms of cytotoxicity and developing acylfulvene-based chemotherapeutics targeting DNA and DNA repair-associated enzymes.



Shana J. Sturla was born in 1975 in Brooklyn, NY. She obtained her B.S. degree in Chemistry at the University of California at Berkeley in 1996 and Ph.D. degree in Chemistry at the Massachusetts Institute of Technology in 2001. From 2004 to 2009 was an Assistant Professor at the University of Minnesota. Since 2009, she has been a Professor at the ETH Zurich. The goal of her research is to understand how chemicals impact disease incidence and treatment. Researchers in her lab address the chemical basis of molecular mechanisms of toxicity by investigating relationships between chemical structure, biotransformation, and cellular responses. Their website is [www.toxicology.ethz.ch](http://www.toxicology.ethz.ch).

## ACKNOWLEDGMENTS

We thank Melissa Stauffer, Ph.D., of Scientific Editing Solutions and Heidi Dahlmann for editorial assistance and Professor D. Tyler McQuade for helpful suggestions. We acknowledge the contributions of past and present researchers in our lab who contributed to the scientific basis of significant portions of this review, including Dr. Jiachang Gong, Dr. Xiaodan Liu, James Neels, Kathryn Pietsch, as well as Dr. Xiang Yu.

## REFERENCES

- (1) Anchel, M.; Hervey, A.; Robbins, W. J. *Proc. Natl. Acad. Sci. U.S.A.* **1950**, *36*, 300.
- (2) Anchel, M.; Hervey, A.; Robbins, W. J. *Proc. Natl. Acad. Sci. U.S.A.* **1952**, *38*, 927.
- (3) Nakai, K. *Med. Biol.* **1958**, *49*, 129.
- (4) Shirahama, S. F.; Matsumoto, T. *Bull. Chem. Soc., Jpn.* **1962**, *35*, 1047.
- (5) Nakanishi, K.; Ohashi, M.; Tada, M.; Yamada, Y. *Tetrahedron* **1965**, *21*, 1231.
- (6) Matsumoto, T.; Shirahama, H.; Ichihara, A.; Fukuoka, Y.; Takahashi, Y.; Mori, Y.; Watanabe, M. *Tetrahedron* **1965**, *21*, 2671.
- (7) McMorris, T. C.; Moon, S.; Ungab, G.; Kerekes, R. J. *J. Nat. Prod.* **1989**, *52*, 380.
- (8) Engler, M.; Anke, T.; Sterner, O. *Z. Naturforsch. C.* **1998**, *53*, 318.
- (9) Kirchmair, M.; Poder, R.; Huber, C. G. *J. Chromatogr. A.* **1999**, *832*, 247.
- (10) McMorris, T. C.; Anchel, M. *J. Am. Chem. Soc.* **1965**, *87*, 1594.
- (11) Hanson, J. R.; Marten, T.; Nyfeler, R. *J. Chem. Soc., Perkin Trans. I* **1976**, *8*, 876.
- (12) Hanzlik, R. P.; Kishore, V.; Tullman, R. *J. Med. Chem.* **1979**, *22*, 759.
- (13) Burgess, M. L.; Barrow, K. D. *J. Chem. Soc., Perkin Trans. I* **1999**, *17*, 2461.
- (14) Smith, B. L.; Embling, P. P.; Lauren, D. R.; Agnew, M. P.; Ross, A. D.; Greentree, P. L. *Aust. Vet. J.* **1989**, *66*, 230.
- (15) Alonsoamelot, M. E.; Perezmena, M.; Calcagno, M. P.; Jaimesespinoza, R.; Castillo, U. *J. Chem. Ecol.* **1992**, *18*, 1405.
- (16) Matoba, M.; Saito, E.; Saito, K.; Koyama, K.; Natori, S.; Matsushima, T.; Takimoto, M. *Mutagenesis* **1987**, *2*, 419.



- (17) Nagao, T.; Saito, K.; Hirayama, E.; Uchikoshi, K.; Koyama, K.; Natori, S.; Morisaki, N.; Iwasaki, S.; Matsushima, T. *Mutat. Res.* **1989**, 2430, 215, 173.
- (18) Yamada, K.; Ojika, M.; Kigoshi, H. *Angew. Chem., Int. Ed.* **1998**, 2432, 37, 1819.
- (19) Kelner, M. J.; McMorris, T. C.; Beck, W. T.; Zamora, J. M.; Taetle, R. *Cancer Res.* **1987**, 47, 3186.
- (20) Woynarowska, B. A.; Woynarowski, J. M.; Herzig, M. C.; Roberts, K.; Higdon, A. L.; MacDonald, J. R. *Biochem. Pharmacol.* **2000**, 59, 1217.
- (21) Woynarowska, B.; Woynarowski, J. M.; Herzig, M. C. S.; Roberts, K.; Higdon, A. L.; MacDonald, J. R. *Ann. Oncol.* **1998**, 9, 106.
- (22) Poindessous, V.; Koepfel, F.; Raymond, E.; Comisso, M.; Waters, S. J.; Larsen, A. K. *Clin. Cancer Res.* **2003**, 9, 2817.
- (23) Sato, Y.; Kashimoto, S.; MacDonald, J. R.; Nakano, K. *Eur. J. Cancer.* **2001**, 37, 1419.
- (24) Woo, M. H.; Peterson, J. K.; Billups, C.; Liang, H.; Bjornsti, M. A.; Houghton, P. J. *Cancer Chemother. Pharmacol.* **2005**, 55, 411.
- (25) Van Laar, E. S.; Izbicka, E.; Weitman, S.; Medina-Gundrum, L.; Macdonald, J. R.; Waters, S. J. *Int. J. Gynecol. Cancer* **2004**, 14, 824.
- (26) Serova, M.; Calvo, F.; Lokiec, F.; Koepfel, F.; Poindessous, V.; Larsen, A. K.; Laar, E. S.; Waters, S. J.; Cvitkovic, E.; Raymond, E. *Cancer Chemother. Pharmacol.* **2006**, 57, 491.
- (27) Alexandre, J.; Raymond, E.; Kaci, M. O.; Brain, E. C.; Lokiec, F.; Kahatt, C.; Faivre, S.; Yovine, A.; Goldwasser, F.; Smith, S. L.; MacDonald, J. R.; Misset, J. L.; Cvitkovic, E. *Clin. Cancer Res.* **2004**, 10, 3377.
- (28) Thomas, J. P.; Arzoomanian, R.; Alberti, D.; Feierabend, C.; Binger, K.; Tutsch, K. D.; Steele, T.; Marnocha, R.; Smith, C.; Smith, S.; MacDonald, J.; Wilding, G.; Bailey, H. *Cancer Chemother. Pharmacol.* **2001**, 48, 467.
- (29) Alexandre, J.; Kahatt, C.; Bertheault-Cvitkovic, F.; Faivre, S.; Shibata, S.; Hilgers, W.; Goldwasser, F.; Lokiec, F.; Raymond, E.; Weems, G.; Shah, A.; MacDonald, J. R.; Cvitkovic, E. *Invest. New Drugs* **2007**, 25, 453.
- (30) Matsumoto, T.; Shirahama, H.; Ichihara, A.; Shin, H.; Kagawa, S.; Sakan, F.; Matsumoto, S.; Nishida, S. *J. Am. Chem. Soc.* **1968**, 90, 3280.
- (31) Kinder, F. R.; Bair, K. W. *J. Org. Chem.* **1994**, 59, 6965.
- (32) McMorris, T. C.; Yu, J.; Hu, Y.; Estes, L. A.; Kelner, M. J. *J. Org. Chem.* **1997**, 62, 3015.
- (33) McMorris, T. C.; Hu, Y.; Yu, J.; Kelner, M. J. *Chem. Commun.* **1997**, 3, 315.
- (34) McMorris, T. C.; Staake, M. D.; Kelner, M. J. *J. Org. Chem.* **2004**, 69, 619.
- (35) Brummond, K. M.; Lu, J. L.; Petersen, J. *J. Am. Chem. Soc.* **2000**, 122, 4915.
- (36) Gong, J.; Neels, J. F.; Yu, X.; Kensler, T. W.; Peterson, L. A.; Sturla, S. J. *J. Med. Chem.* **2006**, 49, 2593.
- (37) Movassaghi, M.; Piizzi, G.; Siegel, D. S.; Piersanti, G. *Angew. Chem., Int. Ed.* **2006**, 45, 5859.
- (38) Movassaghi, M.; Piizzi, G.; Siegel, D. S.; Piersanti, G. *Tetrahedron Lett.* **2009**, 50, 5489.
- (39) Arnone, A.; Merlini, L.; Nasini, G.; de Pava, O. V.; Zunino, F. J. *Chem. Soc., Perkin Trans. 1* **2001**, 6, 610.
- (40) Kinder, F. R.; Wang, R. M.; Bauta, W. E.; Bair, K. W. *Bioorg. Med. Chem. Lett.* **1996**, 6, 1029.
- (41) McMorris, T. C.; Cong, Q.; Kelner, M. J. *J. Org. Chem.* **2003**, 68, 9648.
- (42) Tanaka, K.; Inoue, T.; Kadota, S.; Kikuchi, T. *Xenobiotica* **1990**, 20, 671.
- (43) Tanaka, K.; Inoue, T.; Kadota, S.; Kikuchi, T. *Xenobiotica* **1992**, 22, 33.
- (44) Tanaka, K.; Inoue, T.; Kanai, M.; Kikuchi, T. *Xenobiotica* **1994**, 24, 1237.
- (45) Tanaka, K.; Inoue, T.; Tezuka, Y.; Kikuchi, T. *Chem. Pharm. Bull.* **1996**, 44, 273.
- (46) McMorris, T. C.; Kelner, M. J.; Chadha, R. K.; Siegel, J. S.; Moon, S. S.; Moya, M. M. *Tetrahedron* **1989**, 45, 5433.
- (47) Herzig, M. C.; Arnett, B.; MacDonald, J. R.; Woynarowski, J. M. *Biochem. Pharmacol.* **1999**, 58, 217.
- (48) McMorris, T. C.; Kelner, M. J.; Wang, W.; Moon, S.; Taetle, R. *Chem. Res. Toxicol.* **1990**, 3, 574.
- (49) Tanaka, K.; Inoue, T.; Tezuka, Y.; Kikuchi, T. *Xenobiotica* **1996**, 26, 347.
- (50) Kelner, M. J.; McMorris, T. C.; Montoya, M. A.; Estes, L.; Rutherford, M.; Samson, K. M.; Taetle, R. *Cancer Chemother. Pharmacol.* **1997**, 40, 65.
- (51) Kelner, M. J.; McMorris, T. C.; Montoya, M. A.; Estes, L.; Uglik, S. F.; Rutherford, M.; Samson, K. M.; Bagnell, R. D.; Taetle, R. *Cancer Chemother. Pharmacol.* **1998**, 41, 237.
- (52) Kelner, M. J.; McMorris, T. C.; Montoya, M. A.; Estes, L.; Uglik, S. F.; Rutherford, M.; Samson, K. M.; Bagnell, R. D.; Taetle, R. *Cancer Chemother. Pharmacol.* **1999**, 44, 235.
- (53) Dick, R. A.; Yu, X.; Kensler, T. W. *Clin. Cancer Res.* **2004**, 10, 1492.
- (54) Neels, J. F.; Gong, J.; Yu, X.; Sturla, S. J. *Chem. Res. Toxicol.* **2007**, 20, 1513.
- (55) Liu, X.; Sturla, S. J. *Mol. Biosyst.* **2009**, 5, 1013.
- (56) Liu, X.; Pietsch, K. E.; Sturla, S. J. *Chem. Res. Toxicol.* **2011**, 24, 726.
- (57) Woynarowski, J. M.; Napier, C.; Koester, S. K.; Chen, S. F.; Troyer, D.; Chapman, W.; MacDonald, J. R. *Biochem. Pharmacol.* **1997**, 54, 1181.
- (58) Gong, J.; Vaidyanathan, V. G.; Yu, X.; Kensler, T. W.; Peterson, L. A.; Sturla, S. J. *J. Am. Chem. Soc.* **2007**, 129, 2101.
- (59) Kelner, M. J.; McMorris, T. C.; Estes, L.; Rutherford, M.; Montoya, M.; Goldstein, J.; Samson, K.; Starr, R.; Taetle, R. *Biochem. Pharmacol.* **1994**, 48, 403.
- (60) Jaspers, N. G.; Raams, A.; Kelner, M. J.; Ng, J. M.; Yamashita, Y. M.; Takeda, S.; McMorris, T. C.; Hoeijmakers, J. H. *DNA Repair* **2002**, 1, 1027.
- (61) Koepfel, F.; Poindessous, V.; Lazar, V.; Raymond, E.; Sarasin, A.; Larsen, A. K. *Clin. Cancer Res.* **2004**, 10, 5604.
- (62) Schobert, R.; Knauer, S.; Seibt, S.; Biersack, B. *Curr. Med. Chem.* **2011**, 18, 790.
- (63) Chybowski, J.; Wikipedia: [http://en.wikipedia.org/wiki/File:Omphalotus\\_olearius\\_in\\_NE\\_IL.JPG#filehistory](http://en.wikipedia.org/wiki/File:Omphalotus_olearius_in_NE_IL.JPG#filehistory) (accessed Dec 29, 2011).
- (64) Nakanishi, K.; Ohashi, M.; Suzuki, N.; Tada, M.; Yamada, Y.; Inagaki, S. *Yakugaku Zasshi* **1963**, 83, 377.
- (65) Hidekazu, Y.; Yasutaka, K.; Harumi, I.; Toyoko, K.; Makoto, Y. *Jpn. J. Clin. Radiat.* **2003**, 48, 879.
- (66) Nakanishi, K.; Tada, M.; Yamada, Y.; Ohashi, M.; Komatsu, N.; Terakawa, H. *Nature* **1963**, 197, 292.
- (67) McMorris, T. C.; Anchel, M. J. *Am. Chem. Soc.* **1963**, 85, 831.
- (68) Gonzalez del Val, A.; Platas, G.; Arenal, F.; Orihuela, J. C.; Garcia, M.; Hernandez, P.; Royo, I.; De Pedro, N.; Silver, L. L.; Young, K.; Vicente, M. F.; Pelaez, F. *Mycol. Res.* **2003**, 107, 1201.
- (69) Reina, M.; Orihuela, J. C.; Gonzalez-Coloma, A.; de Ines, C.; de la Cruz, M.; Gonzalez del Val, A.; Torno, J. R.; Fraga, B. M. *Phytochemistry* **2004**, 65, 381.
- (70) Arnone, A.; Cardillo, R.; Nasini, G.; Depava, O. V. *J. Chem. Soc., Perkin Trans. 1* **1991**, 4, 733.
- (71) Arnone, A.; Cardillo, R.; Nasini, G.; Depava, O. V. *J. Chem. Soc., Perkin Trans. 1* **1991**, 8, 1787.
- (72) Lee, I. K.; Jeong, C. Y.; Cho, S. M.; Yun, B. S.; Kim, Y. S.; Yu, S. H.; Koshino, H.; Yoo, I. D. *J. Antibiot.* **1996**, 49, 821.
- (73) Arnone, A.; Cardillo, R.; Modugno, V.; Nasin, G. *Gazz. Chim. Ital.* **1991**, 121, 345.
- (74) Dufresne, C.; Young, K.; Pelaez, F.; DelVal, A. G.; Valentino, D.; Graham, A.; Platas, G.; Bernard, A.; Zink, D. J. *Nat. Prod.* **1997**, 60, 188.
- (75) Twentyman, P. R.; Luscombe, M. Br. *J. Cancer* **1987**, 56, 279.
- (76) Taetle, R.; Jones, O. W.; Honeysett, J. M.; Abramson, I.; Bradshaw, C.; Reid, S. *Cancer* **1987**, 60, 1836.
- (77) Hara, M.; M., Y.; Morimoto, M.; Nakano, H. *J. Antibiot.* **1987**, 40, 1643.

- (78) Kelner, M. J.; McMorris, T. C.; Taetle, R. J. *Natl. Cancer Inst.* **1990**, *82*, 1562.
- (79) Komatsu, N.; Hamada, M.; Nakasawa, S.; Ogata, S.; Yamamoto, A.; Terakawa, H.; Yamamoto, T. *J. Ferment. Assoc.* **1961**, *19*, 464.
- (80) Jin'ichi, S.; Hiromi, O.; Yasuko, K.; Chiaki, Y.; Rie, N.; Hiroyuki, N. *BCG, BRM Ryoho Kenkyukai Kaishi* **2002**, *26*, 17.
- (81) Walser, J.; Heinsteins, P. F. *Antimicrob. Agents Chemother.* **1973**, *3*, 357.
- (82) Hanson, J. R.; Marten, T. *Chem. Commun.* **1973**, *5*, 171.
- (83) Kelner, M. J.; McMorris, T. C.; Estes, L.; Starr, R.; Samson, K.; Varki, N.; Taetle, R. *Anticancer Res.* **1995**, *15*, 867.
- (84) McMorris, T. C.; Kelner, M. J.; Wang, W.; Yu, J.; Estes, L. A.; Taetle, R. *J. Nat. Prod.* **1996**, *59*, 896.
- (85) Kelner, M. J.; McMorris, T. C.; Estes, L.; Starr, R. J.; Rutherford, M.; Montoya, M.; Samson, K. M.; Taetle, R. *Cancer Res.* **1995**, *55*, 4936.
- (86) MacDonald, J. R.; Muscoplat, C. C.; Dexter, D. L.; Mangold, G. L.; Chen, S. F.; Kelner, M. J.; McMorris, T. C.; Von Hoff, D. D. *Cancer Res.* **1997**, *57*, 279.
- (87) Kelner, M. J.; McMorris, T. C.; Estes, L.; Wang, W.; Samson, K. M.; Taetle, R. *Invest. New Drugs* **1996**, *14*, 161.
- (88) Leggas, M.; Stewart, C. F.; Woo, M. H.; Fouladi, M.; Cheshire, P. J.; Peterson, J. K.; Friedman, H. S.; Billups, C.; Houghton, P. J. *Clin. Cancer Res.* **2002**, *8*, 3000.
- (89) Kelner, M. J.; McMorris, T. C.; Estes, L.; Samson, K. M.; Trani, N. A.; MacDonald, J. R. *Leukemia* **2000**, *14*, 136.
- (90) Kelner, M. J.; McMorris, T. C.; Estes, L.; Samson, K. M.; Bagnell, R. D.; Taetle, R. *Eur. J. Cancer.* **1998**, *34*, 908.
- (91) Kelner, M. J.; McMorris, T. C.; Estes, L. A.; Oval, M. Y.; Rojas, R. J.; Lynn, J. R.; Lanham, K. A.; Samson, K. M. *Anticancer Drugs* **2000**, *11*, 217.
- (92) Poindessous, V.; Koepfel, F.; Raymond, E.; Cvitkovic, E.; Waters, S. J.; Larsen, A. K. *Int. J. Oncol.* **2003**, *23*, 1347.
- (93) Boel, K.; Van Poppel, H.; Goethuys, H.; Derluyn, J.; Vandenbroucke, F.; Popelier, G.; Casselman, J.; Billiet, I.; Vanuytsel, L.; Paridaens, R.; Baert, L. *Anticancer Res.* **1999**, *19*, 2157.
- (94) Holtz, K. M.; Rockwell, S.; Tomasz, M.; Sartorelli, A. C. *J. Biol. Chem.* **2003**, *278*, 5029.
- (95) Hofheinz, R. D.; Beyer, U.; Al-Batran, S. E.; Hartmann, J. T. *Onkologie* **2008**, *31*, 271.
- (96) Niwa, H.; Ojika, M.; Wakamatsu, K.; Yamada, K.; Hirono, I.; Matsushita, K. *Tetrahedron Lett.* **1983**, *24*, 4117.
- (97) Niwa, H.; Ojika, M.; Wakamatsu, K.; Yamada, K.; Ohba, S.; Saito, Y.; Hirono, I.; Matsushita, K. *Tetrahedron Lett.* **1983**, *24*, 5371.
- (98) Padwa, A.; Curtis, E. A.; Sandanayaka, V. P. *J. Org. Chem.* **1997**, *62*, 1317.
- (99) Aungst, R. A. Jr.; Chan, C.; Funk, R. L. *Org. Lett.* **2001**, *3*, 2611.
- (100) Brummond, K. M.; Wan, H. H.; Kent, J. L. *J. Org. Chem.* **1998**, *63*, 6535.
- (101) Brummond, K. M.; Wan, H. *Tetrahedron Lett.* **1998**, *39*, 931.
- (102) Hudrlík, P. F.; Kassim, A. M.; Agwaramgbo, E. L. O.; Doonquah, K. A.; Roberts, R. R.; Hudrlík, A. M. *Organometallics* **1993**, *12*, 2367.
- (103) Kent, J. L.; Wan, H.; Brummond, K. M. *Tetrahedron Lett.* **1995**, *36*, 2407.
- (104) Evans, D. A.; Burgey, C. S.; Kozlowski, M. C.; Tregay, S. W. *J. Am. Chem. Soc.* **1999**, *121*, 686.
- (105) Choie, D. D.; Delcampo, A. A.; Guarino, A. M. *Toxicol. Appl. Pharmacol.* **1980**, *55*, 245.
- (106) Ishikawa, T. *Trends Biochem. Sci.* **1992**, *17*, 463.
- (107) Ishikawa, T.; Aliosman, F. *J. Biol. Chem.* **1993**, *268*, 20116.
- (108) McMorris, T. C.; Elayadi, A. N.; Yu, J.; Hu, Y.; Kelner, M. J. *Drug. Metab. Dispos.* **1999**, *27*, 983.
- (109) McMorris, T. C.; Elayadi, A. N.; Yu, J.; Kelner, M. J. *Biochem. Pharmacol.* **1999**, *57*, 83.
- (110) McMorris, T. C.; Moon, S. S.; Kelner, M. J. *J. Nat. Prod.* **2003**, *66*, 310.
- (111) Brandsteterova, E.; Kelner, M. J.; McMorris, T. C.; Estes, L.; Bagnell, R.; Montoya, M. *Neoplasma* **1992**, *39*, 369.
- (112) Arnone, A.; De Gregorio, C.; Mele, A.; Nasini, G.; Vajna de Pava, O. *J. Chem. Soc., Perkin Trans. 1* **2000**, *5*, 745.
- (113) McMorris, T. C.; Yu, J.; Estes, L. A.; Kelner, M. J. *Tetrahedron* **1997**, *53*, 14579.
- (114) Liu, X.; Sharpless, C.; Sturla, S. J. *Chem. Biol.* **2012**, in revision.
- (115) Yokomizo, A.; Ono, M.; Nanri, H.; Makino, Y.; Ohga, T.; Wada, M.; Okamoto, T.; Yodoi, J.; Kuwano, M.; Kohno, K. *Cancer Res.* **1995**, *55*, 4293.
- (116) Kelner, M. J.; McMorris, T. C.; Rojas, R. J.; Trani, N. A.; Estes, L. *Cancer Chemother. Pharmacol.* **2002**, *49*, 412.
- (117) Marzano, C.; Gandin, V.; Pellei, M.; Colavito, D.; Papini, G.; Lobbia, G. G.; Del Giudice, E.; Porchia, M.; Tisato, F.; Santini, C. *J. Med. Chem.* **2008**, *51*, 798.
- (118) Tanner, J. J.; Parsons, Z. D.; Cummings, A. H.; Zhou, H.; Gates, K. S. *Antioxid. Redox. Signal.* **2011**, *15*, 77.
- (119) Chen, C. Y.; Willard, D.; Rudolph, J. *Biochemistry* **2009**, *48*, 1399.
- (120) Kinder, F. R.; Chen, C.-P.; Bair, K. W. *Synth. Commun.* **1997**, *27*, 271.
- (121) Bose, G.; Bracht, K.; Bednarski, P. J.; Lalk, M.; Langer, P. *Bioorg. Med. Chem.* **2006**, *14*, 4694.
- (122) McMorris, T. C.; Yu, J.; Lira, R.; Dawe, R.; MacDonald, J. R.; Waters, S. J.; Estes, L. A.; Kelner, M. J. *J. Org. Chem.* **2001**, *66*, 6158.
- (123) McMorris, T. C.; Chimmami, R.; Gurram, M.; Staake, M. D.; Kelner, M. J. *Bioorg. Med. Chem. Lett.* **2007**, *17*, 6770.
- (124) Kelner, M. J.; McMorris, T. C.; Chimmami, R.; Alisala, K.; Staake, M. D.; Banda, G. *J. Med. Chem.* **2010**, *53*, 1109.
- (125) Reed, M. W.; Lukhtanov, E. A.; Gorn, V.; Kutayavin, I.; Gall, A.; Wald, A.; Meyer, R. B. *Bioconjugate Chem.* **1998**, *9*, 64.
- (126) Schobert, R.; Biersack, B.; Knauer, S.; Ocker, M. *Bioorg. Med. Chem.* **2008**, *16*, 8592.
- (127) Knauer, S.; Biersack, B.; Zoldakova, M.; Effenberger, K.; Milius, W.; Schobert, R. *Anticancer Drugs* **2009**, *20*, 676.
- (128) Dick, R. A.; Kensler, T. W. *J. Biol. Chem.* **2004**, *279*, 17269.
- (129) Tanaka, K.; Inoue, T.; Kadota, S.; Kikuchi, T. *Xenobiotica* **1992**, *22*, 33.
- (130) Rase, B.; Bartfai, T.; Ernster, L. *Arch. Biochem. Biophys.* **1976**, *172*, 380.
- (131) Rajagopalan, K. V.; Handler, P.; Fridovich, I. *J. Biol. Chem.* **1962**, *237*, 922.
- (132) Felsted, R. L.; Bachur, N. R. *Drug Metab. Rev.* **1980**, *11*, 1.
- (133) Kitamura, S. *Yakugaku Zasshi, J. Pharm. Soc. Jpn.* **1988**, *108*, 296.
- (134) Theorell, H.; Yonetani, T. *Biochemische Zeitschrift* **1963**, *338*, 537.
- (135) Clish, C. B.; Levy, B. D.; Chiang, N.; Tai, H. H.; Serhan, C. N. *J. Biol. Chem.* **2000**, *275*, 25372.
- (136) Yokomizo, T.; Izumi, T.; Takahashi, T.; Kasama, T.; Kobayashi, Y.; Sato, F.; Taketani, Y.; Shimizu, T. *J. Biol. Chem.* **1993**, *268*, 18128.
- (137) Yokomizo, T.; Ogawa, Y.; Uozumi, N.; Kume, K.; Izumi, T.; Shimizu, T. *J. Biol. Chem.* **1996**, *271*, 2844.
- (138) Ensor, C. M.; Zhang, H.; Tai, H. H. *Biochem. J.* **1998**, *330*, 103.
- (139) Eder, E.; Hoffman, C.; Deininger, C. *Chem. Res. Toxicol.* **1991**, *4*, 50.
- (140) Dick, R. A.; Kwak, M. K.; Sutter, T. R.; Kensler, T. W. *J. Biol. Chem.* **2001**, *276*, 40803.
- (141) Kelner, M. J.; McMorris, T. C.; Montoya, M. A.; Estes, L.; Uglik, S. F.; Rutherford, M.; Samson, K. M.; Bagnell, R. D.; Taetle, R. *Cancer Chemother. Pharmacol.* **1999**, *44*, 235.
- (142) Pietsch, K. E.; Neels, J. F.; Yu, X.; Gong, J.; Sturla, S. J. *Chem. Res. Toxicol.* **2011**, *24*, 2044.
- (143) McMorris, T. C.; Kelner, M. J.; Wang, W.; Diaz, M. A.; Estes, L. A.; Taetle, R. *Experientia* **1996**, *52*, 75.
- (144) McMorris, T. C. *Bioorg. Med. Chem.* **1999**, *7*, 881.
- (145) Wiltshire, T.; Senft, J.; Wang, Y.; Konat, G. W.; Wenger, S. L.; Reed, E.; Wang, W. *Mol. Pharmacol.* **2007**, *71*, 1051.
- (146) Kaufmann, S. H.; Mesner, P. W.; Samejima, K.; Tone, S.; Earnshaw, W. C. *Method. Enzymol.* **2000**, *322*, 3.



- (147) Hampton, M. B.; Orrenius, S. *Biofactors* **1998**, *8*, 1.  
 (148) Kusenda, J. *Neoplasma* **1998**, *45*, 117.  
 (149) Khan, S. M.; Cassarino, D. S.; Abramova, N. N.; Keeney, P. M.; Borland, M. K.; Trimmer, P. A.; Krebs, C. T.; Bennett, J. C.; Parks, J. K.; Swerdlow, R. H.; Parker, W. D.; Bennett, J. P. *Ann. Neurol.* **2000**, *48*, 148.  
 (150) Koizumi, H.; Ohkawa, I.; Tsukahara, T.; Momoi, T.; Nakada, K.; Uchikoshi, T. *J. Pathol.* **1999**, *189*, 410.  
 (151) Nakagawara, A.; Nakamura, Y.; Ikeda, H.; Hiwasa, T.; Kuida, K.; Su, M. S.; Zhao, H. Q.; Cnaan, A.; Sakiyama, S. *Cancer Res.* **1997**, *57*, 4578.  
 (152) Herzig, M. C. S.; Liang, H. Y.; Johnson, A. E.; Woynarowska, B.; Woynarowski, J. M. *Breast Cancer Res. Treat.* **2002**, *71*, 133.  
 (153) Yang, X. H.; Sladek, T. L.; Liu, X. S.; Butler, B. R.; Froelich, C. J.; Thor, A. D. *Cancer Res.* **2001**, *61*, 348.  
 (154) Blanc, C.; Deveraux, Q. L.; Krajewski, S.; Janicke, R. U.; Porter, A. G.; Reed, J. C.; Jaggi, R.; Marti, A. *Cancer Res.* **2000**, *60*, 4386.  
 (155) Umansky, V.; Ushmorov, A.; Ratter, F.; Chlichlia, K.; Bucur, M.; Lichtenauer, A.; Rocha, M. *Int. J. Oncol.* **2000**, *16*, 109.  
 (156) Kim, Y. M.; Kim, T. H.; Seol, D. W.; Talanian, R. V.; Billiar, T. R. *J. Biol. Chem.* **1998**, *273*, 31437.  
 (157) Woynarowski, J. M.; Koester, S.; Woynarowska, B.; Arnett, B.; Trevino, A. V.; Chan, D.; Higdon, A. L.; Munoz, R.; Herzig, M. C. S.; Faive, S. *Proc. Am. Assoc. Cancer Res.* **1999**, *40*.  
 (158) Liang, H.; Munoz, R. M.; Higdon, A. L.; Waters, S. J.; Woynarowska, B. A. *Clin. Cancer Res.* **2000**, *6*, 4526s.  
 (159) Sgorbissa, A.; Benetti, R.; Marzinotto, S.; Schneider, C.; Brancolini, C. *J. Cell Sci.* **1999**, *112*, 4475.  
 (160) Woynarowska, B. A.; Roberts, K.; Woynarowski, J. M.; MacDonald, J. R.; Herman, T. S. *Radiat. Res.* **2000**, *154*, 608.  
 (161) Branch, P.; Masson, M.; Aquilina, G.; Bignami, M.; Karran, P. *Oncogene* **2000**, *19*, 3138.  
 (162) Reles, A.; Wen, W. H.; Schmider, A.; Gee, C.; Runnebaum, I. B.; Kilian, U.; Jones, L. A.; El-Naggar, A.; Minguillon, C.; Schonborn, L.; Reich, O.; Kreienberg, R.; Lichtenegger, W.; Press, M. F. *Clin. Cancer Res.* **2001**, *7*, 2984.  
 (163) Belotserkovskii, B. P.; De Silva, E.; Tornaletti, S.; Wang, G.; Vasquez, K. M.; Hanawalt, P. C. *J. Biol. Chem.* **2007**, *282*, 32433.  
 (164) Chehab, N. H.; Malikzay, A.; Appel, M.; Halazonetis, T. D. *Genes. Dev.* **2000**, *14*, 278.  
 (165) Shieh, S. Y.; Ahn, J.; Tamai, K.; Taya, Y.; Prives, C. *Genes Dev.* **2000**, *14*, 289.  
 (166) Falck, J.; Mailand, N.; Syljuasen, R. G.; Bartek, J.; Lukas, J. *Nature* **2001**, *410*, 842.  
 (167) Sorensen, C. S.; Syljuasen, R. G.; Falck, J.; Schroeder, T.; Ronnstrand, L.; Khanna, K. K.; Zhou, B. B.; Bartek, J.; Lukas, J. *Cancer Cell* **2003**, *3*, 247.  
 (168) Blasina, A.; de Weyer, I. V.; Laus, M. C.; Luyten, W. H.; Parker, A. E.; McGowan, C. H. *Curr. Biol.* **1999**, *9*, 1.  
 (169) Furnari, B.; Blasina, A.; Boddy, M. N.; McGowan, C. H.; Russell, P. *Mol. Biol. Cell* **1999**, *10*, 833.  
 (170) Hanawalt, P. C.; Spivak, G. *Nat. Rev. Mol. Cell. Biol.* **2008**, *9*, 958.  
 (171) Laine, J. P.; Egly, J. M. *EMBO J.* **2006**, *25*, 387.  
 (172) Svejstrup, J. Q. *Nat. Rev. Mol. Cell Biol.* **2002**, *3*, 21.  
 (173) Koepfel, F.; Poindessous, V.; Lazar, V.; Raymond, E.; Sarasin, A.; Larsen, A. K. *Clin. Cancer Res.* **2004**, *10*, 5604.  
 (174) Hoeijmakers, J. H. J. *Nature* **2001**, *411*, 366.  
 (175) Hanawalt, P. C. *Oncogene* **2002**, *21*, 8949.  
 (176) Surrallés, J.; Ramirez, M. J.; Marcos, R.; Natarajan, A. T.; Mullenders, L. H. *Proc. Natl. Acad. Sci. U.S.A.* **2002**, *99*, 10571.  
 (177) Protic-Sabljic, M.; Kraemer, K. H. *Proc. Natl. Acad. Sci. U.S.A.* **1985**, *82*, 6622.  
 (178) Hanawalt, P. C. *Nature* **2000**, *405*, 415.  
 (179) Bootsma, D.; Kraemer, K. H.; Cleaver, J. E.; Hoeijmakers, J. H. J. *The Metabolic and Molecular Basis of Inherited Disease*; McGraw-Hill: New York, 2001.  
 (180) Cleaver, J. E.; Thompson, L. H.; Richardson, A. S.; States, J. C. *Hum. Mutat.* **1999**, *14*, 9.  
 (181) Wakasugi, M.; Sancar, A. *Proc. Natl. Acad. Sci. U.S.A.* **1998**, *95*, 6669.  
 (182) Staresincic, L.; Fagbemi, A. F.; Enzlin, J. H.; Gourdin, A. M.; Wijgers, N.; Dunand-Sauthier, I.; Giglia-Mari, G.; Clarkson, S. G.; Vermeulen, W.; Scharer, O. D. *EMBO J.* **2009**, *28*, 1111.  
 (183) Iyer, N.; Reagan, M. S.; Wu, K. J.; Canagarajah, B.; Friedberg, E. C. *Biochemistry* **1996**, *35*, 2157.  
 (184) Selby, C. P.; Sancar, A. *Proc. Natl. Acad. Sci. U.S.A.* **1997**, *94*, 11205.  
 (185) Bradsher, J.; Auriol, J.; de Santis, L. P.; Iben, S.; Vonesch, J. L.; Grummt, I.; Egly, J. M. *Mol. Cell* **2002**, *10*, 819.  
 (186) VanderHorst, G. T. J.; vanSteeg, H.; Berg, R. J. W.; vanGool, A. J.; deWit, J.; Weeda, G.; Morreau, H.; Beems, R. B.; vanKreijl, C. F.; deGrujil, F. R.; Bootsma, D.; Hoeijmakers, J. H. J. *Cell* **1997**, *89*, 425.  
 (187) Citterio, E.; Van Den Boom, V.; Schnitzler, G.; Kanaar, R.; Bonte, E.; Kingston, R. E.; Hoeijmakers, J. H.; Vermeulen, W. *Mol. Cell. Biol.* **2000**, *20*, 7643.  
 (188) Mu, D.; Sancar, A. *J. Biol. Chem.* **1997**, *272*, 7570.  
 (189) Jones, C. J.; Wood, R. D. *Biochemistry* **1993**, *32*, 12096.  
 (190) Matsuda, T.; Saijo, M.; Kuraoka, I.; Kobayashi, T.; Nakatsu, Y.; Nagai, A.; Enjoji, T.; Masutani, C.; Sugawara, K.; Hanaoka, F.; et al. *J. Biol. Chem.* **1995**, *270*, 4152.  
 (191) Mellon, I.; Spivak, G.; Hanawalt, P. C. *Cell* **1987**, *51*, 241.  
 (192) Leadon, S. A.; Lawrence, D. A. *Mutat. Res.* **1991**, *255*, 67.  
 (193) Venema, J.; Bartosova, Z.; Natarajan, A. T.; Vanzeeland, A. A.; Mullenders, L. H. F. *J. Biol. Chem.* **1992**, *267*, 8852.  
 (194) Evans, E.; Fellows, J.; Coffey, A.; Wood, R. D. *EMBO J.* **1997**, *16*, 625.  
 (195) Kamiuchi, S.; Saijo, M.; Citterio, E.; de Jager, M.; Hoeijmakers, J. H.; Tanaka, K. *Proc. Natl. Acad. Sci. U.S.A.* **2002**, *99*, 201.  
 (196) Foustier, M.; Vermeulen, W.; van Zeeland, A. A.; Mullenders, L. H. *Mol. Cell* **2006**, *23*, 471.  
 (197) Sarker, A. H.; Tsutakawa, S. E.; Kostek, S.; Ng, C.; Shin, D. S.; Peris, M.; Campeau, E.; Tainer, J. A.; Nogales, E.; Cooper, P. K. *Mol. Cell* **2005**, *20*, 187.  
 (198) Escargueil, A. E.; Poindessous, V.; Soares, D. G.; Sarasin, A.; Cook, P. R.; Larsen, A. K. *J. Cell Sci.* **2008**, *121*, 1275.  
 (199) Tornaletti, S.; Reines, D.; Hanawalt, P. C. *J. Biol. Chem.* **1999**, *274*, 24124.  
 (200) Donahue, B. A.; Yin, S.; Taylor, J. S.; Reines, D.; Hanawalt, P. C. *Proc. Natl. Acad. Sci. U.S.A.* **1994**, *91*, 8502.  
 (201) Kristjahan, A.; Reid, J.; Svejstrup, J. Q. *Yeast* **2003**, *20*, S25.  
 (202) Yang, L. Y.; Jiang, H.; Rangel, K. M. *Int. J. Oncol.* **2003**, *22*, 683.  
 (203) McKay, B. C.; Becerril, C.; Ljungman, M. *Oncogene* **2001**, *20*, 6805.  
 (204) Bregman, D. B.; Halaban, R.; Henning, K. A.; Friedberg, E. C.; Warren, S. L. *FASEB J.* **1996**, *10*, 1658.  
 (205) Bregman, D. B.; Luo, Z. H.; Zheng, J. H.; Lu, Y. *Mutat. Res.* **2001**, *486*, 259.  
 (206) Tornaletti, S.; Hanawalt, P. C. *Biochimie* **1999**, *81*, 139.  
 (207) Cheng, L.; Eicher, S. A.; Guo, Z. Z.; Hong, W. K.; Spitz, M. R.; Wei, Q. Y. *Cancer Epidemiol. Biomark. Prev.* **1998**, *7*, 465.  
 (208) Yangfeng, T. L.; Li, S. B.; Han, H.; Schwartz, P. *Int. J. Cancer* **1992**, *52*, 575.  
 (209) Spitz, M. R.; Wu, X. F.; Wang, Y. F.; Wang, L. E.; Shete, S.; Amos, C. I.; Guo, Z. Z.; Lei, L.; Mohrenweiser, H.; Wei, Q. Y. *Cancer Res.* **2001**, *61*, 1354.  
 (210) Takebayashi, Y.; Nakayama, K.; Kanzaki, A.; Miyashita, H.; Ogura, O.; Mori, S.; Mutoh, M.; Miyazaki, K.; Fukumoto, M.; Pommier, Y. *Cancer Lett.* **2001**, *174*, 115.  
 (211) Miyashita, H.; Mori, S.; Tanda, N.; Nakayama, K.; Kanzaki, A.; Sato, A.; Morikawa, H.; Motegi, K.; Takebayashi, Y.; Fukumoto, M. *Oncol. Rep.* **2001**, *8*, 1133.  
 (212) Cheng, L.; Sturgis, E. M.; Eicher, S. A.; Spitz, M. R.; Wei, Q. Y. *Cancer* **2002**, *94*, 393.  
 (213) Wang, Y.; Wiltshire, T.; Senft, J.; Wenger, S. L.; Reed, E.; Wang, W. *Mol. Cancer Ther.* **2006**, *5*, 3153.  
 (214) Narod, S. A.; Foulkes, W. D. *Nat. Rev. Cancer* **2004**, *4*, 665.



- (215) Garcia-Higuera, I.; Taniguchi, T.; Ganesan, S.; Meyn, M. S.; Timmers, C.; Hejna, J.; Grompe, M.; D'Andrea, A. D. *Mol. Cell* **2001**, 2843, 7, 249.
- (216) Nakanishi, K.; Yang, Y. G.; Pierce, A. J.; Taniguchi, T.; Digweed, M.; D'Andrea, A. D.; Wang, Z. Q.; Jasin, M. *Proc. Natl. Acad. Sci. U.S.A.* **2005**, 102, 1110.
- (217) Venkitaraman, A. R. *Nat. Rev. Cancer* **2004**, 4, 266.
- (218) Rothfuss, A.; Grompe, M. *Mol. Cell. Biol.* **2004**, 24, 123.
- (219) Lindahl, T.; Nyberg, B. *Biochemistry* **1972**, 11, 3610.
- (220) Almeida, K. H.; Sobol, R. W. *DNA Repair* **2007**, 6, 695.
- (221) Devanesan, P.; Todorovic, R.; Zhao, J.; Gross, M. L.; Rogan, E. G.; Cavalieri, E. L. *Carcinogenesis* **2001**, 22, 489.
- (222) Terashima, I.; Suzuki, N.; Itoh, S.; Yoshizawa, I.; Shibutani, S. *Biochemistry* **1998**, 37, 8803.
- (223) Banerjee, S.; Brown, K. L.; Egli, M.; Stone, M. P. *J. Am. Chem. Soc.* **2011**, 133, 12556.
- (224) Mikes, P.; Korinek, M.; Linhart, I.; Krouzelka, J.; Dabrowska, L.; Stransky, V.; Mraz, J. *Toxicol. Lett.* **2010**, 197, 183.
- (225) Boger, D. L. *Pure Appl. Chem.* **1994**, 66, 837.
- (226) Boger, D. L.; Mesini, P. *J. Am. Chem. Soc.* **1994**, 116, 11335.
- (227) Asai, A.; Yano, K.; Mizukami, T.; Nakano, H. *Cancer Res.* **1999**, 59, 5417.
- (228) Kushida, T.; Uesugi, M.; Sugiura, Y.; Kigoshi, H.; Tanaka, H.; Hirokawa, J.; Ojika, M.; Yamada, K. *J. Am. Chem. Soc.* **1994**, 116, 479.
- (229) Nagao, T.; Saito, K.; Hirayama, E.; Uchikoshi, K.; Koyama, K.; Natori, S.; Morisaki, N.; Iwasaki, S.; Matsushima, T. *Mutat. Res.* **1989**, 215, 173.
- (230) Hirono, I.; Shibuya, C.; Shimizu, M.; Fushimi, K. *J. Natl. Cancer. Inst.* **1972**, 48, 1245.
- (231) Alonso-Amelot, M. E.; Castillo, U.; Smith, B. L.; Lauren, D. R. *Nature* **1996**, 382, 587.
- (232) Alonso-Amelot, M. E. *Nutrition* **1997**, 13, 694.
- (233) Alonso-Amelot, M. E.; Avendano, M. *Curr. Med. Chem.* **2002**, 9, 675.
- (234) Yamada, K.; Ojika, M.; Kigoshi, H. *Nat. Prod. Rep.* **2007**, 24, 798.
- (235) Hirono, I.; Ogino, H.; Fujimoto, M.; Yamada, K.; Yoshida, Y.; Ikagawa, M.; Okumura, M. *J. Nat. Cancer I* **1987**, 79, 1143.
- (236) Evans, I. A. *Chemical Carcinogens*, 2nd ed.; ACS Monograph 182; American Chemical Society: Washington, D.C., 1984; Vol. 2.
- (237) Hirono, I.; Yamada, K. *Naturally Occuring Carcinogens of Plant Origin*; Kodansha-Elsevier: Tokio, Amsterdam, 1987.
- (238) Evans, I. A.; Mason, J. *Nature* **1965**, 208, 913.
- (239) Ojika, M.; Sugimoto, K.; Okazaki, T.; Yamada, K. *J. Chem. Soc., Chem. Commun.* **1989**, 1775.
- (240) Hanka, L. J.; Dietz, A.; Gerpheide, S. A.; Kuentzel, S. L.; Martin, D. G. *J. Antibiot.* **1978**, 31, 1211.
- (241) Martin, D. G.; Hanka, L. J.; Neil, G. L. *Proc. Am. Assoc. Cancer Res.* **1978**, 19, 99.
- (242) Boger, D. L.; Wolkenberg, S. E. *Chem. Rev.* **2002**, 102, 2477.
- (243) Boger, D. L.; Trzupek, J. D.; Gottesfeld, J. M. *Nat. Chem. Biol.* **2006**, 2, 79.
- (244) Parrish, J. P.; Kastrinsky, D. B.; Hwang, I.; Boger, D. L. *J. Org. Chem.* **2003**, 68, 8984.
- (245) Boger, D. L.; Hertzog, D. L.; Bollinger, B.; Johnson, D. S.; Cai, H.; Goldberg, J.; Turnbull, P. *J. Am. Chem. Soc.* **1997**, 119, 4977.
- (246) Parrish, J. P.; Kastrinsky, D. B.; Wolkenberg, S. E.; Igarashi, Y.; Boger, D. L. *J. Am. Chem. Soc.* **2003**, 125, 10971.
- (247) Boger, D. L.; Bollinger, B.; Hertzog, D. L.; Johnson, D. S.; Cai, H.; Mesini, P.; Garbaccio, R. M.; Jin, Q.; Kitos, P. A. *J. Am. Chem. Soc.* **1997**, 119, 4987.
- (248) Boger, D. L.; Machiya, K.; Hertzog, D. L.; Kitos, P. A.; Holmes, D. J. *J. Am. Chem. Soc.* **1993**, 115, 9025.
- (249) Moore, H. W. *Science* **1977**, 197, 527.
- (250) Tomasz, M. *Chem. Biol.* **1995**, 2, 575.
- (251) Nagaoka, K.; Matsumoto, M.; Oono, J.; Yokoi, K.; Ishizeki, S.; Nakashima, T. *J. Antibiot.* **1986**, 39, 1527.
- (252) Saito, I.; Fujiwara, T.; Sugiyama, H. *Tetrahedron Lett.* **1999**, 40, 315.
- (253) Armstrong, R. W.; Salvati, M. E.; Nguyen, M. *J. Am. Chem. Soc.* **1992**, 114, 3144.
- (254) Ishizeki, S.; Ohtsuka, M.; Irinoda, K.; Kukita, K. I.; Nagaoka, K.; Nakashima, T. *J. Antibiot.* **1987**, 40, 60.
- (255) Hartley, J. A.; Hazrati, A.; Kelland, L. R.; Khanim, R.; Shipman, M.; Suzenet, F.; Walker, L. F. *Angew. Chem., Int. Ed.* **2000**, 39, 3467.
- (256) Zang, H.; Gates, K. S. *Biochemistry* **2000**, 39, 14968.
- (257) Coleman, R. S.; Burk, C. H.; Navarro, A.; Brueggemeier, R. W.; Diaz-Cruz, E. S. *Org. Lett.* **2002**, 4, 3545.
- (258) Searcey, M.; Casely-Hayford, M. A.; Pors, K.; James, C. H.; Patterson, L. H.; Hartley, J. A. *Org. Biomol. Chem.* **2005**, 3, 3585.
- (259) Sakai, R.; Rinehart, K. L.; Guan, Y.; Wang, A. H. J. *Proc. Nat. Acad. Sci. U.S.A.* **1992**, 89, 11456.
- (260) Erba, E.; Bergamaschi, D.; Bassano, L.; Damia, G.; Ronzoni, S.; Faircloth, G. T.; D'Incalci, M. *Eur. J. Cancer* **2001**, 37, 97.
- (261) Damia, G.; Silvestri, S.; Carrassa, L.; Filiberti, L.; Faircloth, G. T.; Liberi, G.; Foiani, M.; D'Incalci, M. *Int. J. Cancer* **2001**, 92, 583.
- (262) Soares, D. G.; Escargueil, A. E.; Poindessous, V.; Sarasin, A.; de Gramont, A.; Bonatto, D.; Henriques, J. A.; Larsen, A. K. *Proc. Natl. Acad. Sci. U.S.A.* **2007**, 104, 13062.
- (263) Pommier, Y.; Kohlhagen, G.; Bailly, C.; Waring, M.; Mazumdar, A.; Kohn, K. W. *Biochemistry* **1996**, 35, 13303.
- (264) Raymond, E.; Lawrence, R.; Izbic, E.; Faivre, S.; Von Hoff, D. *Ann. Oncol.* **1998**, 9, 38.
- (265) Pommier, Y.; Takebayashi, Y.; Pourquier, P.; Zimonjic, D. B.; Nakayama, K.; Emmert, S.; Ueda, T.; Urasaki, Y.; Kanzaki, A.; Akiyama, S.; Popescu, N.; Kraemer, K. H. *Nat. Med.* **2001**, 7, 961.
- (266) Moore, B. M.; Seaman, F. C.; Hurley, L. H. *J. Am. Chem. Soc.* **1997**, 119, 5475.
- (267) Hurley, L. H.; Zewail-Foote, M. *J. Med. Chem.* **1999**, 42, 2493.
- (268) Jin, S. K.; Hu, Z.; Scotto, K. W. *Clin. Cancer Res.* **1999**, 5, 3790s.
- (269) Takebayashi, Y.; Pourquier, P.; Yoshida, A.; Kohlhagen, G.; Pommier, Y. *Proc. Natl. Acad. Sci. U.S.A.* **1999**, 96, 7196.
- (270) Eckhardt, S. G.; Baker, S. D.; Britten, C. D.; Hidalgo, M.; Siu, L.; Hammond, L. A.; Villalona-Calero, M. A.; Felton, S.; Drengler, R.; Kuhn, J. G.; Clark, G. M.; Smith, S. L.; MacDonald, J. R.; Smith, C.; Moczygamba, J.; Weitman, S.; Von Hoff, D. D.; Rowinsky, E. K. *J. Clin. Oncol.* **2000**, 18, 4086.
- (271) Urien, S.; Alexandre, J.; Raymond, E.; Brain, E.; Smith, S.; Shah, A.; Cvitkovic, E.; Lokiec, F. *Anticancer Drugs* **2003**, 14, 353.
- (272) Hilgers, W.; Faivre, S.; Chieze, S.; Alexandre, J.; Lokiec, F.; Goldwasser, F.; Raymond, E.; Kahatt, C.; Taamma, A.; Weems, G.; MacDonald, J. R.; Misset, J. L.; Cvitkovic, E. *Invest. New Drugs* **2006**, 24, 311.
- (273) Bomgaars, L. R.; Megason, G. C.; Pullen, J.; Langevin, A. M.; Dale Weitman, S.; Hershon, L.; Kuhn, J. G.; Bernstein, M.; Blaney, S. *M. Pediatr. Blood. Cancer.* **2006**, 47, 163.
- (274) Giles, F.; Cortes, J.; Garcia-Manero, G.; Kornblau, S.; Estey, E.; Kwari, M.; Murgo, A.; Kantarjian, H. *Invest. New Drugs* **2001**, 19, 13.
- (275) Berg, W. J.; Schwartz, L.; Yu, R.; Mazumdar, M.; Motzer, R. J. *Invest. New Drugs* **2001**, 19, 317.
- (276) Pierson, A. S.; Gibbs, P.; Richards, J.; Russ, P.; Eckhardt, S. G.; Gonzalez, R. *Invest. New Drugs* **2002**, 20, 357.
- (277) Dowell, J. E.; Johnson, D. H.; Rogers, J. S.; Shyr, Y.; McCullough, N.; Krozely, P.; DeVore, R. F. *Invest. New Drugs* **2001**, 19, 85.
- (278) Sherman, C. A.; Herndon, J. E. 2nd; Watson, D. M.; Green, M. R. *Lung Cancer* **2004**, 45, 387.
- (279) Yeo, W.; Boyer, M.; Chung, H. C.; Ong, S. Y.; Lim, R.; Zee, B.; Ma, B.; Lam, K. C.; Mo, F. K.; Ng, E. K.; Ho, R.; Clarke, S.; Roh, J. K.; Beale, P.; Rha, S. Y.; Jeung, H. C.; Soo, R.; Goh, B. C.; Chan, A. T. *Cancer Chemother. Pharmacol.* **2007**, 59, 295.
- (280) Seiden, M. V.; Gordon, A. N.; Bodurka, D. C.; Matulonis, U. A.; Penson, R. T.; Reed, E.; Alberts, D. S.; Weems, G.; Cullen, M.; McGuire, W. P. III *Gynecol. Oncol.* **2006**, 101, 55.
- (281) Schilder, R. J.; Blessing, J. A.; Pearl, M. L.; Rose, P. G. *Invest. New Drugs* **2004**, 22, 343.

2978 (282) Raymond, E.; Kahatt, C.; Rigolet, M. H.; Sutherland, W.;  
2979 Lokiec, F.; Alexandre, J.; Tombal, B.; Elman, M.; Lee, M. S.;  
2980 MacDonald, J. R.; Cullen, M.; Misset, J. L.; Cvitkovic, E. *Clin. Cancer*  
2981 *Res.* **2004**, *10*, 7566.